Exploring the potential of earthworms to reduce microplastic pollution in soils

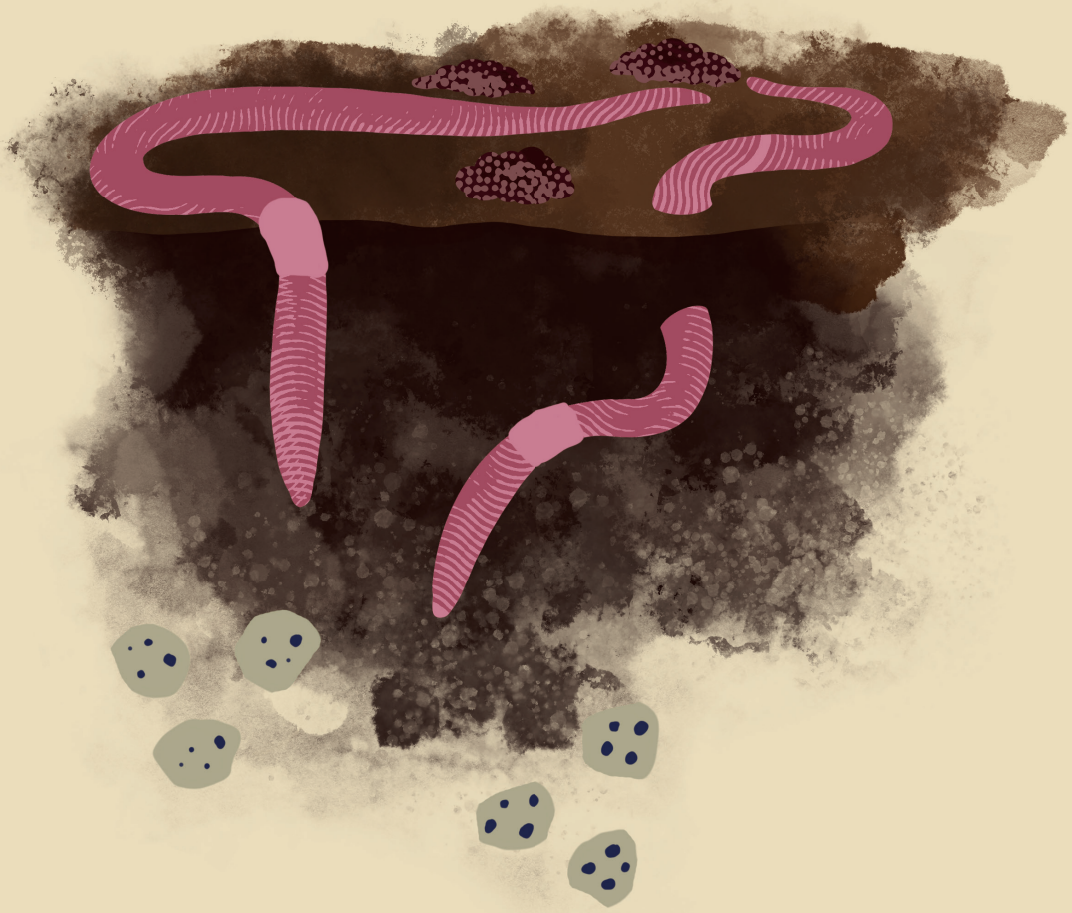

Ke Meng

Propositions

1. Earthworms' gut process and cast aging process are double-edged swords in solving microplastic pollution in soils.
   (this thesis)

2. Biodegradable plastics are not savior for solving microplastic pollution in soils.
   (this thesis)

3. Academic publishing boom reduces quality of scientific publications.

4. Profiling research objects from different disciplinary perspectives stimulates new ideas in environmental research.

5. The conflicts between the academia and industry are beneficial for society.

6. Efficiency, quality, and cost form a trilemma in all human activities.

Propositions belonging to the thesis, entitled

Exploring the potential of earthworms to reduce microplastic pollution in soils

Ke Meng
Wageningen, 10 June 2024

Exploring the potential of earthworms to reduce microplastic pollution in soils

Ke Meng

Thesis committee

Promotor

Prof. Dr Violette Geissen

Personal chair at Soil Physics and Land Management Group

Wageningen University & Research

Co-promotor

Dr Esperanza Huerta Lwanga

Researcher, Soil Physics and Land Management Group

Wageningen University & Research

Other members

Prof. Dr Bart Koelmans, Wageningen University & Research

Dr. Andres Rodriguez Seijo, University of Vigo, Spain

Dr Paula da Silva Tourinho, Masaryk University, Czech Republic

Dr Melanie Braun, University of Bonn, Germany

This research was conducted under the auspices of the Graduate School for Socio-Economic and Natural Sciences of the Environment (SENSE)

Exploring the potential of earthworms to reduce microplastic pollution in soils

Ke Meng

Thesis

submitted in fulfilment of the requirements for the degree of doctor

at Wageningen University

by the authority of the Rector Magnificus,

Prof. Dr C. Kroeze,

in the presence of the

Thesis Committee appointed by the Academic Board

to be defended in public

on Monday 10 June 2024

at 11 a.m. in the Omnia Auditorium.

Ke Meng

Exploring the potential of earthworms to reduce microplastic pollution in soils,

164 pages.

PhD thesis, Wageningen University, Wageningen, the Netherlands (2024)
With references, with summary in English

DOI https://doi.org/10.18174/649352

Table of contents

1. General introduction

1.1 The production and use of plastics

Plastics are a wide range of synthetic or semi-synthetic materials that use polymers as a main ingredient. They are versatile materials used in many industrial segments including packaging, building & construction, auto manufacture, electronics, agriculture, houseware, etc. The global plastics production has increased steadily since 1950 (**Fig 1.1**), and 400 Mt of plastics were produced in 2022 (Plastics Europe, 2023).

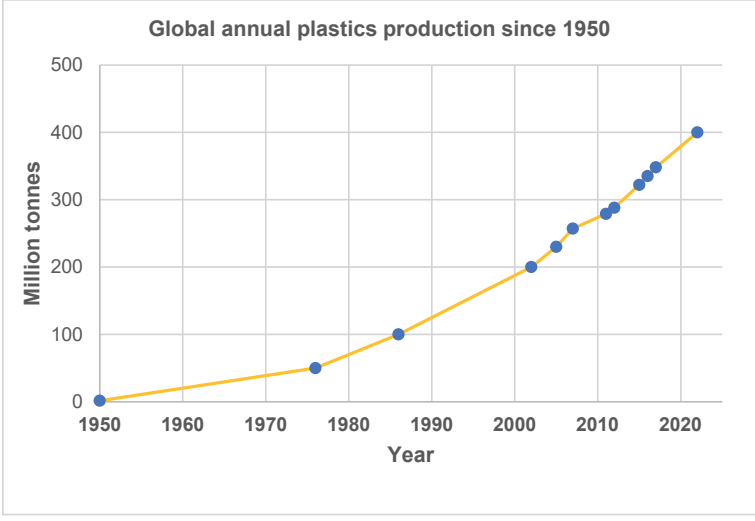

Figure 1.1 Global plastics production since 1950. (Based on data of annual reports by Plastics Europe)

In the past 10 years, the production of biodegradable plastics has also experienced a significant boom, as people have been seeking more sustainable and environmentally friendly alternatives to the non-biodegradable fossil-based plastics. The latest data in Europe shows that the production of bioplastics (either bio-based or biodegradable) accounted for only 1% of the total plastic production in 2022 (Plastics Europe, 2023), nevertheless, the global production capacity of biodegradable plastics has exceeded 1 million tonnes in 2021 (**Fig 1.2**) and is expected to exceed 3.5 million tonnes by 2027 (European Bioplastics, 2023a).

The agricultural and horticultural sector is one of the sectors where biodegradable plastics are actively promoted. In 2022, the proportion of plastics produced for agriculture and gardening was around 4% of the total plastic production, while ~8% of the produced biodegradable plastics were used in agriculture and horticulture (European Bioplastics, 2023a). Therefore, soil, especially agricultural soil, is an environmental matrix into which non-biodegradable and biodegradable plastics potentially end up.

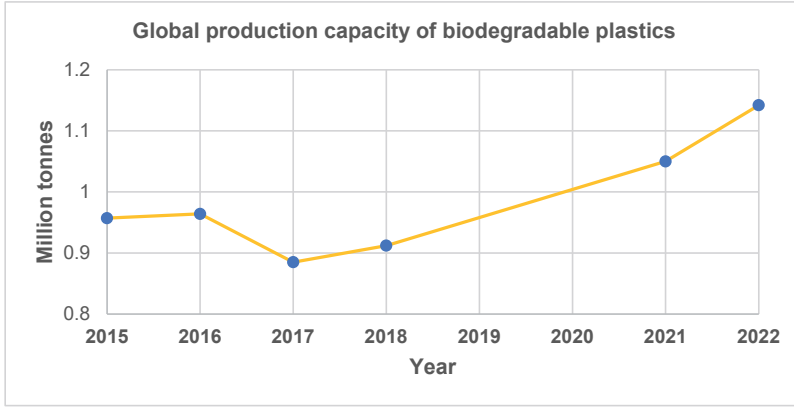

Figure 1.2 Global production capacity of biodegradable plastics (Based on data from European Bioplastics)

1.2 Source of plastic residues in soils

Plastic residues in soils can derive from direct sources such as from intentional plastic use, as well as indirect sources from unintentional use (Lwanga et al., 2022). Potential direct sources are agricultural mulch films for keeping the soil temperature and humidity, plastic pipes for irrigation, twine, and coated fertilizers and pesticides. Indirect sources can be the application of plastics-containing sewage sludge, biosolids, and compost. A recent study also showed that the atmospheric deposition also adds significant amounts of plastic particles in farmlands (Adhikari et al., 2024). Plastics could be broken up into small debris due to the ploughing activity, photodegradation, and the activities of soil organisms, and these small plastic debris with a diameter < 5 mm are now named as microplastics (MPs) (Hartmann et al., 2019).

Figure 1.3 Plastic mulch residues in farmlands. Left: LDPE mulch films. Right: biodegradable mulch films. (by Nicolas Bériot, 2018, south Spain)

Among the abovementioned sources, the massive use and incomplete recovery of plastic mulch films (Fig 1.3) makes one of the most significant inputs of plastic residues into the soil (Liu et al., 2014). Most non-biodegradable plastic mulch films are made from low-density polyethylene (LDPE) with a thickness of 8–20 μm in different regions. Driven by

the need to control the input and accumulation of MPs in the soil, biodegradable plastics are promoted worldwide as promising substitutes for non-biodegradable plastics. A few biodegradable polymers have been explored to replace LDPE to produce agricultural mulch films (Fig 1.4), e.g., polylactic acid (PLA), polybutylene adipate terephthalate (PBAT), polyhydroxyalkanoate (PHA), polybutylene succinate (PBS) and thermoplastic starch (TPS).

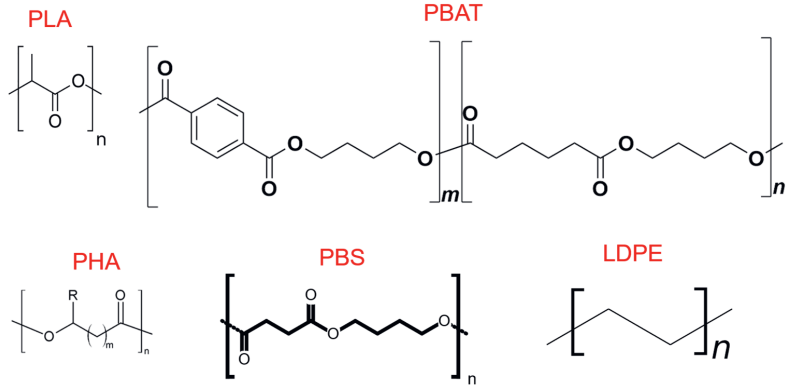

Figure 1.4 Chemical structures of common polymers used for plastic mulch production. **LDPE**: low-density polyethylene, non-biodegradable. **PLA**: polylactic acid, biodegradable. **PBAT**: polybutylene adipate terephthalate. **PHA**: polyhydroxyalkanoate, biodegradable. **PBS**: polybutylene succinate, biodegradable. (The structure of PHA: https://commons.wikimedia.org/w/index.php?curid=25432949)

Several standards and labels are currently available for certifying/labeling the soil-biodegradable mulch films, e.g., EN 17033:2018, ISO 23517:2021 and OK biodegradable SOIL, etc. Both the EN 17033:2018 and ISO 23517:2021 norms required a conversion of a minimum of 90% of the organic carbon in the plastic films into carbon dioxide in 2 years. Nevertheless, several unresolved issues remain for the reliability of the certification process, for example, the differences in testing conditions (controlled lab conditions VS variable field conditions), in the form of testing materials (powder in the norm VS large debris in the field), in the soil type (artificial soil VS various natural soils), etc. (Hayes and Flury, 2018).

Under controlled lab conditions, the biodegradability of some polymers has been demonstrated. For example, the biodegradation of PBAT and PBS has been tracked with the stable carbon isotope labelling technique in microcosm systems in the soil (Zumstein et al., 2018; Nelson et al., 2022). However, the degradation performance of biodegradable plastic products in different regions and under different environmental conditions remains uncertain.

In a field scale experiment, researchers found that the degradation of different biodegradable mulches (made from PLA, PBAT, PHA, starch and their blends) in soil can take several years, depending on the climate, soil type and other environmental factors (Sintim et al., 2020). In another study by the same group, researchers were able to recover

a constant level of fragments from biodegradable mulch films tested in different fields in the US (Griffin-LaHue et al., 2022). It is worth noting that these studies quantified the degradation rate of biodegradable mulch films by calculating the ratio of the total area of

Figure 1.5 Residues of biodegradable seedling trays (main composition: PLA, PBAT and starch) in paddy fields in China. Left and middle: newly applied seedling trays. Right: residues from previous years. (by Ke Meng, 2018, Jiangsu, China)

recoverable fragments to the initial area of the mulch films, potentially overestimating the extent of degradation as the non-recoverable parts (e.g. microplastics) were considered as "area loss". Therefore, the real in-field degradation performance of biodegradable mulch films could be even slower. A previous work conducted at optimal temperature (30 °C) and moisture content (30%) showed that the degradation of a commercial biodegradable seedling tray in soils was limited by the relatively recalcitrant components in the plastic, i.e., PLA and PBAT, posing the potential accumulation in soils (Meng et al., 2023b). Others have also reported low degradation rates of currently popular biodegradable plastics/polymers under various conditions in soils (Satti et al., 2018; Liao and Chen, 2021; Borelbach et al., 2023; Slezak et al., 2023). The degradation rate of plastics not only on their intrinsic properties—the polymer type—but also depends on the environment conditions to which they are exposed. Temperature, pH, moisture contents, UV irradiation, and other biotic factors significantly affect the biodegradation performance of plastics (Chamas et al., 2020). The importance of soil type, which is accountable for the soil physicochemical properties and the availability of potential plastic degraders, in affecting the degradation rate of plastic mulch films has been revealed for PBAT (Han et al., 2021).

Meanwhile, according to the information published by European Bioplastics—"*the association representing the interests of the thriving bioplastics industry in Europe*" (https://www.european-bioplastics.org/about-us/)—soil-biodegradable mulch films possess the advantages where "*In contrast to non-biodegradable mulch films, certified soil-biodegradable ones do not need to be removed but are ploughed under after the harvest where they will completely biodegrade in the soil*." (European Bioplastics, 2023b). It is concerning that the so-called biodegradable plastics are promoted in such a way while their biodegradability and degradation performance have not been thoroughly investigated. Therefore, considering the recommended way of applying biodegradable plastic products (mulch films or others) during agricultural production, the potential accumulation of debris derived from biodegradable plastics in the soil is not impossible (Fig 1.5).

1.3 Occurrence, fate and potential ecotoxicological risks of microplastics in the soil ecosystem

Occurrence of MPs in soils

The occurrence of MPs in soils, especially in agricultural soils, has been widely reported. Due to the fact that most studies applied a density separation method to extract MPs from soils and used Infrared or Raman spectroscopy to identify polymer type, most studies reported the content of MPs in item numbers per gram or kilogram of soil. A survey on farmlands in the US with 23 years of biosolid application history showed that the MPs contents were 360–500 items kg^{-1} soil (Adhikari et al., 2024). In another study, soils from vegetable farms in southeast Spain were found to contain ~2×10^3 items kg^{-1} (equivalent to ~60 cm^2 kg^{-1}) MPs (Beriot et al., 2023). A study involving 19 provinces in China showed that the abundances of MPs increased over time in the locations where plastic mulching was continuously employed, with concentrations of 80.3 ± 49.3, 308 ± 138.1, and 1075.6 ± 346.8 items kg^{-1} soil in fields with 5, 15, and 24 years of continuous mulching, respectively (Huang et al., 2020). A few studies have reported MP contents in soils based on mass. For, example, Li et al. (2020) reported that the abundance of MPs with a size within 0.9–2.0 mm could reach up to 40.35 mg kg^{-1} in fields where plastic film has been applied for 30 years. Scheurer and Bigalke (2018) found up to 55.5 mg kg^{-1} MPs in Swiss floodplain soils.

Fate of MPs in soils

MPs can be transported by abiotic forces in the soil. It was reported that MPs were vertically transported by preferential flows through macropores, and biogenic pores created by *Lumbricus terrestris* (Yu et al., 2019). Wind erosion could also act as a force driving the spreading of MPs from the terrestrial environments to the surroundings (Rezaei et al., 2019; Bullard et al., 2021). The biogenic transport of MPs in the soil is by contrast more studied. The transport of LDPE MPs and (polystyrene, PS) PS nanoplastics (NPs) by the earthworm's ingestion and excretion activity into deeper soil layers has been revealed (Huerta Lwanga et al., 2017a; Heinze et al., 2021; Ju et al., 2023). The presence of MPs in different links along a food chain (soil–earthworm cast–chicken organs) was reported (Huerta Lwanga et al., 2017b), indicating the potential transfer of MPs along the food chain. The uptake of PS NPs by edible plants (wheat and lettuce) was also demonstrated recently (Luo et al., 2022), leaving a question about the potential risks of NPs on the food safety. The drilling, rasping, and grinding activities of soil macrofauna could lead to the fragmentation of plastic debris and even certain level of degradation (Adhikari et al., 2023; Meng et al., 2023a; Rambacher et al., 2023), generating more small-sized plastic particles.

1.4 Ecotoxicological risks of microplastics in the soil ecosystem

Effects of MPs on soil physicochemical properties

Studies have shown that the presence of MPs could affect soil physicochemical properties, exert certain extents of influence on soil organisms, and potentially affect the nutrient cycling in the soil ecosystem. The application of high dosages (7–28%, w/w) of polypropylene (PP) MPs was associated with higher nutrient contents and high-molecular-weight humic-like material and fulvic acid in the soil (Liu et al., 2017). The presence of polyacrylic, polyamide, polyester, and PE at dosages of 0.05–2% (w/w) was found to affect the bulk density, water holding capacity, water stable aggregates in the soil (de Souza Machado et al., 2018). While another study reported that PBAT-based MPs and LDPE MPs showed no influence on soil physicochemical properties at low dosage (0.5%, w/w) but affected soil porosity, bulk density, field capacity, etc. at dosage > 1% (w/w) (Qi et al., 2020). In a more comprehensive investigation, researchers reported that MPs (at a dosage of 0.4%, w/w) could affect soil pH, respiration and enzymatic activities depending on microplastic shape and polymer type (Zhao et al., 2021).

Effects of MPs on plants

Researchers have studied the influence of MPs on plants from different aspects. A meta-analysis has suggested that the phytotoxicity of MPs depends on the polymer types (Zhang et al., 2022). Several studies using MPs derived from LDPE and biodegradable plastics (mainly comprised of PBAT and PLA) have reported that biodegradable MPs in general exerted stronger negative effects (e.g., vegetative, and reproductive growth) on plants, such as wheat, radish, and soybean (Qi et al., 2018; Meng et al., 2021; Ju et al., 2024). It has also been found that the sensitivities of different plant species to MPs are different, for example, meta-analysis showed that maize is in general more sensitive than rice and wheat within the Poaceae family (Zhang et al., 2022). A recent study using different species (barley, wheat, carrot, and lettuce) showed that PS MPs significantly affected the early development of lettuce and carrot, indicating that dicot species are more sensitive to PS MPs than monocot species.

Effects of MPs on soil organisms and nutrient cycles

The impacts of MPs on soil organisms have also been investigated intensively in the past years. The harmful effects of non-biodegradable MPs have been reported on soil fauna including earthworms (e.g. *Lumbricus terrestris*), nematodes (e.g. *Caenorhabditis elegans*), and springtails (e.g. *Folsomia candida*) (Huerta Lwanga et al., 2016; Ju et al., 2019; Kim et al., 2021). On the other hand, some have reported negligible effects of MPs on the fitness of *Eisenia fetida* (Wang et al., 2019), and biodegradable polymers (e.g. PLA) were found to even boost the reproduction of *Eisenia fetida* (Holzinger et al., 2023). The influence of MPs on soil microorganisms has also received much research attention. A meta-analysis based on 92 published articles summarized that MPs pollution has positive effects on soil microbial biomass, induces shifts in soil microbial community structure and

reduce bacterial diversity, in addition biodegradable MPs were found to have greater effects on soil fungal diversity and bacterial community structure that non-biodegradable MPs (Liu et al., 2023).

Several studies have reported that MPs could potentially affect the nutrient cycling in soils, but no consensus has been achieved on this issue. Depending on different experimental settings, MPs were found to either accelerate nitrification (Guo et al., 2023) or inhibit nitrification (Lan et al., 2024) in the soil.

1.5 Counter measurements for microplastic pollution in soils

Due to the various potential ecotoxicological risks mentioned in section 1.3, the importance of adopting appropriate countermeasures for MPs pollution in the soil is highlighted. As a general principle for curbing the plastic pollution, it is crucial to switch from a "take–make–waste" economy to one which materials are reused, recycled, composted or biodegraded (Ward et al., 2024). On this basis, efforts should be made in several aspects to deal with the issue.

Reducing the input of (micro)plastics into the soil

Reducing the use of plastic agricultural tools can be a very direct and efficient way to cut off the input of (micro)plastics in the soil. Land management could be optimized by tuning the crop–climate match, for example, discouraging the production of crops highly dependent on irrigation and mulching in arid or semi-arid regions. The recovery of post-use agricultural tools like mulch films could also be improved in a few ways, e.g., applying better-quality mulch films which are easier to recover, and developing lightweight, simple, and multi-functional machinery for the recovery of mulch film remainings (Liu et al., 2014). Finally, the application of sewage sludge, compost and manure should be conducted with caution to avoid bringing large amounts of MPs into the soil.

Replacing non-biodegradable plastics with biodegradable plastics

The development of biodegradable plastics could provide potential solutions to the (micro)plastics pollution in the soil. However, due to the concerns discussed in section 1.2, this approach should be promoted with caution.

Biodegradation of (micro)plastics

Most plastic products are chemically inert, and resistant to degradation under natural conditions. An early survey has reported that almost no biodegradation was observed for plastic products (polyvinyl chloride (PVC), LDPE, PS, etc.) buried in soil for over 32 years (Otake et al., 1995). Nevertheless, efforts have been made to degrade plastics with biological approaches and several studies have reported promising progress. For example, two bacterial strains (*Enterobacter asburiae YT1* and *Bacillus sp. YP1*) isolated from the gut of waxworms were found to be capable of degrading 6.1–10.7% of the PE over 60 days in liquid mediums (Yang et al., 2014). *Ideonella sakaiensis 201-F6*, isolated from the biofilm on the polyethylene terephthalate (PET) debris presents the ability to degrade low-

crystallinity PET films effectively (Yoshida et al., 2016). Auta et al. (2017) screened microplastics degrading strains from mangrove ecosystems and found that two Bacillus strains (*Bacillus cereus* and *Bacillus gottheilii*) were able to utilize PE, PP, PET, and PS as their sole carbon sources in liquid medium. With the increasing discovery of microbial plastic-degraders, isolated and engineered enzymes could also serve as valuable resources for plastic degradation, and the potential application of plastic-degrading enzymes in agricultural soils is underdevelopment (Palacios-Mateo et al., 2023).

Challenges of solving MPs pollution in the soil

Despite the above-mentioned counter measurements, a few challenges remain for solving MPs pollution in the soil:

1. The recovery of large plastic debris such as macroplastics and post-use mulch films by manpower or machine is possible. However, the recovery of small debris, e.g. MPs and NPs from the soil is extremely difficult, if not impossible. Therefore, potential in-situ remediation strategies need to be explored.
2. Most plastic biodegradation studies were carried out in liquid medium or sterile environmental matrices. However, in real fields the functional strains must compete with indigenous microbial community. It is also highly possible that the degradation of plastics is carried out by a complex microbial community with different individuals playing different roles. Therefore, the single-strain biodegradation might work well in the lab but malfunction in fields.
3. MPs pollution levels in soils largely vary, one study reported the average concentration of 4.5 mg kg^{-1} in current global soils (Büks and Kaupenjohann, 2020). There has not been a widely accepted pollution threshold which defines the need for bioremediation or safe land use. Nevertheless, moderate in-situ mitigation strategies should be explored in advance for future needs.
4. Biodegradable plastics are actively promoted in agricultural production but their residues in soils have not received enough attention. The “future” concentrations of biodegradable MPs could be much higher than expected if biodegradable plastics are blindly used. Therefore, strategies enhancing the degradation of biodegradable plastics in soils should also be explored.

1.6 Role of earthworms in soil bioremediation

The contribution of earthworms to mitigating existing soil pollution

Earthworms, as an important member of the soil fauna, have shown the potential for bioremediating soils polluted with organic contaminants (Hickman and Reid, 2008) and heavy metals (Zeb et al., 2020). For example, *Eisenia fetida* exhibited the ability to remove metals Zn, Fe, Mn, and Cu from the sludge by bioaccumulation in the tissues (Suthar, 2008). The biodegradation of benzo (a) pyrene in the soil could be enhanced by introducing an endogeic earthworm *Pontoscolex corethrurus* into the soil (Hernández-Castellanos et al., 2013). Similarly, the presence of *Eisenia fetida* was found to promote the biodegradation of herbicide metolachlor via stimulating the microbial functional strains (Sun et al., 2019), and facilitate the removal of heavy crude oil in 200 days (Martinkosky

et al., 2017). Based on existing studies where earthworms were introduced to enhance soil bioremediation, several possible mechanisms behind the earthworm-mediated soil bioremediation have been summarized, i.e. the stimulation of soil microorganisms, the enhancement of phytoextraction, the influence on the enzymatic activities and bioaccumulation of pollutants in the tissues (Zeb et al., 2020).

Interactions between earthworms and microplastics

Previous studies have demonstrated that earthworms could interact with plastic debris including MPs in different manners. It has been reported that *Lumbricus terrestris* could drag PE and biodegradable plastic mulch fragments into their burrows when foraging for food (Zhang et al., 2018). The transportation of MPs and NPs from the soil surface to deeper layers by anecic species was also revealed (Huerta Lwanga et al., 2017a; Heinze et al., 2021). In addition, the ingestion of MPs of various polymer types, shapes, and sizes by different earthworm species has been demonstrated under different experimental settings (Huerta Lwanga et al., 2016; Prendergast-Miller et al., 2019; Wang et al., 2022; Adhikari et al., 2023). Furthermore, the abrasion and digestion activity in the gut of *Eisenia fetida* is likely to break up PE MPs and generate small-sized particles (Kwak and An, 2021). Recently, the fragmentation of PLA MPs by *Eisenia fetida* has been confirmed in another study (Wang et al., 2022).

1.7 Research questions and outline of this PhD thesis

With the aim of seeking potential counter measurements which could help mitigate the existing plastic pollution in soils and prevent the potential accumulation of biodegradable plastic debris in the future (which might be happening in some regions), the current thesis explored the potential role of earthworms in the degradation of MPs in the soil.

Objectives of the PhD project

With knowledge derived from existing findings, it is reasonable and logical to ask whether earthworms could play a role in mitigating MPs pollution in soils. Similar proposals have been raised by Sanchez-Hernandez et al. (2020) when the current PhD project just started. Sanchez-Hernandez et al. (2020) proposed that earthworm activities could potentially facilitate plastic (mainly biodegradable plastics) biodegradation in soils via approaches including physical contact between earthworms and plastics, earthworm-mediated microbial proliferation and colonization, enzyme secretion by the earthworms, and the absorption of hydrolysis products by earthworms. As one of the first attempts, the current thesis mainly focused on earthworm gut-related processes, i.e. ingestion, digestion, casting, and cast aging (Fig 1.6). We aimed to provide a relatively complete picture describing the fate of MPs during the soil–gut–cast journey and evaluate the potential of MPs bioremediation mediated by earthworms in soils. The research objectives are as follows:

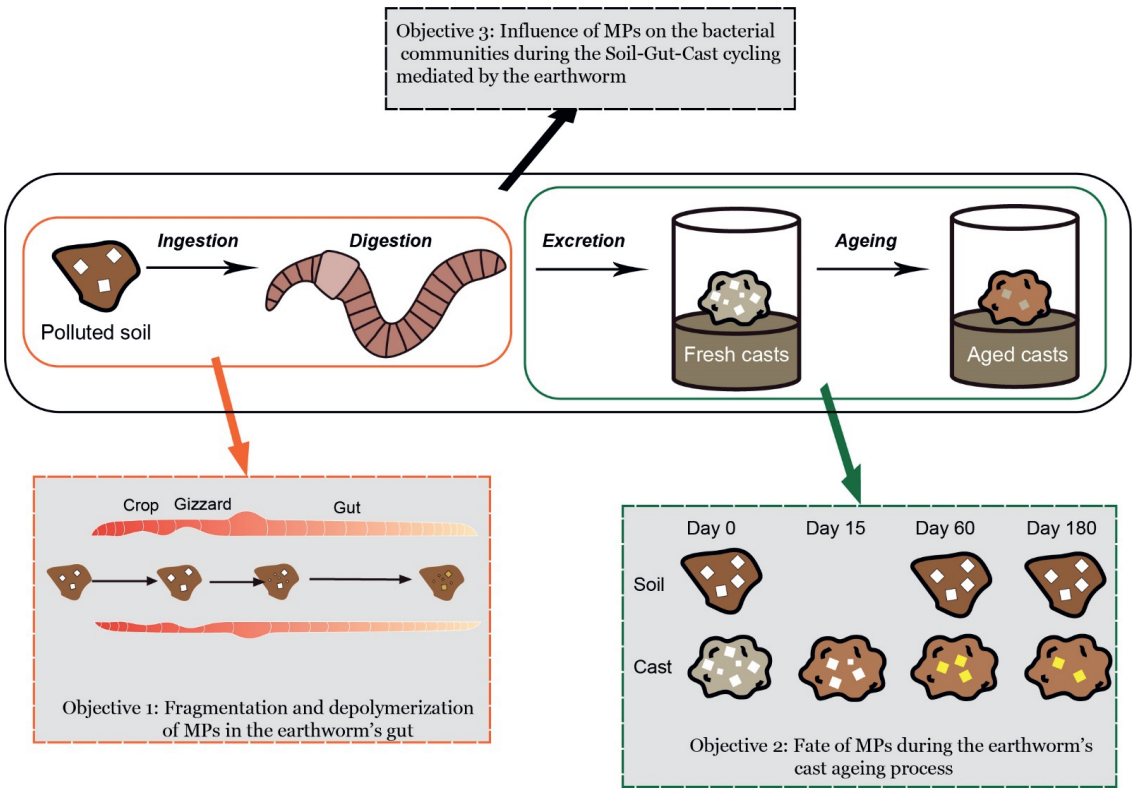

Figure 1.6 Research objectives of the current PhD thesis

Objective 1 (chapter 2): To evaluate the potential of MPs bioremediation in the earthworm gut, we studied the physicochemical changes (e.g., size distribution, chemical composition, and molecular weight distribution) of MPs during ingestion and digestion by *Lumbricus terrestris* in a mesocosm experiment and a Petri Dish experiment. We used three most popular polymers for producing mulch films (LDPE, PLA and PBAT) as test materials and aimed at exploring 1) whether earthworms could survive in a microplastic-contaminated soil (1%, w/w), 2) whether the ingestion of microplastics by earthworms is size-dependent, and 3) the potential changes, e.g., fragmentation and depolymerization of microplastics, during the ingestion and digestion processes.

Objective 2 (chapter 3): Revealing the fate of MPs in earthworm casts is crucial for the full-cycle assessment of the feasibility of MPs bioremediation with earthworms. It is important to know whether gut-processed MPs continue to degrade in the cast and what physicochemical changes happen to MPs during cast aging. In a microcosm experiment, we explored the fate of MPs (LDPE, PLA and PBAT) during the cast aging process. The study was carried out under controlled lab conditions at microcosm scale which simulates the aging of earthworm casts deposited on the soil surface. MPs, where applicable, were recovered and quantified by two extraction–quantification approaches based on different principles to ensure reliable results of MPs contents. The physicochemical properties of MPs during the cast aging process were characterized by multiple techniques to help explain the potential mechanisms associated with the fate of MPs.

Objective 3 (chapter 4): Revealing the response of soil microbial community to MPs in different earthworm gut-related niches (gut contents, casts of different aging stages) can provide useful information for understanding the mechanisms behind the earthworm-mediated MPs bioremediation strategy. With this chapter we aimed to 1) explore the potential influence of MPs on the physicochemical properties of earthworm casts. 2) reveal the influence of MPs on the bacterial communities residing in the earthworm gut and aged casts (for up to 180 days). By targeting both the total community and the active community, we tried to provide realistic and comprehensive information that could help complete a holistic picture of MPs influence on the bacterial community succession during the soil–gut–cast journey.

2. Fragmentation and depolymerization of microplastics in the earthworm gut: A potential for microplastic bioremediation?

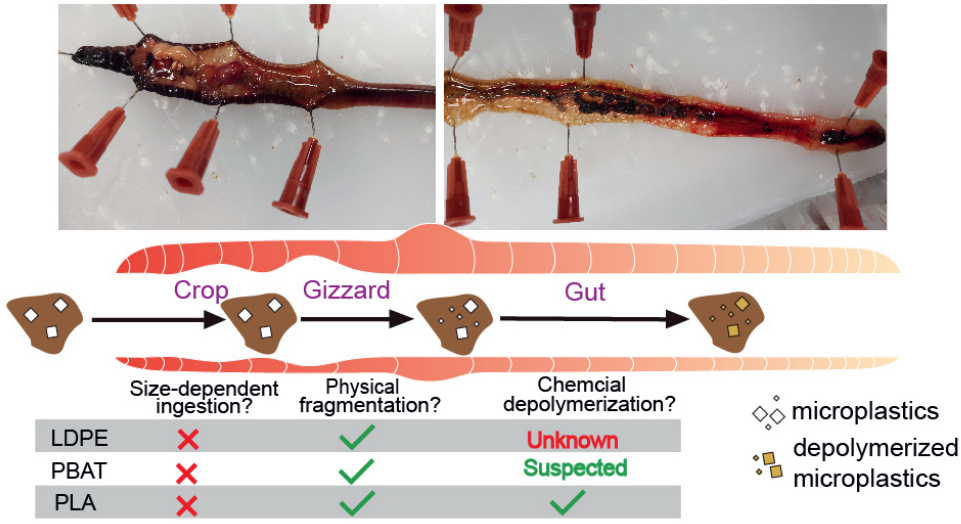

Based on:

Meng, K., Lwanga, E. H., Van der zee, M., Munhoz, D. R., & Geissen, V. (2023). Fragmentation and depolymerization of microplastics in the earthworm gut: A potential for microplastic bioremediation? Journal of Hazardous Materials, 447, Article 130765. https://doi.org/10.1016/j.jhazmat.2023.130765

Abstract

The accumulation of microplastics poses potential risks to soil health. Here, we did a preliminary exploration on the potential of *Lumbricus terrestris* (Oligochaeta) to reduce low-density polyethylene (LDPE), polylactic acid (PLA), and polybutylene adipate terephthalate (PBAT) microplastic (20-648 μm) contamination in soils. The ingestion of microplastics-contaminated soil (1% of microplastics, dw/dw) in a mesocosm system and the ingestion of pure microplastics in the Petri Dish by earthworms were studied. Results show that earthworms survived in the microplastics-contaminated soil (0% mortality in 35 days) but barely when exposed solely to microplastics (30-80% mortality in 4 days). Size-dependent ingestion of microplastics was not observed. The fragmentation of LDPE microplastics in the gizzard facilitated by soil was confirmed by the significantly increased ratio of small-sized (20-113 μm) microplastics from the bulk soil to the gut (from 8.4% to 18.8%). PLA and PBAT microplastics were fragmented by gizzard without the facilitation of soil, the ratios of small-sized (20-113 μm) PLA and PBAT microplastics in the gut were 55.5% and 108.2% higher than in respective pristine distributions. Substantial depolymerization of PLA (weight-average molar mass reduced by 17.7% with shift in molecular weight distribution) and suspected depolymerization of PBAT were observed in the worm gut, while no change in the molar mass was observed for PLA and PBAT microplastics buried in the soil for 49 days. Our results suggest that ingested microplastics could undergo fragmentation and depolymerization (for certain polymers) in the earthworm gut. Further research is needed to reveal the mechanisms of polymer depolymerization in the earthworm gut and to evaluate the feasibility of microplastic bioremediation with earthworms.

2.1 Introduction

The global production of non-biodegradable plastics has reached 368 million tonnes in 2019 (Plastics Europe, 2019), while the bio/biodegradable plastics market has reached 2.1 million tonnes by 2020 and its market share is expected to grow and reach 2.9 million tonnes by 2025 (European Bioplastics, 2020). Plastic products are used in various segments, including agriculture. In 2019, agricultural products accounted for 3.4% and 9% of the total market demand for non-biodegradable and biodegradable plastics, respectively (European Bioplastics, 2019; Plastics Europe, 2019). Consequently, plastic debris derived from agricultural products, such as mulch films, could enter the soil, ending up as small fragments (e.g., micro(nano)plastics) due to various physical, chemical, or biological processes.

The increasing use of bio/biodegradable plastics leads to the potential accumulation of bio-microplastics in the soil, as micro(nano)plastics could be released upon their degradation (Sintim et al., 2019). The degradation performance of biodegradable plastics in the soil has been investigated and concerns have increased over their fate and impacts on the soil environment (Liu et al., 2022). Poor biodegradability of some popular bio/biodegradable polymers and commercial biodegradable plastic products in the soil has been reported under lab conditions and in the field (Sintim et al., 2020; Liao and Chen, 2021; Griffin-LaHue et al., 2022), which might be explained by that the rate of plastic degradation depends not only on the intrinsic properties (e.g., polymer type, molecular weight, fillers, etc.) and environmental conditions, but also on the extrinsic properties such as the size and shape(Chamas et al., 2020). For example, the biodegradability of polybutylene adipate terephthalate (PBAT) in the soil has been verified (Zumstein et al., 2018), but its degrading performance highly depends on the soil type and the native soil microbial community (Han et al., 2021). The poor biodegradability of polylactic acid (PLA) in the soil at ambient temperature was also reported(Shogren et al., 2003; Kamiya et al., 2007), probably due to its critical requirement for temperature. Plastic contamination in the soil has been investigated in different areas with different analytical techniques (Scheurer and Bigalke, 2018; Zhang and Liu, 2018; Corradini et al., 2019; Meng et al., 2020), and its impacts on soil biophysical properties, plant growth and their transfer along the terrestrial food chain have been assessed (Huerta Lwanga et al., 2017b; de Souza Machado et al., 2018, 2019; Qi et al., 2018). At the nano-scale, plastic particles could even accumulate in edible plants (Luo et al., 2022).

To disentangle plastic contamination, efforts are underway to develop methods to remediate soils by plastic biodegradation. The biodegradation of polymers in the soil mainly consists of three steps, i.e., colonization of polymer surface by microbes, depolymerization by extracellular enzymes, and utilization of degrading products by soil microorganisms (Sander, 2019). Attempts have been made by directly screening microbial degraders from environmental samples (Hadad et al., 2005; Yoshida et al., 2016), or using the gut microbiome of soil animals to trigger the degradation. For example, waxworms (the larvae of *Plodia interpunctella*), wax moths (*Galleria mellonella*), earthworms (*Lumbricus terrestris*) and the larvae of *Zophobas atratus* were reported to biodegrade polyethylene

(PE) with their gut microbiome (Yang et al., 2014; Huerta Lwanga et al., 2018; Zhang et al., 2020; Peng et al., 2022), expanded polystyrene could be ingested and biodegraded by dark mealworms (*Tenebrio obscurus*), yellow mealworms (*Tenebrio molitor*), and land snails (*Achatina fulica*) (Peng et al., 2019; Song et al., 2020). In addition, yellow mealworms were also reported to be able to carry out the biodegradation of PLA and polyvinyl chloride (PVC) (Peng et al., 2020, 2021).

Previous studies have proven that soil-dwelling earthworms (e.g., *Lumbricus terrestris*) could transport and ingest plastic debris in the soil. They could drag PE and biodegradable plastic mulch fragments into their burrows when foraging for food (Zhang et al., 2018). The transportation of micro(nano)plastics from the soil surface to deeper layers by anecic species was also reported (Huerta Lwanga et al., 2017a; Heinze et al., 2021). Earthworms could ingest polyester microfibers (Prendergast-Miller et al., 2019) and low-density polyethylene (LDPE) microplastics (Huerta Lwanga et al., 2016) from the food source and potentially trigger the LDPE degradation with the help of the microbial consortium in the gut (Huerta Lwanga et al., 2018). It is therefore interesting to further explore the potential use of earthworms to reduce existing (micro)plastic contamination in soils and prevent the accumulation of bio-based and biodegradable plastics due to their unclear degrading performance under field conditions.

The potential impacts of earthworm activity on plastic biodegradation in the soil include microbial proliferation, physical contact, microbial colonization, enzyme secretion, absorption of hydrolysis products, etc. (Sanchez-Hernandez et al., 2020). Among them, we believe the ingestion of microplastics and the sequential exposure to the gut environment (digestion) might play a key role since the worm gut could host up to 4,000 times more microorganisms than the surrounding soil (Drake and Horn, 2007), making it an ideal place for the degradation of polymers. In the current research we take three most popular polymers for producing mulch films (LDPE, PLA and PBAT) as test materials and aim at exploring (1) whether earthworms could survive in a microplastic-contaminated soil, (2) whether the ingestion of microplastics by earthworms is size-dependent, and (3) the potential changes, e.g., fragmentation and depolymerization of microplastics, during the ingestion and digestion processes. Given the feeding ecology of earthworms, our hypotheses are as follows: (i) the ingestion of microplastics by earthworms might be size-dependent, (ii) microplastic size distributions in the gut might be different from the pristine and gizzard distribution, (iii) a gradual shift in the size distribution and chemical properties of microplastics may occur during their passage through different sections of the gut.

2.2 Materials and methods

2.2.1 Preparation of microplastics

Fossil-based non-biodegradable low-density polyethylene (LDPE, Dow™ LDPE 310E), bio-based compostable PLA (NatureWorks® Ingeo™ Biopolymer 2003D, $M_N/M_W/M_Z$: 73/164/257 kg mol^{-1}), and fossil-based biodegradable (in soil) PBAT (Ecoflex® F Blend

C1200, $M_N/M_W/M_Z$: 23/76/183 kg mol^{-1}) were used in our experiment. Thoroughly cleaned additive-free plastic polymers were used to produce microplastics. Pellets were fed into an ultra-centrifugal mill (ZM200, Retsch GmbH) with liquid nitrogen at 14,000 rpm. A ring sieve with a trapezoid hole size of 1.5 mm was used for the cryogenic fragmentation. Fragmented polymers were collected and sieved with 212 µm and 420 µm metal sieves. Due to different material properties, microplastics with different average diameters and size distributions were produced. The sizes of our artificially prepared microplastics were determined by Laser Direct Infrared (LDIR) chemical imaging system, under the 'particle analysis' mode (see Section 2.5). The area of each particle was measured by the software and the diameter was calculated from the area based on a round shape by the software. The average diameters are 362 ± 119 µm (n = 1720), 300 ± 167 µm (n = 1421), and 234 ± 139 µm (n = 1743) for LDPE, PLA, and PBAT, respectively.

2.2.2 Earthworms and soil

Lumbricus terrestris, a widespread anecic species, was selected for the experiments due to its wide food preferences, including pure soil, soil-litter mixture, and soil-cow dung mixture (Doube et al., 1997), and its aptitude for survival under different microplastic concentrations (0–60% of microplastics in food sources) (Huerta Lwanga et al., 2016). *Lumbricus terrestris* was purchased from Star Food Company (Barneveld, The Netherlands). Adult worms with a clear clitellum and similar body weights were selected. Clean soil was prepared with the following composition, 26% loamy sand, 24% quartz sand, and 50% loamy silt, as described by Huerta Lwanga et al. (2016) and sieved through a 2 mm mesh. The loamy sand and loamy silt (containing organic matter) were collected from clean fields in Unifarm (Wageningen University & Research), and the quartz sand (free of organic matter) was ordered. The final measured soil texture was 1.75% clay, 50.36% silt, 16.42% very fine sand, 10.53% fine sand, 20.87% medium sand, and 0.07% coarse sand (volume-based) (Table S2.1). The final soil pH was 6.4 and contained 0.2% organic matter.

2.2.3 Experimental set-up

Experiment 1: changes in microplastics during the passage through the earthworm gut in a mesocosm system containing a microplastics-contaminated soil

A 35-day mesocosm experiment was conducted to study the changes of microplastics during the passage through the earthworm gut. The experiment was carried out in a 40×30×3 cm glass box (Photo S2.1A, containing 1500 grams of dry clean soil or microplastics-contaminated soil) as described by Huerta Lwanga et al. (2017). Four treatments were set up, namely Control (free of microplastics), LDPE (1% of LDPE microplastics, dw/dw), PBAT (1% of PBAT microplastics, dw/dw), and PLA (1% of PLA microplastics, dw/dw).

To prepare a mesocosm containing 1500 grams of microplastics-contaminated soil, 495 grams of dry clean soil were thoroughly mixed with 5 grams of respective microplastics, then transferred into the glass box. This step was repeated twice to fill 1500 grams into the

mesocosm and to achieve a homogeneous distribution of microplastics. For Control treatment, 1500 grams of dry clean soil were filled in the glass box. The soil moisture was adjusted to 20% by adding distilled water, and the mesocosms were pre-incubated for 2 weeks. After 48 h of gut purging in the dark, four worms with clean guts were rinsed with cold distilled water, dried with a paper towel, weighed on an electronic balance, and placed on the soil surface in the mesocosm. Four replicates were prepared for each treatment, and the mesocosms were kept in the dark at 16 °C for 35 days. Distilled water was added to the mesocosm weekly to maintain the soil moisture at 20% (based on gravimetric measurements). The average fresh body weight of all worms before the experiment was 4.47 ± 0.53 g (n = 64), and there was no difference in initial weights between different treatments. Worms that escaped during the experiment were collected and removed from further analyses (Table S2.3).

After 35 days, mesocosms were opened for sampling (Photo S2.1C). Worms that survived were immediately rinsed with ice-cold distilled water, dried with a paper towel, weighed, and kept at −20 °C. After 1 h, frozen worms were defrosted and dissected as follows (Barois et al., 1993) (Fig S2.1, a–d): the worm was first divided into three equivalent portions, the anterior section consisting of the pharynx, esophagus, crop, gizzard, and the foregut. The middle and posterior sections are midgut and hindgut. The opening was made carefully with a sterile surgical scissor from the dorsal side of the body. The gut content of each section was collected separately with sterile spatulas and preserved in microcentrifuge tubes (1.5 mL). The length of galleries created by worms in each mesocosm was measured to estimate the ingestion rate of worms. Bulk soil, which was not processed by earthworms, was visually identified as per Photo S2.1C and sampled on day 35 (total incubation time 49 days). All samples were stored at 4 °C for further analysis.

Experiment 2: changes in microplastics during the ingestion and digestion processes by *Lumbricus terrestris* in Petri Dishes containing only microplastics

After Experiment 1, another experiment was performed to assess whether there is a size-dependent selection of microplastics during the ingestion (by checking microplastic distributions in the crop and gizzard) and if fragmentation happens in the gizzard (by comparing size distributions in the gizzard and the gut). Briefly, two grams of microplastics (LDPE, PLA, and PBAT) were added to each Petri Dish, and the moisture was adjusted to 20% with distilled water. Two worms with clean gut and known weight were then placed in the Petri Dish (Photo S2.1B). The experiment was carried out in the dark at 16 °C for 4 days, and five replicates were prepared for each polymer type (ten worms in total for each polymer type). The initial fresh body weight of earthworms was 4.15 ± 0.39 g (n = 30), and there was no difference in the fresh weight between different treatments before the experiment. A microplastic-free treatment was also prepared to check the mortality of *Lumbricus terrestris* when no food was provided.

After 4 days, worms that survived were collected, rinsed with ice-cold distilled water, dried with a paper towel, and kept in the −20 °C freezer immediately. After 1 h, frozen worms were defrosted at room temperature and dissected with sterile tools. In this experiment, the worm dissection was conducted differently (Fig S2.1, e–g). Crop, gizzard, and gut

contents were collected separately and subjected to the extraction of microplastics right after the dissection. Due to the crop and gizzard's limited contents, replicates of these two sections were pooled as one sample for extraction.

2.2.4 Extraction of microplastics

A sequential density-based extraction method, modified from Corradini et al. (2021) and Zhang et al. (2020) was established to recover target microplastics (LDPE/PLA/PBAT) from the soil, gut contents, and worm casts. Briefly, for LDPE (density ~0.94 g cm^{-3}), dried samples were extracted with two solutions: firstly with 70% ethanol solution (density 0.88 g cm^{-3}) to remove light impurities and then with distilled water (density 1.0 g cm^{-3}) to recover microplastics. For PLA (density 1.24 g cm^{-3}) and PBAT (density 1.26 g cm^{-3}), dried samples were firstly extracted with distilled water to remove light impurities and then with sodium dihydrogen phosphate (NaH_2PO_4) solution (density 1.28 g cm^{-3}) to recover microplastics. The main procedures are depicted in Figure S2.2, and the detailed extraction protocol is provided in Text S2.1. A weight-based recovery test for this extraction protocol was conducted (Table S2), and the recovery rates of LDPE, PBAT, and PLA microplastics were 103.9 ± 4.6%, 104.0 ± 2.9%, and 102.2 ± 2.1%, respectively.

2.2.5 Identification of microplastics with LDIR and generation of microplastic size distributions

Dried particles preserved in glass scintillation vials were re-suspended by adding 0.5 mL of 96% ethanol solution and treated with an ultrasonic bath for up to 30 s. The suspension was then transferred with a Pasteur pipet onto an infrared-reflective glass slide (7.5 × 2.5 cm; MirrIR, Kevley Technologies). The slide was covered with a glass lid and left to air dry. Sample slides were subjected to microplastics identification on the Agilent 8700 LDIR using the Clarity software with a customized library. Settings for identification and library information are provided in Text S2.2. Besides polymer identification, LDIR also measures the size of detected microplastics. Detected microplastics were sorted in the order of particle area (µm²) since the particle area was the direct measurement from LDIR. Microplastic size distributions were calculated based on the ratio (%) of microplastics in each size fraction (the number of microplastics per size fraction divided by total number of microplastics). As the smallest detectable particle size with current LDIR settings was 325 µm² (equivalent to 20 µm), and the biggest particle detected across all samples was 329,425 µm² (equivalent to 648 µm), 33 size fractions (i.e., from 325–10,000 µm², 10,000–20,000 µm² to 320,000–330,000 µm², bin size 10,000 µm²) were defined. For ease of understanding, size distributions were alternatively displayed based on calculated diameter (20–113 µm, 113–226 µm, 226–339 µm, 339–451 µm and 451–648 µm). Size distributions were calculated for pristine microplastics (PristineMPs), microplastics extracted from bulk soils (Experiment1-BulkSoil), and worm guts (Experiment1-Gut) in Experiment 1, microplastics extracted from crops (Experiment2-Crop), gizzards (Experiment2-Gizzard) and worm guts (Experiment2-Gut) in Experiment 2.

2.2.6 Characterization of microplastics recovered from bulk soil and the worm gut

Pristine microplastics, microplastics extracted from bulk soils and worm guts in Experiment 1, and microplastics extracted from worm guts in Experiment 2 were subjected to a cleaning procedure (Text S2.3) to remove residual biomass and soil organic matters on the particle surface. Cleaned particles were measured with Gel Permeation Chromatography (GPC) to determine molar mass. Detailed procedures for GPC analysis are provided in Text S2.4. Weight-average molecular weight (M_W), Number-average molecular weight (M_N), Z-average molecular weight (M_Z), and polydispersity index (PDI = M_W/M_N) were generated from the measured molecular weight distributions (MWDs). Cleaned pristine microplastics, microplastics extracted from bulk soils and worm guts in Experiment 1 were also characterized by Fourier transform infrared spectroscopy with attenuated total reflectance accessory (FTIR-ATR). Samples were measured in duplicate to generate an average spectrum.

2.2.7 Calculations

Mortality, gross growth rate (*gGR*), and ingestion rate (*IR*) were calculated to profile the physiological conditions of earthworms:

(1) $Mortality: M = \frac{N_0 - N_t}{N_0} \times 100\%$ (for Experiment 1 and 2)

where N_0 and $N_t$represent the numbers of worms that survived at the beginning and by the end of the experiment, respectively.

(2) $Gross\ growth\ rate: gGR = \frac{gM_t - gM_0}{M_0} \times 100\%$ (for Experiment 1 only)

as gut purging was not conducted by the end of Experiment 1 (immediate dissection instead), the *gGR* was calculated to profile the growth of worms with the assumption that adult worms with similar body weights contain similar amounts of gut contents and gut content to body weight ratios. M_0 (g) is the initial weight (without gut contents) before the experiment, *gMt* (g) is the final weight (with gut contents) at the end of the experiment,

(3) $Ingestion\ rate: IR = \frac{V_g}{\sum gM_t}$ (cm^3 soil g^{-1} worm) (for Experiment 1 only)

since no additional food was added to the mesocosms, earthworms could only ingest soil, leading to the forming of galleries in the mesocosm. V_g (cm^3) is the volume of galleries estimated based on the total length of galleries (galleries were treated as cylinders with a diameter of 1 cm) in each mesocosm, and $\sum gM_t$ (g) is the total final body weight of survival worms in each mesocosm on day 35. The occurrence of microplastics in the bulk soil and different gut sections were measured and reported in mass concentration (*Cmpm*, %, w/w) and number-based concentration (*Cmpn*, p g^{-1}). The equations are as follows:

(4) $Cmpm\ (in\ soil/gut):\ Cmpm = \frac{M_{mp}}{M_s} \times 100\%$ (for Experiment 1 only)

(5) $Cmpn\ (in\ soil/gut):\ Cmpn = \frac{N_{mp}}{M_s}$ (p g^{-1}) (for Experiment 1 only)

where M_{mp} (g) and N_{mp} represent the weight and number of microplastics extracted from the sample, and M_s (g) is the dry weight of samples used for microplastic extraction.

2.2.8 Statistics and data analysis

One-way analysis of variance (ANOVA) and student's t-test were used to test significant differences between values of different treatments. Levene's test was used to test the homogeneity of variance. Duncan's test (for equal variance) and Games–Howell test (for unequal variance) were utilized to conduct the post hoc test. Kolmogorov–Smirnov test was used to test whether normal distribution occurred and whether two microplastic size distributions were different. The significant level was set as 0.05.

2.3 Results and discussion

2.3.1 Impacts of microplastics on basic physiological indicators of *Lumbricus terrestris*

No mortality was found in Experiment 1 (35 days), except for one removed replicate from LDPE treatment. Replicate LDPE-D was removed at the early stage because the worms were abnormally inactive from the beginning and all four worms died within 2 weeks. Based on our previous experience with commercially purchased earthworms, this could be a result of using unhealthy worms (e.g., worms carrying pathogens or diseases). The information on individual worms in the mesocosms is provided in Table S2.3. In Experiment 2 (4 days), the mortality was 30% (7 survivors), 40% (6 survivors), and 80% (2 survivors) for worms fed with solely PBAT, PLA, and LDPE microplastics, respectively, and 0% for worms without food. The zero mortality for Experiment 1 was expected since the concentration of microplastics in the soil was 1% (dw/dw), and the exposure time was relatively short. While the mortalities in Experiment 2 indicate that microplastics could cause lethal damage to earthworms if they are ingested in large quantities at exceedingly high concentrations, despite the polymer types. We speculate that the death of worms fed with solely microplastics might be resulted from gut damage caused by plastic particles, which was confirmed for another species *Eisenia andrei* by histopathological analysis (Rodriguez-Seijo et al., 2017).

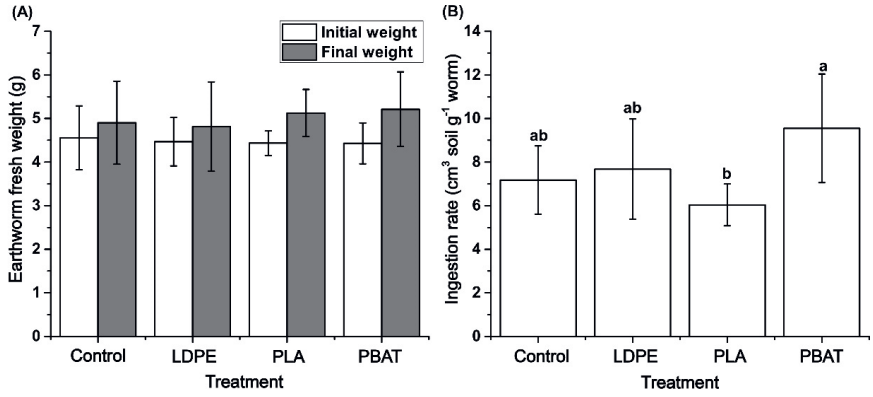

Figure 2.1 (A) Fresh body weights of *Lumbricus terrestris* before and after Experiment 1. The initial weight is the net weight without gut contents, while the final weight is with gut contents. (B) Ingestion rate of *Lumbricus terrestris* in different treatments in Experiment 1. Error bars represent standard deviations and significant difference between different treatments is labeled with different letters.

In Experiment 1, there was no significant difference in initial body weights between different treatments and no significant difference in final body weights between different treatments (Fig 2.1A). The *gGR* was 7.7% for Control, 7.8% for LDPE, 15.6% for PLA, and 17.7% for PBAT. Worms fed with PBAT-contaminated soil showed the highest *IR* (9.55 ± 2.50 $cm^3\ g^{-1}$ worm), while those fed with PLA-contaminated soil showed the lowest (6.04 ± 0.97 $cm^3\ g^{-1}$ worm). The *IR* in the PBAT treatment was significantly higher than that in the PLA treatment ($p < 0.05$). However, no significant difference was found between control and microplastic-addition treatments (Fig 2.1B). This could suggest that the presence of microplastics (1%, dw/dw) in the soil did not affect the activity of earthworms in 35 days of incubation period.

As microplastics of all polymer types were found in the worm gut in both experiments, it is possible to point out that *Lumbricus terrestris* could ingest LDPE, PLA, and PBAT microplastics within the given size ranges when they are either provided as sole food or mixed with soil. Our findings also indicate that the presence of 1% (dw/dw) of LDPE, PLA, and PBAT microplastics in the soil did not significantly impact the earthworms' health after 35 days, reverberating existing findings on the same or other species (Huerta Lwanga et al., 2016; Rodriguez-Seijo et al., 2017; Prendergast-Miller et al., 2019). Although the approach-avoidance behavior of earthworms to different microplastic-contaminated soils was not studied in the current research, some studies reported that *Lumbricus terrestris* did not actively avoid polyester fibers at the concentration of 1% (dw/dw) (Prendergast-Miller et al., 2019), and *Eisenia fetida* avoided the food source when the microplastic concentration exceeded 4% (dw/dw) (Ding et al., 2021). Recent research even observed that *Eisenia fetida* preferred soils contaminated with certain polymer types, e.g., PET and PLA, rather than clean soil (Wang et al., 2022). The robustness of earthworms against microplastic-contaminated soil provides the potential for bioremediation with earthworms.

2.3.2 Microplastics in different gut sections

One of our hypotheses was that microplastics might undergo a gradual change in the size distribution during the passage through different gut sections, which was explored in Experiment 1. Microplastics were separately extracted from different gut sections, and their concentrations were measured in Experiment 1 (Table 2.1). The average *Cmpm* in the bulk soil on day 35 was 0.98% for the LDPE treatment, 1.14% for the PBAT treatment, and 1.26% for the PLA treatment, while the corresponding average *Cmpn* was 1419 p g^{-1}, 2837 p $g^{-1}$and 946 p g^{-1}, respectively (Table 2.1). From the bulk soil to the hindgut, no clear trend in *Cmpm* or *Cmpn* could be observed for any polymer type. Both *Cmpm* and *Cmpn* were calculated in the whole gut by pooling different gut sections, and the average concentrations of microplastics in the entire gut were 0.83% (1143 p g^{-1}) for LDPE, 1.08% (1407 p g^{-1}) for PBAT and 1.15% (523 p g^{-1}) for PLA.

Several studies have reported the ingestion of microplastics by soil invertebrates; however, quantitative studies on the microplastic concentrations in the digestive tract or excreta are scarce. Existing information was derived from different polymer types, particle sizes, feeding strategies, extraction methodologies, and identification methods. For example, Huerta Lwanga et al. (2016) reported that when fed with an LDPE-litter mixture, the microplastic concentration in the cast of *Lumbricus terrestris* varied about 0.20 to 2.0 times compared with those in the LDPE-litter mixture, depending on the ratio of microplastics in the food. Up to 1.6 p mg^{-1} of particles was found in the cast of *Eisenia fetida* exposed to soil mixed with 0.15% of LDPE microplastics (Chen et al., 2020). Small-sized PS microplastics (0.1 and 1.3 μm) were found to accumulate heavily in the intestine of *Eisenia fetida*, and microplastic concentration in the intestine can be up to 800 times that in the soil (Jiang et al., 2020). In Experiment 1, the *Cmpm* was not different between the bulk soil and the gut. While a noteworthy reduction in the *Cmpn* was observed in the gut, especially for PLA and PBAT, the *Cmpn*s of the respective polymers in the gut were 44.7% ($p = 0.128$) and 50.4% ($p = 0.057$) lower than corresponding values for the bulk soil.

Table 2.1 Concentrations of microplastics in the bulk soil and different gut sections (foregut, midgut, hindgut, and whole gut) in Experiment 1. *Cmpm* represents the concentration of microplastics in weight percentage (%), and *Cmpn* represents the number-based concentration of microplastics (p g^{-1}). Data was presented as mean ± SD, for *Cmpm*, N=3–4; For *Cmpn*, N=3. One-way ANOVA was tested for bulk soil, foregut, midgut, and hindgut (significant difference labeled with lowercase letters). Student's *t*-test was tested between bulk soil and whole gut (significant difference labeled with uppercase letters).

Sections	LDPE		PLA		PBAT	
	***Cmpm* (%)**	***Cmpn* (p g^{-1})**	***Cmpm* (%)**	***Cmpn* (p g^{-1})**	***Cmpm* (%)**	***Cmpn* (p g^{-1})**
Bulk Soil	$0.98\pm0.25^{ab,A}$	$1419\pm501^{a,A}$	$1.26\pm0.20^{ab,A}$	$946\pm258^{a,A}$	$1.14\pm0.14^{a,A}$	$2837\pm839^{a,A}$
Foregut	1.34 ± 0.37^{a}	1628 ± 267^{a}	1.15 ± 0.54^{ab}	421 ± 203^{a}	1.26 ± 0.51^{a}	1861 ± 1172^{ab}
Midgut	0.78 ± 0.30^{ab}	1254 ± 414^{a}	0.80 ± 0.53^{b}	468 ± 424^{a}	0.94 ± 0.29^{a}	957 ± 286^{b}
Hindgut	0.74 ± 0.41^{b}	819 ± 608^{a}	2.16 ± 1.37^{a}	618 ± 277^{a}	1.13 ± 0.18^{a}	1630 ± 484^{ab}
Whole Gut	0.83 ± 0.23^{A}	1143 ± 265^{A}	1.15 ± 0.38^{A}	523 ± 283^{A}	1.08 ± 0.18^{A}	1407 ± 416^{A}

The inconsistency between the *Cmpm* and *Cmpn* in our research might be caused by the limitations to extract and identify microplastics. The *Cmpm* was measured for all particles larger than 5 μm (due to the use of a filter membrane with a pore size of 5 μm), while the *Cmpn* calculations included all detectable microplastics under LDIR (>20 μm). The contribution of small-sized microplastics to the *Cmpm* is minimal, but their contribution to the *Cmpn* is noticeable. The observed lower *Cmpn*s in the worm gut in Experiment 1 could be resulted from the fast degradation of small-sized microplastics in the gut due to their substantial surface area. Another possible explanation is that some processes, which occurred during ingestion and digestion, led to particles below the detection limit of LDIR (20 μm). To our knowledge, except for a recent work by Wang et al. (2022) which reported the mass concentration and number-based concentration of PET and PLA microplastics in the cast of *Eisenia fetida*, there is a lack of studies quantifying microplastic concentrations both mass-wise and number-wise.

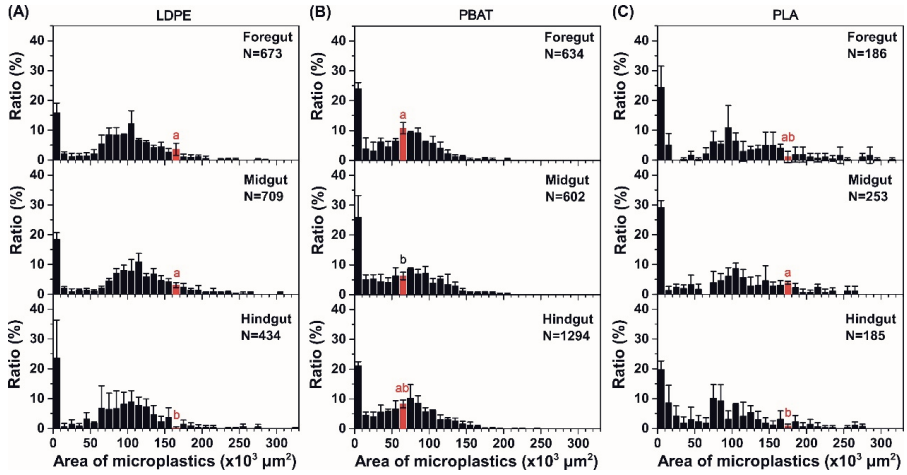

Figure 2.2 Size distributions of (A) LDPE, (B) PBAT, and (C) PLA microplastics in different sections of the gut in Experiment 1. Microplastic sizes were calculated from three replicates for each section. N is the total number of microplastic particles recovered from the triplicate samples. One-way ANOVA was conducted to test whether the ratios of certain size fraction in different gut sections were different. Error bars represent standard deviations and significant differences were labeled vertically across different distributions with letters. Size fractions with significant difference between gut sections were highlighted in red. Calculated diameters (based on a circle) were provided as a reference, e.g., 10×10^3 µm² ~ 113 µm, 50×10^3 µm² ~ 252 µm, 100×10^3 µm² ~ 357 µm, 10×10^3 µm² ~ 437 µm.

Size distributions of microplastics in different gut sections were measured (Fig 2.2). In general, a minimal difference was observed in size distributions from foregut to hindgut for all polymer types. For LDPE, ratios in the foregut and midgut exceeded the ones in the hindgut ($p < 0.05$), standing out as the only significant difference in the fraction 160,000–170,000 µm². For PBAT, the only significant difference was found in the fraction 60,000–70,000 µm², where the ratio in the foregut was higher than in the midgut ($p < 0.05$). For PLA, the only significant difference was found in the fraction 170,000–180,000 µm², where the ratio in the midgut was higher than in the hindgut ($p < 0.05$). In addition, the comparison using distributions pooled from three replicates of each gut section showed that the distributions of microplastics in the foregut and the hindgut were always the same for all polymer types (Fig S2.3), which indicates that no gradual shift in the microplastic size distribution during the passage through the gut.

Indeed, the earthworm gut is a complex environment where different biological processes occur in several sections, and the foregut, midgut, and hindgut take on different tasks during digestion (Drake and Horn, 2007). However, combining the results of microplastic concentrations and size distributions in different gut sections led to an unclear gradual shift in these indicators during the passage through the gut (foregut–midgut–hindgut). Therefore, the earthworm gut was treated as a single environment and studied in our research.

2.3.3 Microplastics after different ingestion and digestion processes

The size distributions and cumulative size distributions of microplastics in different samples in both experiments are displayed in Figure 2.3 (A–C) and Figure S2.4. As only a few microplastics could be extracted from the crops of worms in Experiment 2 (14 LDPE particles, 66 PLA particles, and 190 PBAT particles recovered), microplastic size distributions from the worm crop were disregarded.

In Experiment 1, microplastic size distributions were traced from the pristine microplastics (PristineMPs) to both the bulk soil (Experiment1-BulkSoil, buried in the soil for 49 days), and the worm gut (Experiment1-Gut, by the end of the experiment). The size distributions of PristineMPs and Experiment1-BulkSoil were about the same for all polymer types. Only 1–2 out of the 33 size fractions showed a significant ($p < 0.05$) but slight difference in the ratio (Table S2.4 to S2.6), which indicates that natural fragmentation of LDPE, PBAT, and PLA microplastics did not happen in the soil in 49 days. Interestingly, a distinctly different LDPE microplastic size distribution was observed in the worm gut (Fig 2.3A and inset), where the ratio of the smallest size fraction 325–10,000 μm^2 (18.8 ± 1.7%) was significantly higher than that in the pristine distribution (8.6 ± 0.2%) and in the bulk soil (8.4 ± 0.8%) ($p < 0.05$). For PBAT and PLA, size distributions in the gut were not perceptibly different from those in the bulk soil and the pristine distribution (Fig 2.3, B–C).

In Experiment 2, microplastic size distributions were traced from the pristine distribution (PristineMPs) to the gizzard (Experiment2-Gizzard) and the worm gut (Experiment2-Gut). The aim of measuring microplastic size distributions in the gizzard was to check whether the potentially observed size changes in the gut could result from size-dependent selection during ingestion. For LDPE, there seemed to be a slight shift in the size distribution and cumulative size distribution (Fig 2.3A, Fig S2.4) from PristineMPs to Experiment2-Gizzard. However, we cannot conclude that there was a size-dependent selection during ingestion as the gizzard samples were pooled as one for the microplastic extraction and the observed difference was minimal. The same happened for PBAT and PLA since no size-dependent selection occurred during the ingestion of microplastics by the worm. However, after passing through the gizzard, some changes in the size distribution occurred depending on polymer types. For LDPE, no distinctly different size distribution stood out between Experiment2-Gut and Experiment2-Gizzard (Fig 2.3A and inset). Despite the high variance, the ratio of PBAT microplastics in the smallest fraction, i.e., 325–10,000 $\mu m,^2$ was 55.5% higher in the gut than in the gizzard (Fig 2.3B and inset). While for PLA, Experiment2-Gut was noticeably different from PristineMPs and Experiment2-Gizzard. The ratio of the size fraction 325–10,000 μm^2 was 48.3 ± 5.6% in the gut, significantly.

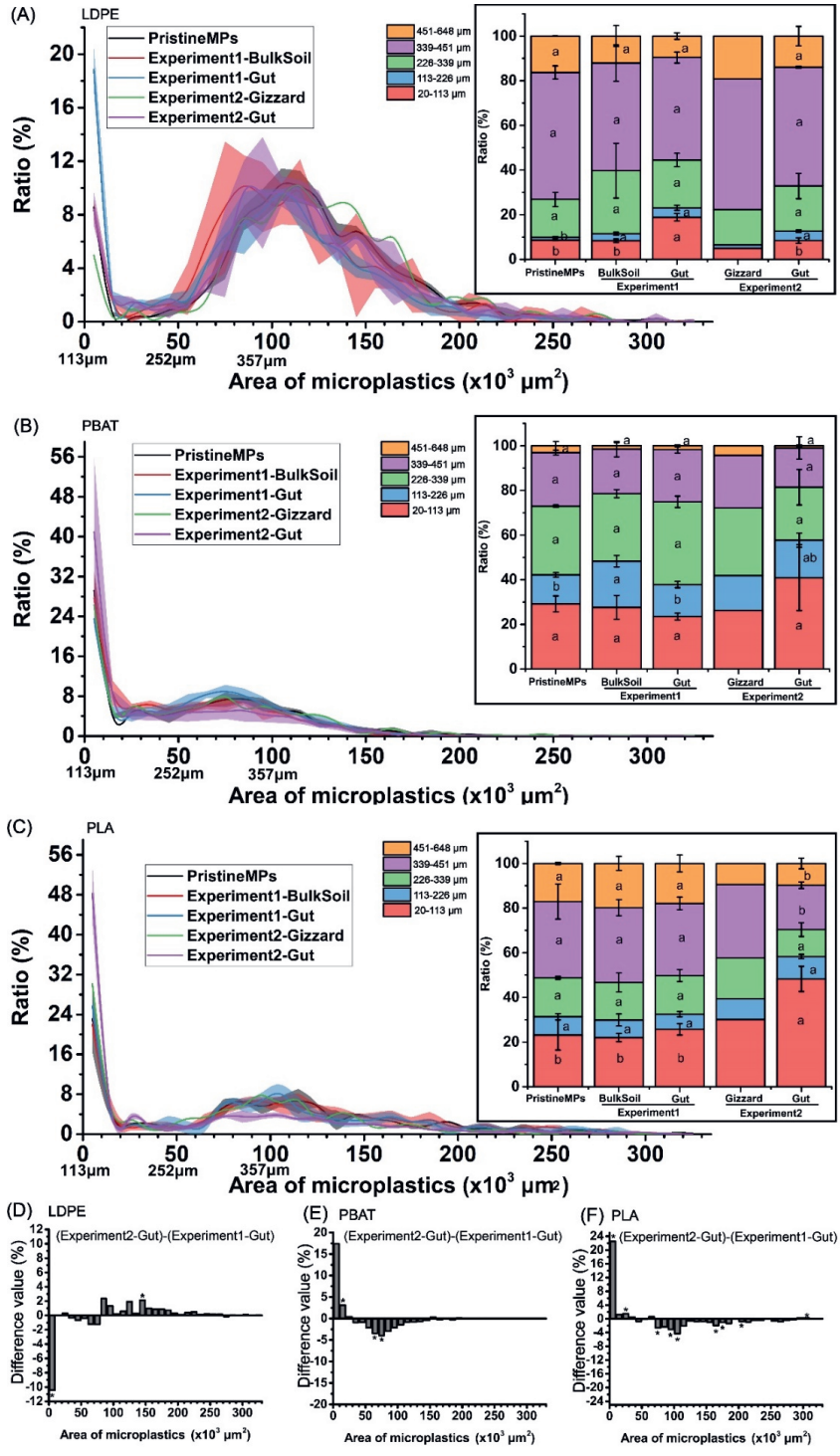
(A) LDPE
PristineMPs
Experiment1-BulkSoil
Experiment1-Gut
Experiment2-Gizzard
Experiment2-Gut
451-648 μm
339-451 μm
226-339 μm
113-226 μm
20-113 μm
Ratio (%)
Area of microplastics (x10³ μm²)
113μm
252μm
357μm
PristineMPs
BulkSoil
Gut
Gizzard
Gut
Experiment1
Experiment2
(B) PBAT
(C) PLA
(D) LDPE
(E) PBAT
(F) PLA
(Experiment2-Gut)-(Experiment1-Gut)
Difference value (%)

Figure 2.3 (A–C) Size distributions (sorted by particle area) of LDPE, PBAT, and PLA microplastics in different samples in Experiment 1 and 2. The shadow area above and under the curve represents standard deviations. Inset bar charts in (A–C) provide an overview of size distributions sorted by calculated diameters (significant difference tested with One-way ANOVA, except for Experiment2-Gizzard). All PristineMPs distributions and Experiment2-Gut distribution in the LDPE treatment were generated from duplicate measurements. All Experiment2-Gizzard distributions were generated from one pooled sample (one measurement). Other distributions were generated from triplicate measurements. Error bars in the inset bar charts represent standard deviations. (D–F) Comparison (per size fraction) between Experiment2-Gut and Experiment1-Gut distributions (significant increase/decrease tested with Student's t-test). Calculated diameters were provided as a reference, e.g., 10×10^3 μm² ~ 113 μm, 50×10^3 μm² ~ 252 μm, 100×10^3 μm² ~ 357 μm, 10×10^3 μm² ~ 437 μm. Detailed size distributions can be found in Table S2.4 to S2.6.

higher than 23.2 ± 6.7% in the pristine distribution ($p < 0.05$) (Fig 2.3C and inset). In addition, significantly lower ratios were also found for size fractions of 80,000–90,000 μm², 100,000–110,000 μm², 120,000–130,000 μm², 150,000–170,000 μm², 180,000–205,000 μm² in the gut ($p < 0.05$).

In Experiment 1, worms were incubated in mesocosms with the microplastics-contaminated soil for 35 days, which means microplastics were ingested together with the soil. While in Experiment 2, worms were incubated in glass Petri Dishes with moist microplastics for 4 days, where microplastics acted as the only food source. By comparing the size distributions of microplastics in two different gut environments (Experiment1-Gut and Experiment2-Gut) (Fig 2.3, D–F), we found more considerably small-sized LDPE microplastics (325–10,000 μm²) in Experiment1-Gut, and the ratios of larger microplastics were, in general, lower in Experiment1-Gut. On the contrary, more small-sized PBAT and PLA microplastics (325–10,000 μm²) were present in Experiment2-Gut, and the ratios of larger microplastics were generally lower in Experiment1-Gut.

PLA and PBAT microplastics recovered in Experiment 1 and 2 were subjected to GPC analysis to study the potential changes in their molecular weight distribution (MWD). The cleaning efficiency for recovered microplastics with SDS solution has been shown and the presence of SDS residues on microplastics has been ruled out (Text S2.3). For PLA (Fig 2.4A), microplastics in the bulk soil (BulkSoil) did not show any significant difference in the weight average molecular weight (M_W) and Z-average molecular weight (M_Z) compared with pristine ones (Pristine) after burial in the soil for 49 days. However, the M_W and M_Z of PLA microplastics in the worm gut (Gut) was 17.7% and 12.3% lower than BulkSoil ($p < 0.05$), indicating a substantial depolymerization given the relatively short gut transit time of 11.6 h for *Lumbricus terrestris* (Taylor and Taylor, 2013). The PDIs of PLA microplastics in Pristine, BulkSoil and Gut were 2.28, 1.92 and 1.94 respectively. In addition, the entire MWD curve of PLA-Gut shifted clearly to low molecular weight area compared with Pristine and BulkSoil (Fig 2.4C). However, in Experiment 2, no significant change in the M_W, M_Z, PDI, and the MWD was observed for PLA microplastics after entering the worm gut (Fig S2.5A). Characterization with FTIR showed that a broad peak around 3340 cm^{-1}

occurred in the BulkSoil and Gut but not in the Pristine, and the absorbance was higher in the Gut than

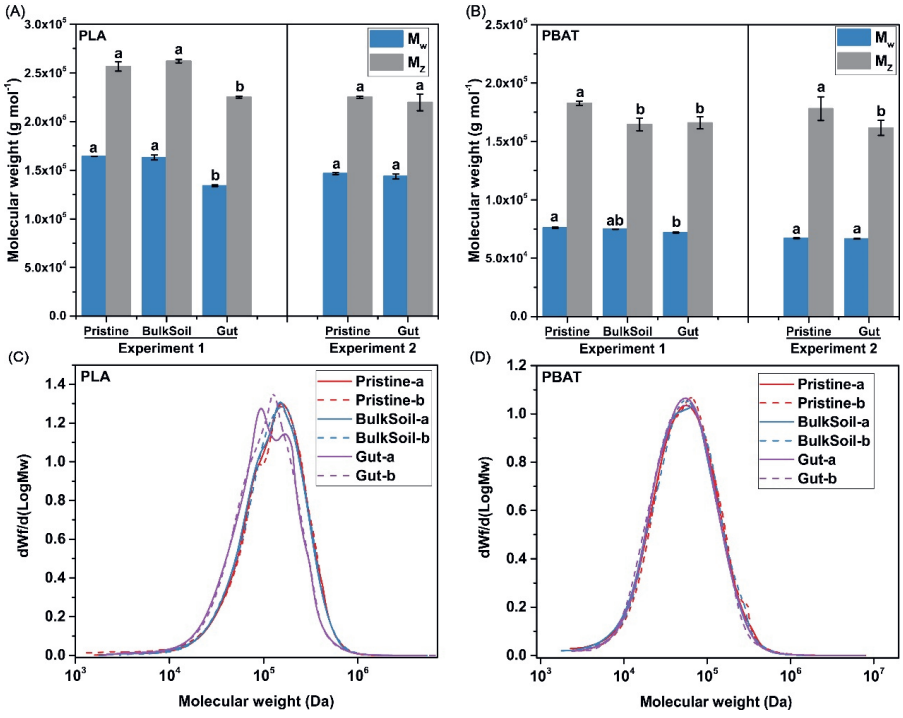

Figure 2.4 (A–B) Weight average molecular weight (M_W) and Z-average molecular weight (M_Z) of PLA and PBAT microplastics in Experiment 1 and 2. Error bars represent standard deviations and significant differences were labeled with different letters. (C–D) GPC molecular weight distribution (MWD) curves of PLA and PBAT microplastics in Experiment 1. 'Pristine' represents pristine microplastics used for the experiment, 'BulkSoil' represents microplastics recovered from the bulk soil in Experiment 1, 'Gut' represents microplastics recovered from the worm gut. Duplicate analyses (-a and -b) were performed for each sample.

BulkSoil (Fig S2.6). This peak could possibly be caused by the stretching of –OH groups in the alcohol end and the carboxylic end of depolymerized PLA, which were generated during chain scission at the ester bond.

In Experiment 1, the M_W of PBAT in the Gut was 5.3% lower than Pristine ($p < 0.05$) and the M_Z of BulkSoil and Gut were 9.9% and 9.2% lower than Pristine ($p < 0.05$) (Fig 2.4B). The PDIs of Pristine, Bulksoil and Gut were 3.30, 2.84 and 2.56, respectively. Nevertheless, the MWD curves of PBAT microplastics showed minimal difference between Pristine, BulkSoil and Gut (Fig 2.4D). No significant difference was found for M_W between Pristine and Gut in Experiment 2 but a slight reduction of M_Z in Gut was observed (–9.2%, $p < 0.05$). It is necessary to point out that the observed changes in M_W and M_Z in the earthworm

gut may not necessarily lead to the conclusion that depolymerization of PBAT happened in the gut, as no synchronous shift in the MWD curves was observed (Fig 2.4D, Fig S2.5B). However, it is possible that the PBAT depolymerization in the gut followed a surface erosion mechanism (Haider et al., 2019) that could have triggered the peeling of surface materials by worm gut enzymes, and the remaining part stayed the same. This is also supported by the FTIR spectra (Fig S2.6). Therefore, we suspect that PBAT depolymerization could have happened in the worm gut in our experiment.

Considering the feeding ecology of earthworms (Curry and Schmidt, 2007), we propose three biological processes where earthworms could interact with microplastics and potentially lead to some changes in microplastic properties. The first is the size-dependent selection during the ingestion of microplastics, which would determine the initial size distribution of microplastics entering the earthworm's digestive system. A second process is the fragmentation of microplastics due to the grinding action in the gizzard, which could lead to the generation of smaller particles and the reduction of larger particles. A third process is the biodegradation of microplastics that takes place simultaneously with the assimilation of nutrients in the gut.

In Experiment 2, we ruled out the size-dependent ingestion of microplastics by checking the size distribution in the gizzard. Some studies have reported that *Lumbricus terrestris* actively select small-sized sands/seeds over big-sized sands/seeds when they forage for food (Zhang and Schrader, 1993; Shumway and Koide, 1994; Schulmann and Tiunov, 1999). However, these studies were usually conducted with larger particles (0.5–3.0 mm in diameter), and the observed size selection possibly reflected the limitation of ingestible particle sizes by the diameter of the intestinal tract (Zhang and Schrader, 1993). It has already been reported that earthworms could ingest and excrete PE and polypropylene (PP) microplastics with a diameter up to 1400–1660 µm (Rillig et al., 2017; Li et al., 2021). However, the largest microplastic in our study was 329,425 µm² (equivalent to a circle with a diameter of 648 µm), i.e., not large enough to cause any difficulty for the ingestion by *Lumbricus terrestris*.

Microplastic fragmentation in the gizzard was verified by the observed differences between microplastic size distributions before ingestion, in the gizzard, and in the gut. LDPE microplastics were not broken up by the gizzard when ingested solely (without soil) but fragmented into smaller particles when uptake together with soil (Fig 2.3A). Previous studies on *Lumbricus terrestris* have reported that sand ingestion facilitates assimilation by enhancing the grinding action in the gizzard (Marhan and Scheu, 2005). Moreover, the enrichment of smaller PE microplastics in the worm cast has been reported by Huerta Lwanga et al. (2016) and Chen et al. (2020). Recently, the presence of PE nanoplastics (potentially fragmented from PE microbeads) in the worm cast has also been confirmed (Kwak and An, 2021). Some have also observed that plastic particles at submicron and nanocron scale can be excreted from *Eisenia fetida* at a slower rate than microplastics (Wang et al., 2022), which potentially provides alternative explanation to the higher ratio of smaller microplastics in the gut. However, this is unlikely an explanation to our findings because size distributions were compared section by section from bulk soil to hindgut in our experiment. Together with already published studies, our results indicate that LDPE

microplastics could be physically fragmented into smaller particles with the assistance of sand grains in the soil, but the gizzard itself may not be strong enough to break up LDPE microplastics. The generation of smaller LDPE microplastics or even nanoplastics suggests that LDPE microplastics are biodegraded in the earthworm gut at extremely slow rate or not biodegraded at all, although the presence of LDPE-degrading gut microbes cannot be ruled out. Nevertheless, PE in other forms, e.g., films and expanded foams have been reported to be biodegraded by other macroinvertebrates (waxworms and mealworms) with their saliva or synergistic enzymatic reactions of the host and gut microbiome (Brandon et al., 2018; Yang et al., 2021; Sanluis-Verdes et al., 2022). More evidence is needed to confirm the biodegradability of LDPE microplastics in the earthworm' gut.

Interestingly, opposing phenomena were observed for PLA and PBAT microplastics. When ingested solely (without soil), a larger ratio of small-sized PLA and PBAT microplastics were found in the gut. In contrast, no significant change in the size distribution was found in the earthworm gut compared with the bulk soil when ingested with soil (Fig 2.3, B–C). In addition, GPC results showed that depolymerization only happened to PLA microplastics (potentially also to PBAT microplastics) when exposed to the gut environment with the presence of soil (Fig 2.4). It has been reported that a wide range of enzymes, such as lipase, chitinase, cellulase, protease, and carboxylesterase, are secreted into the gut by ingested microbes and the worm itself (Drake and Horn, 2007; Sanchez-Hernandez et al., 2009). Furthermore, several studies indicate that the microbial composition of the earthworm gut reflects that of the ingested soil (Curry and Schmidt, 2007). Since both PBAT and PLA are polyesters, it is highly possible that the unique gut environment of *Lumbricus terrestris*, where microbial activity and enzymatic activity are much higher than the surrounding soil, triggered the hydrolysis of ester bonds, accelerating their biodegradation. Therefore, we propose a possible explanation for these results: PLA and PBAT microplastics could be fragmented by the grinding action in the gizzard even without the presence of soil (Fig 2.3, B–C) due to their material properties (e.g., strength and ductility), which could be corroborated by the size distributions and average diameters of different pristine microplastics produced by the same cryogenic grinding process. In Experiment 2, PLA and PBAT microplastics were physically fragmentized into smaller particles. However, the worm gut could not trigger the hydrolysis of these polyesters with its indigenous microbial community and enzymatic activity (Fig 2.4, A–B). In Experiment 1, alternatively, PLA and PBAT microplastics went through both physical fragmentation and depolymerization during their passage through the digestive tract due to the high microbial and enzymatic activity in the gut environment boosted after soil ingestion. The freshly generated small particles were either too small to be detected by the LDIR or assimilated by the gut in a short time.

2.3.4 Environmental implications and limits

The presence of microplastics in the soil and their impacts on the soil properties, soil microorganisms, plants, and soil animals have been reviewed (Zhou et al., 2020). Challenges arise when tackling microplastic contamination in the soil due to their strenuous recovery from the soil at a large scale and limited contamination levels in this

environment, which highlights that conducting a large-scale cleaning for contaminated sites is inessential and not feasible. Therefore, we propose the approach of in-situ bioremediation, seeking help from earthworms inhabiting the soil and carrying out the remediation in the long term. Sanchez-Hernandez et al. (2020) also proposed that the decaying of biodegradable plastics could be enhanced by earthworm activities in the soil, e.g., the formation of middens and burrows, the excretion of casts, and the passage through the gastrointestinal lumen of earthworms. In the current research, we mainly focused on ingestion and digestion processes of earthworms. Given the results of our study, we foresee earthworm gut as a potential 'factory' for the bioremediation of microplastic-contaminated soil, especially for polymers with a relatively easy-to-degrade structure (e.g., PLA and PBAT).

The current research focused on the processes inside the worm. However, it is also pivotal to study the fate of microplastics after excretion back into the soil together with the worm cast. For PLA and PBAT microplastics, the depolymerization may continue in the cast, or other worms could ingest them again due to the coprophagy, leading to further fragmentation and depolymerization in the worm gut. Due to technical limitations, we could not assess the MWDs of LDPE microplastics and the FTIR spectra alone is not sufficient to lead to any solid conclusion. Therefore, we can only conclude that LDPE microplastics were physically fragmented by the gizzard. In this case, LDPE microplastics in the worm cast could be another source of even smaller and nano-scaled particles. Further studies are needed to provide a holistic picture of the interactions between microplastics and earthworms in the soil. Finally, the current study was conducted at mesocosm scale in the lab that mimicked natural conditions. In future work, field experiments are needed to evaluate the feasibility of this bioremediation approach.

2.4 Conclusions

In this study, the potential of earthworms to reduce microplastic contamination in the soil was explored, focused on the ingestion and digestion processes. No mortality was recorded for *Lumbricus terrestris* in microplastics-contaminated (LDPE, PBAT and PLA) soils (1%, dw/dw), and their ingestion rates and growth rates were not affected. The ingestion of microplastics by earthworms was not size-dependent. Fragmentation of microplastics in the gizzard was confirmed by comparing microplastic size distributions in different gut sections. Substantial depolymerization of PLA and suspected depolymerization of PBAT were observed in the gut, while no sign of biodegradation was found for PLA and PBAT microplastics in the soil after 49 days incubation. In general, the results of the current study suggest that ingested microplastics could undergo fragmentation and depolymerization (depending on polymer type) in the earthworm gut. No significant evidence supported biodegradation of LDPE in earthworms although the presence of PE-degrading gut bacteria, which perform degradation at extremely slow rate, cannot be ruled out. Further research is needed to reveal the mechanisms of polymer depolymerization in the earthworm gut and to evaluate the feasibility of bioremediation.

Acknowledgement

We are thankful for the financial support from the China Scholarship Council (CSC: 201904910443). We would also like to acknowledge the financial support from European Union's Horizon 2020 research and innovation programme under the Marie Skłodowska-Curie grant agreement No 955334. We would like to thank Hennie Gertsen and Piet Peters for helping in preparing materials for the experiment, and Wouter Teunissen for the GPC analysis.

Supplementary Materials

Table S2.1 The composition of soil texture (non-dispersed). "Under" and "Upper" represent the under and upper boundaries of diameters. V% represents the volume-based proportion of certain size fraction.

Under (μm)	Upper (μm)	V %	Under (μm)	Upper (μm)	V%	Under (μm)	Upper (μm)	V%	Under (μm)	Upper (μm)	V %
0.02	0.40	0.00	2.52	2.83	0.18	17.83	20.00	1.94	126.19	141.59	2.35
0.40	0.45	0.01	2.83	3.17	0.21	20.00	22.44	2.40	141.59	158.87	2.52
0.45	0.50	0.05	3.17	3.56	0.23	22.44	25.18	2.89	158.87	178.25	2.73
0.50	0.56	0.09	3.56	3.99	0.26	25.18	28.25	3.39	178.25	200.00	2.92
0.56	0.63	0.12	3.99	4.48	0.29	28.25	31.70	3.85	200.00	224.40	3.05
0.63	0.71	0.14	4.48	5.02	0.33	31.70	35.57	4.23	224.40	251.79	3.09
0.71	0.80	0.15	5.02	5.64	0.37	35.57	39.91	4.48	251.79	282.51	3.00
0.80	0.89	0.15	5.64	6.32	0.40	39.91	44.77	4.58	282.51	316.98	2.81
0.89	1.00	0.15	6.32	7.10	0.44	44.77	50.24	4.52	316.98	355.66	2.50
1.00	1.12	0.15	7.10	7.96	0.47	50.24	56.37	4.30	355.66	399.05	2.13
1.12	1.26	0.15	7.96	8.93	0.52	56.37	63.25	3.96	399.05	447.74	1.71
1.26	1.42	0.15	8.93	10.02	0.58	63.25	70.96	3.55	447.74	502.38	1.29
1.42	1.59	0.14	10.02	11.25	0.67	70.96	79.62	3.12	502.38	563.68	0.88
1.59	1.78	0.15	11.25	12.62	0.79	79.62	89.34	2.74	563.68	632.46	0.41
1.78	2.00	0.15	12.62	14.16	0.98	89.34	100.24	2.45	632.46	709.63	0.07
2.00	2.24	0.16	14.16	15.89	1.23	100.24	112.47	2.29	709.63	2000.00	0.00
2.24	2.52	0.17	15.89	17.83	1.55	112.47	126.19	2.26			

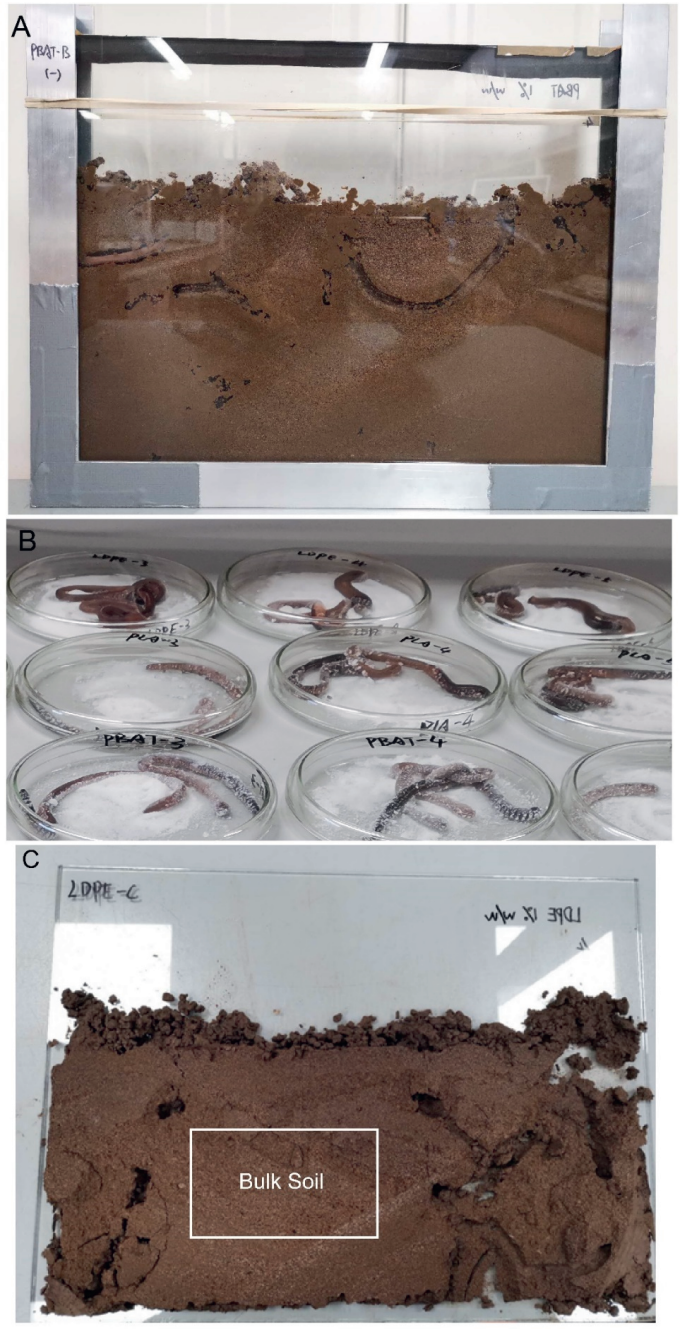

Photo S2.1 Photos of the experimental systems in the study. (A) the mesocosm. (B) the Petri Dish test. (C) Sampling of mesocosm units

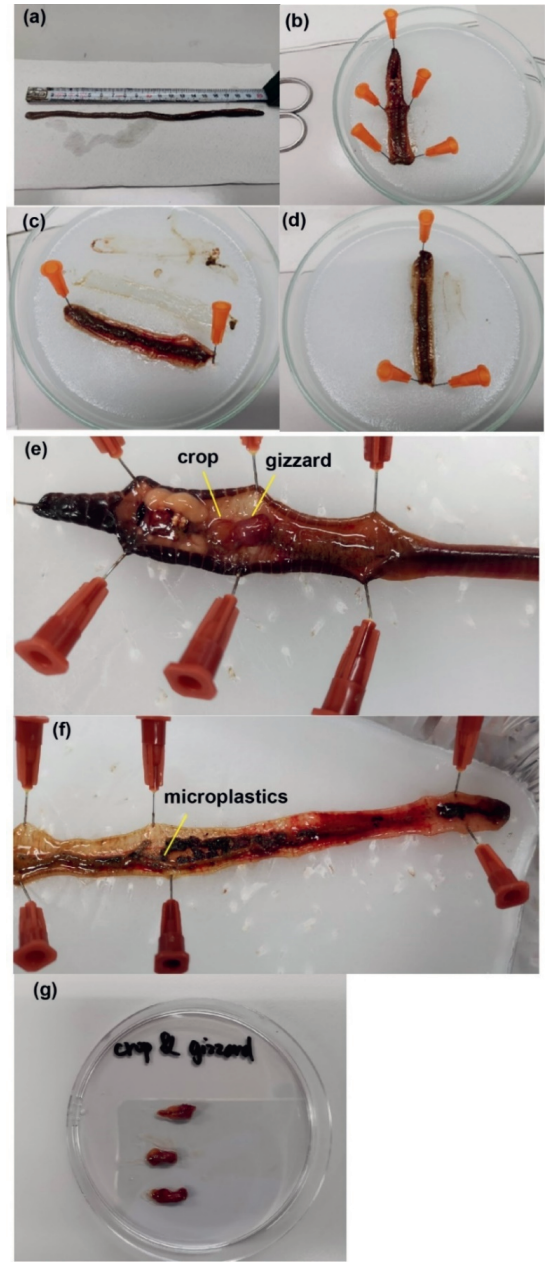

Figure S2.1 Dissection of earthworms. (a) to (d) depict the dissection of earthworms in Experiment 1. (e) to (g) depict the dissection of earthworms after the ingestion of microplastics in Experiment 2.

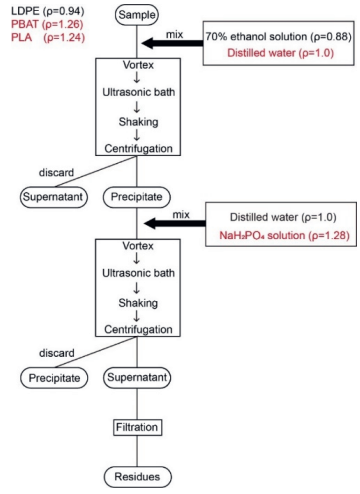

Figure S2.2 Flow chart depicting the extraction of microplastics.

Text S2.1 Protocol for the extraction of microplastics

Dried samples (approx. 0.2-1.0 g depending on sample types) were weighed into a 10 mL glass centrifuge tube and mixed with 8 mL of the first-step solution. The first-step solution varies according to the type of polymer. 70% (v/v) ethanol solution (density ~0.88 g mL^{-1}) was used for LDPE (density ~0.92 g cm^{-3}), while distilled water (density 1.0 g mL^{-1}) was used for PBAT (density ~1.26 g cm^{-3}) and PLA (density ~1.24 g cm^{-3}). The solid-liquid mixture was fully mixed on a vortex shaker until all aggregates were broken and treated with an ultrasonic bath for 10 min and then shaken on a shaker (70 rpm) for 20 min. After shaking, residues in the cap and on the inner wall of the tube were carefully rinsed into the tube with the same solution. Then the mixture was centrifuged at 2,500 rpm for 25 min. After centrifugation, the supernatant was discarded, and the precipitate was extracted again following the above procedures with the second-step solution. The second-step solution also varies according to the type of polymer. Distilled water was used for LDPE, while sodium dihydrogen phosphate (NaH_2PO_4) solution (density ~1.28 g mL^{-1}) was used for PBAT and PLA. After the second centrifugation, the supernatant was filtered through a Whatman® Cyclopore® polycarbonate membrane filter (5 µm, 25 mm) using a vacuum filtration unit. The filtration column was rinsed with distilled water three times and one last time with 70% (v/v) ethanol solution to guarantee that everything in the column was collected onto the filter. The filtration column was covered with a clean lid during filtration to avoid contamination from the lab environment. The polycarbonate filter was then gently recovered with tweezers and deposited in an empty glass scintillation vial with a known weight. The bottleneck of the filtration column was washed out with 70% (v/v) ethanol solution into the scintillation vial, which was treated with an ultrasonic bath to release microplastics from the filter. The filter was rinsed and removed from the vials. The scintillation vials were dried in the oven at 50 °C. Finally, the weights of the vials containing dried particles were recorded.

Text S2.2 Identification of microplastics on the Agilent 8700 LDIR.

The identification was carried out on LDIR with the Clarity software developed by Agilent. Slides with dried samples on the surface were analyzed with the 'Particle Analysis' method, and the detected particles were matched with a customized library. The customized library consists of two parts, the original database 'Agilent Microplastic Starter 1.0' in Clarity software, provided by Primpke et al.[1] under the Creative Commons Attribution 4.0 International License (http://creativecommons.org/licenses/by/4.0/). This database includes most of the plastic polymers in the environment. The second part with the polymers (LDPE, PLA, and PBAT) used in the current study was created using pristine microplastics of different sizes and added to the library by the authors. The sampling parameters of the LDIR were as follows: scanning pixel size 5 μm, spectral range 1800-975 cm^{-1}, sampling step 0.5 cm^{-1} and the target particle size was set as 20-1500 μm. The infrared spectrum of each particle was acquired under transreflectance mode and automatically matched with the customized library. The spectral matching results were given with a hit quality score (from 0 to 1) and a threshold of 0.80 was adopted, as tests with pristine microplastics showed that a rate of correct match could reach 94.75% for LDPE, 98.02% for PBAT, and 98.73% for PLA at current settings. Besides the polymer types, the LDIR also generates the area of each particle.

1. Primpke, S.; Wirth, M.; Lorenz, C.; Gerdts, G., Reference database design for the automated analysis of microplastic samples based on Fourier transform infrared (FTIR) spectroscopy. *Anal Bioanal Chem* **2018,** *410*, (21), 5131-5141.

Table S2.2 Recovery test of LDPE, PBAT, and PLA microplastics from the test soil. Treatment 'Soil-Control-PE' and 'LDPE' used the same extraction method. Treatment 'Soil-Control-PLAPBAT', 'PLA' and 'PBAT' used the same extraction method.

Treatment	Replicate	Soil (mg)	Added MPs (mg)	Recovered mass (mg)	Concentration (%)	Measured concentration (%)	Recovery rate (%)
Soil-Control-PE	1	515.1	0.0	0.2	0.00	0.03	
	2	503.1	0.0	0.0	0.00	0.00	
	3	507.4	0.0	0.2	0.00	0.03	
	4	514.5	0.0	0.1	0.00	0.02	
LDPE	1	499.5	4.6	4.9	0.92	0.98	105.9
	2	512.7	6.6	6.3	1.29	1.24	95.8
	3	541.5	6.0	6.4	1.11	1.18	106.5
	4	485.1	4.4	4.6	0.91	0.95	104.8
	5	507.3	5.4	5.7	1.06	1.13	106.5
Soil-Control-PLAPBAT	1	512.7	0.0	0.2	0.00	0.04	
	2	514.5	0.0	0.4	0.00	0.07	
	3	472.6	0.0	0.3	0.00	0.05	
	4	494.9	0.0	0.9	0.00	0.18	
PLA	1	476.9	4.9	5.1	1.03	1.08	104.5
	2	498.5	6.6	6.7	1.32	1.33	101.1
	3	492.6	5.9	6.4	1.20	1.29	107.8
	4	508.3	5.3	5.4	1.04	1.06	102.5
	5	542.4	4.6	Damaged sample	0.84	Damaged sample	N.A.
PBAT	1	500.1	5.8	6.0	1.15	1.21	104.5
	2	504.7	5.3	5.3	1.05	1.05	100.0
	3	511.2	5.4	5.5	1.06	1.07	100.9
	4	494.3	5.3	5.4	1.08	1.09	101.3
	5	596.1	4.8	5.0	0.81	0.84	104.4

Text S2.3 Cleaning procedures of microplastics before the measurements with GPC

1 Microplastics were mixed with 10 mL of 2% SDS solution (Sodium dodecyl sulfate) in a 20 mL glass vial.

2 The suspension was treated with an ultrasonic bath for 1 h.

3 The suspension was filtrated through a Cyclopore polycarbonate membrane filter (5 µm, 25 mm, Whatman). The glass column was washed with distilled water 5 times (10 mL each time), then with 70% ethanol to remove all particles from the inner wall.

4 The filter membrane was transferred into a 50 mL centrifuge tube (plastic) and particles on the filter were rinsed off with 45 mL distilled water.

5 The centrifuge tube was treated with an ultrasonic bath for another 30 min.

6 Second filtration onto a new filter membrane.

7 Rinse the glass column 5 times with distilled water (10 mL each time) and one last time with 70% ethanol.

8 Transfer the filter into a glass vial and rinse everything off with 70% ethanol.

9 Dry in the oven at 40 °C.

Visual inspection of microplastics before/after cleaning under stereoscopic microscope:

Recovered MPs before cleaning **Recovered MPs after cleaning**

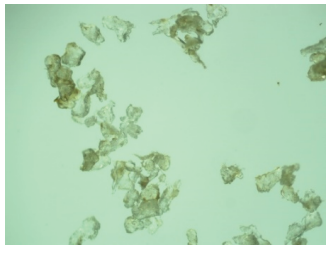

Cleaning procedures do not affect chemical properties of test microplastics

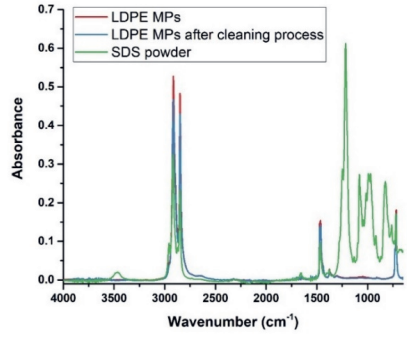

Text S2.4 Methodology for GPC analysis.

An OmniSEC Reveal GPC (model CHR6000) provided with an OmniSEC Resolve (model 7100) Triple Detector Array (RALLS and LALLS light scattering detectors, Refractive Index detector, and Viscometer detector) was used. The selected effluent was 1,1,1,3,3,3-hexafluor-2-propanol (HFIP) + 0.02M KTFA, at a flow of 0.7 ml/min. Columns used are a PSS PFG analytical linear M and guard column, molecular range ~ 300 – 2·10 e^6 D (PMMA in HFIP) at an oven temperature of 35°C. Accurately weighed samples were dissolved overnight in 1.0 ml effluent in 1.5 ml GLC vials. Concentrations were 3 to 4 mg/ml of polymer (accurate weight of sample and liquid). Filtering is done before measuring through 0.45µm PTFE syringe filters. The (standard) injection volume was 100 µl. All measurements were performed in duplicate.

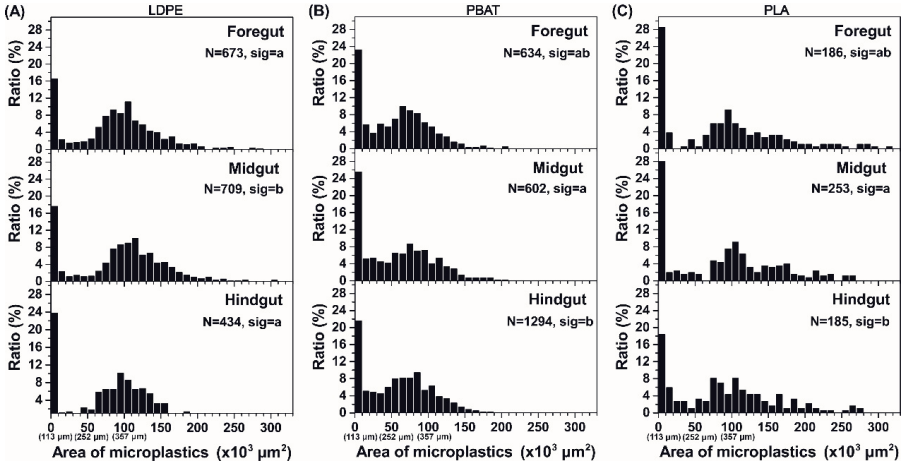

Fig S2.3 Size distribution of (A) LDPE, (B) PBAT, and (C) PLA microplastics in different sections of the gut in Experiment 1. Each distribution was pooled from respective sections of three complete guts. N is the total number of particles used to generate the distribution. Kolmogorov-Smirnov test was used to test whether two distributions are statistically different. Significant difference was labeled with letters. Estimated diameters (based on a circle) were provided as a reference, e.g., 10×10^3 µm² ~ 113 µm, 50×10^3 µm² ~ 252 µm, 100×10^3 µm² ~ 357 µm, 10×10^3 µm² ~ 437 µm.

Table S2.3 Body weights of earthworms before and after mesocosm test. Initial and final weight in the same row do not refer to the same worm.

Treatment	Rep	Initial weight (g)	Final weight (g)	Treatment	Rep	Initial weight (g)	Final weight (g)	Treatment	Rep	Initial weight (g)	Final weight (g)	Treatment	Rep	Initial weight (g)	Final weight (g)
CK	A	5.01	3.70	LDPE	A	4.22	4.56	PLA	A	4.41	4.53	PBAT	A	4.32	5.66
		4.33	5.31			4.26	3.66			4.18	5.11			4.76	6.49
		3.78	6.31			5.24	5.4			5.08	6.36			5.02	Espcape
		5.44	Espcape			4.12	3.69			4.14	4.72			3.61	Espcape
	B	6.32	3.86		B	3.91	5.66		B	4.36	5.30		B	4.75	4.04
		3.77	6.94			5.63	4			4.69	4.48			4.25	6.44
		4.77	4.66			3.94	6.63			4.48	5.73			4.94	4.83
		3.44	5.66			4.52	Espcape			4.21	Espcape			3.72	5.88
	C	5.04	4.68		C	4.84	5.47		C	4.83	5.45		C	5.07	5.11
		4.06	5.24			4.55	4.26			4.04	5.12			4.21	4.70
		4.06	4.21			3.80	Espcape			4.29	5.01			4.64	4.06
		4.99	4.27			4.57	Espcape			4.34	5.06			4.11	4.71
	D	4.68	4.98		D	3.88	Dead		D	4.14	4.40		D	4.21	4.70
		4.92	5.55			4.55	Dead			4.63	5.62			3.8	4.82
		4.16	3.60			5.56	Dead			4.56	4.86			4.62	6.33
		4.09	4.58			3.97	Dead			4.54	Escape			4.85	Espcape

*Replicate LDPE-D was removed from the experiment because the worms were abnormally inactive (not digging the burrows) from the beginning and all four worms died within 2 weeks. Based on our previous experience with commercially purchased earthworms, this could be a result of using unhealthy worms (e.g., worms carrying pathogens or diseases).

Table S2.4 Distribution of LDPE microplastics in different samples in Experiment 1 and 2. One-way ANOVA test was conducted to test whether the ratios of certain size fractions in different samples (Pristine, Experiment1-BulkSoil, Experiment1-Gut, and Experiment2-Gut) were different. Significant difference was labeled with letters.

Size fraction ($x10^3$ μm²)	PristineMPs (%)		Experiment1-BulkSoil (%)		Experiment1-Gut (%)		Experiment2-Gut (%)		Experiment2-Gizzard (%)
	Average	SD	Average	SD	Average	SD	Average	SD	
0.325-10	8.6[b]	0.2	8.4[b]	0.8	18.8[a]	1.7	8.4[b]	1.3	5.0
10-20	0.6[b]	0.1	1.6[a]	0.3	1.8[a]	0.5	1.8[a]	0.2	0.4
20-30	0.3	0.1	0.5	0.5	1.2	0.5	1.5	0.4	0.9
30-40	0.4	0.1	1.1	0.5	1.2	0.4	0.9	0.1	0.2
40-50	0.9	0.5	1.3	0.4	1.7	0.4	1.0	0.8	0.6
50-60	1.2	0.4	2.4	1.9	1.6	0.7	1.2	0.0	0.7
60-70	2.4	0.1	5.8	3.0	4.3	0.3	3.0	0.8	1.7
70-80	4.8	1.6	8.6	4.9	6.4	1.0	5.2	3.3	5.2
80-90	7.8	0.9	10.1	2.3	7.4	2.3	9.7	2.3	7.7
90-100	8.8	1.1	9.3	2.6	8.3	1.6	9.6	4.2	7.4
100-110	10.3	1.2	8.8	1.5	9.6	0.4	9.8	1.1	9.2
110-120	10.1	1.2	9.7	2.5	8.6	1.6	9.1	1.5	10.1
120-130	9.0	0.5	6.3	2.0	6.3	0.3	8.2	1.6	8.7
130-140	6.5	0.9	5.8	0.5	5.4	1.0	5.7	1.2	8.8
140-150	6.8	0.4	4.2	3.9	4.1	0.8	6.3	0.4	8.3
150-160	5.4	0.5	4.1	1.6	3.6	0.5	4.6	1.7	6.1
160-170	3.9	0.6	3.3	0.8	2.7	0.7	3.6	2.4	6.3
170-180	3.2	0.4	2.7	2.0	1.7	0.5	2.6	0.6	3.3
180-190	2.5	0.3	1.3	0.6	1.2	0.7	1.9	0.4	1.3
190-200	1.4	0.1	0.8	0.4	1.1	0.7	1.4	0.0	1.8
200-210	1.4	0.3	0.9	1.2	0.6	0.2	0.7	0.3	1.7
210-220	1.2	0.0	1.3	0.5	0.5	0.5	0.9	0.5	1.7
220-230	0.5	0.5	0.1	0.2	0.3	0.1	0.7	0.7	0.6
230-240	0.6	0.1	0.4	0.7	0.4	0.0	0.5	0.3	0.7
240-250	0.4	0.1	0.5	0.5	0.2	0.2	0.4	0.1	0.6
250-260	0.2	0.1	0.1	0.2	0.3	0.3	0.4	0.6	0.2
260-270	0.2	0.1	0.4	0.7	0.2	0.2	0.3	0.2	0.4
270-280	0.1	0.2	0.3	0.3	0.2	0.1	0.1	0.1	0.6
280-290	0.1	0.1	0.0	0.0	0.0	0.1	0.1	0.1	0.0
290-300	0.1[a]	0.1	0.0[b]	0.0	0.0[b]	0.0	0.0[b]	0.0	0.0
300-319	0.2	0.1	0.0	0.0	0.2	0.2	0.3	0.4	0.2
310-320	0.0	0.1	0.0	0.0	0.0	0.0	0.0	0.0	0.0
320-330	0.1	0.1	0.0	0.0	0.0	0.1	0.1	0.1	0.0
Total number	1721		1816		711		982		543

Table S2.5 Distribution of PBAT microplastics in different samples in Experiment 1 and 2. One way ANOVA test was conducted to test whether the ratios of certain size fractions in different samples (Pristine, Experiment1-BulkSoil, Experiment1-Gut, and Experiment2-Gut) were different. Significant difference was labeled with letters.

Size fraction ($x10^3$ μm²)	PristineMPs (%)		Experiment1-BulkSoil (%)		Experiment1-Gut (%)		Experiment2-Gut (%)		Experiment2-Gizzard (%)
	Average	SD	Average	SD	Average	SD	Average	SD	
0.325-10	29.2	3.6	27.6	5.4	23.5	1.6	40.9	14.8	26.3
10-20	4.0^{c}	0.5	8.6^{a}	2.5	5.1^{bc}	0.9	8.2^{ab}	1.0	5.2
20-30	4.7	0.8	5.7	0.7	4.2	1.3	4.6	1.3	5.8
30-40	4.3^{b}	0.2	6.3^{a}	0.8	5.0^{ab}	0.9	4.1^{b}	0.9	4.6
40-50	4.3	1.6	5.3	0.8	4.9	1.5	4.1	1.1	4.7
50-60	5.4	0.8	5.7	1.2	6.8	1.6	4.7	1.7	5.6
60-70	6.4^{ab}	0.5	6.2^{ab}	0.7	8.3^{a}	0.7	4.9^{b}	1.7	6.5
70-80	7.3	1.5	6.3	1.3	8.9	1.3	5.0	1.5	7.9
80-90	7.4	0.7	6.8	0.5	8.1	1.5	5.1	2.2	5.6
90-100	6.5	1.1	5.3	2.0	6.4	1.5	4.3	1.5	6.0
100-110	5.2	0.7	4.6	0.4	5.4	0.3	4.0	1.4	4.7
110-120	4.7	0.6	3.2	0.3	4.1	0.3	3.3	0.8	4.3
120-130	2.6	0.6	2.9	0.6	2.9	1.3	2.1	0.4	4.2
130-140	2.2	0.1	2.1	0.4	2.4	0.6	1.8	0.6	2.8
140-150	1.5	0.5	1.4	0.5	1.4	0.6	1.0	0.5	0.8
150-160	1.2	0.3	0.5	0.5	0.8	0.4	1.1	0.3	0.9
160-170	1.0	0.8	0.6	0.4	0.5	0.2	0.3	0.1	1.4
170-180	0.5	0.3	0.3	0.3	0.4	0.1	0.4	0.3	0.4
180-190	0.5	0.7	0.2	0.4	0.4	0.3	0.1	0.1	0.5
190-200	0.4	0.2	0.2	0.3	0.1	0.1	0.1	0.2	0.6
200-210	0.4	0.2	0.1	0.2	0.2	0.1	0.1	0.1	0.1
210-220	0.2	0.1	0.0	0.0	0.0	0.1	0.1	0.1	0.3
220-230	0.1	0.1	0.1	0.2	0.0	0.1	0.0	0.0	0.1
230-240	0.0	0.0	0.0	0.0	0.0	0.0	0.0	0.0	0.1
240-250	0.0	0.0	0.0	0.0	0.0	0.1	0.0	0.0	0.4
250-260	0.1	0.1	0.0	0.0	0.0	0.0	0.0	0.0	0.0
260-270	0.0	0.0	0.1	0.1	0.0	0.0	0.0	0.0	0.1
270-280	0.0	0.0	0.0	0.0	0.0	0.0	0.0	0.0	0.0
280-290	0.0	0.0	0.0	0.0	0.0	0.0	0.0	0.0	0.1
290-300	0.0	0.0	0.0	0.0	0.0	0.0	0.0	0.0	0.0
300-319	0.0	0.0	0.0	0.0	0.0	0.0	0.0	0.0	0.0
310-320	0.0	0.0	0.0	0.0	0.0	0.0	0.0	0.0	0.0
320-330	0.0	0.0	0.0	0.0	0.0	0.0	0.0	0.0	0.1
Total number	1743		1643		2530		4197		788

Table S2.6 Distribution of PLA microplastics in different samples in Experiment 1 and 2. One way ANOVA test was conducted to test whether the ratios of certain size fractions in different samples (Pristine, Experiment1-BulkSoil, Experiment1-Gut, and Experiment2-Gut) were different. Significant difference was labeled with letters.

Size fraction ($x10^3$ μm²)	Pristine MPs (%)		Experiment1-BulkSoil (%)		Experiment1-Gut (%)		Experiment2-Gut (%)		Experiment2-Gizzard (%)
	Average	SD	Average	SD	Average	SD	Average	SD	
0.325-10	23.2^{b}	6.7	22.0^{b}	1.8	25.7^{b}	2.5	48.3^{a}	5.6	30.1
10-20	4.2	0.8	5.0	2.1	3.6	0.4	4.9	0.7	5.3
20-30	1.9^{b}	0.5	1.3^{b}	0.6	1.7^{b}	0.1	3.2^{a}	0.7	2.8
30-40	2.1	0.0	1.6	0.8	1.4	0.7	1.9	0.2	1.1
40-50	1.5	0.4	1.5	1.0	2.1	1.5	1.3	0.9	1.4
50-60	1.3	0.4	1.6	0.1	1.5	1.3	1.4	0.5	3.0
60-70	2.7	0.3	2.8	1.3	1.7	1.2	2.3	0.6	3.4
70-80	5.4^{a}	1.7	4.7^{ab}	0.8	6.2^{a}	0.3	3.5^{b}	0.3	4.8
80-90	6.6	0.2	6.2	1.1	5.9	1.3	3.5	1.2	5.7
90-100	5.6	1.5	6.5	0.9	6.7	1.6	3.6	0.6	7.8
100-110	6.5^{ab}	1.0	6.0^{ab}	1.6	8.1^{a}	1.8	3.8^{b}	0.5	6.4
110-120	6.6	2.5	5.7	2.4	5.1	2.5	3.1	0.3	6.7
120-130	5.7	0.4	4.2	1.8	3.8	1.0	3.2	0.5	3.0
130-140	2.8	2.0	4.2	1.3	3.0	1.4	2.2	0.2	4.1
140-150	3.8	0.4	3.7	0.5	2.8	1.2	2.1	0.0	3.5
150-160	3.1	0.1	3.2	1.1	2.9	1.2	2.0	0.3	1.4
160-170	2.6	0.0	3.1	1.6	3.4	1.0	1.5	0.4	1.6
170-180	1.5	0.4	2.4	1.0	2.5	0.1	1.5	0.1	2.0
180-190	1.8	0.2	2.8	1.6	2.3	0.8	0.9	0.2	1.1
190-200	2.5	0.2	1.7	0.7	0.9	1.2	1.0	0.5	0.5
200-210	1.2	0.2	1.4	0.4	1.3	0.4	0.6	0.1	0.7
210-220	1.2	0.4	1.8	0.5	1.4	0.9	0.5	0.3	0.7
220-230	0.9	0.2	0.9	0.4	0.9	0.5	0.5	0.4	0.9
230-240	1.2	0.8	1.0	0.9	1.1	0.4	0.7	0.3	0.0
240-250	0.7	0.3	1.5	0.2	0.5	0.9	0.5	0.4	0.2
250-260	0.7	0.1	1.1	0.6	0.9	0.6	0.3	0.2	0.2
260-270	0.8	0.2	0.3	0.3	1.1	0.6	0.2	0.2	0.5
270-280	0.7	0.5	0.9	0.1	0.7	0.3	0.2	0.2	0.0
280-290	0.3	0.1	0.4	0.4	0.5	0.9	0.3	0.3	0.5
290-300	0.3	0.0	0.1	0.1	0.1	0.3	0.4	0.2	0.2
300-319	0.2	0.2	0.2	0.3	0.0	0.0	0.2	0.0	0.2
310-320	0.3	0.0	0.1	0.1	0.1	0.3	0.1	0.1	0.2
320-330	0.2	0.1	0.1	0.1	0.0	0.0	0.0	0.1	0.0
Total number	1421		1044		624		3189		564

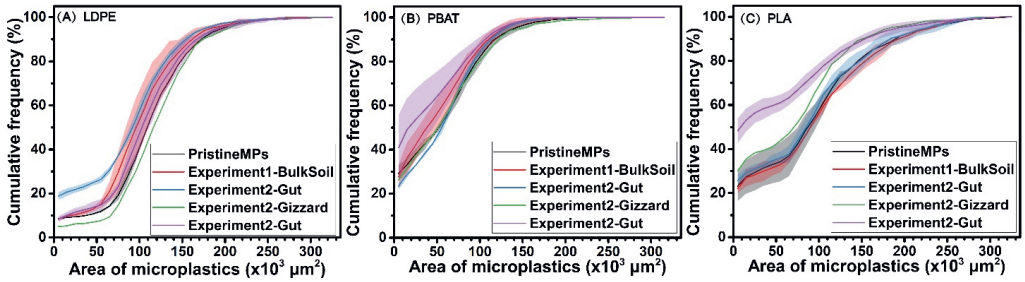

Figure S2.4 Cumulative size distributions of LDPE, PBAT, and PLA microplastics in different samples in Experiment 1 and 2. Distributions of PristineMPs in all treatments and Experiment2-Gut in the LDPE treatment were generated from duplicate measurements. Distributions of Experoment2-Gizzard in all treatments were generated from one pooled sample (one measurement). Other distributions were generated from triplicate measurements. The area above and under the curve represents standard deviations.

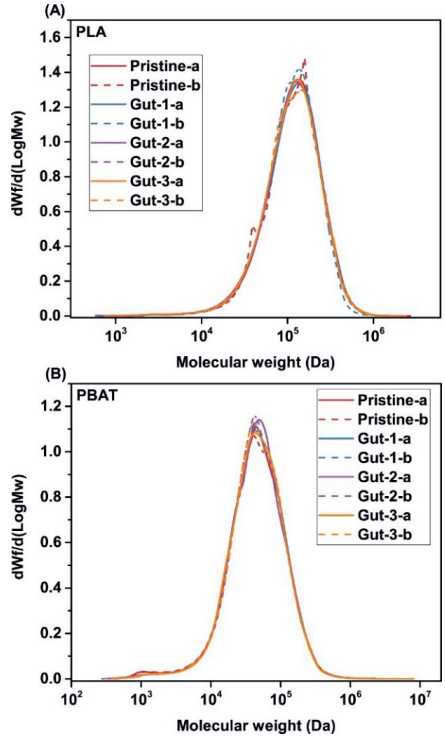

Figure S2.5 GPC molecular weight distribution (MWD) curves of PLA and PBAT microplastics in experiment 2. The term 'pristine' represents pristine microplastics used for the experiment, and 'gut' represents microplastics recovered from the worm gut. Triplicate gut samples were measured and duplicate analysis (-a and -b) was performed for each sample.

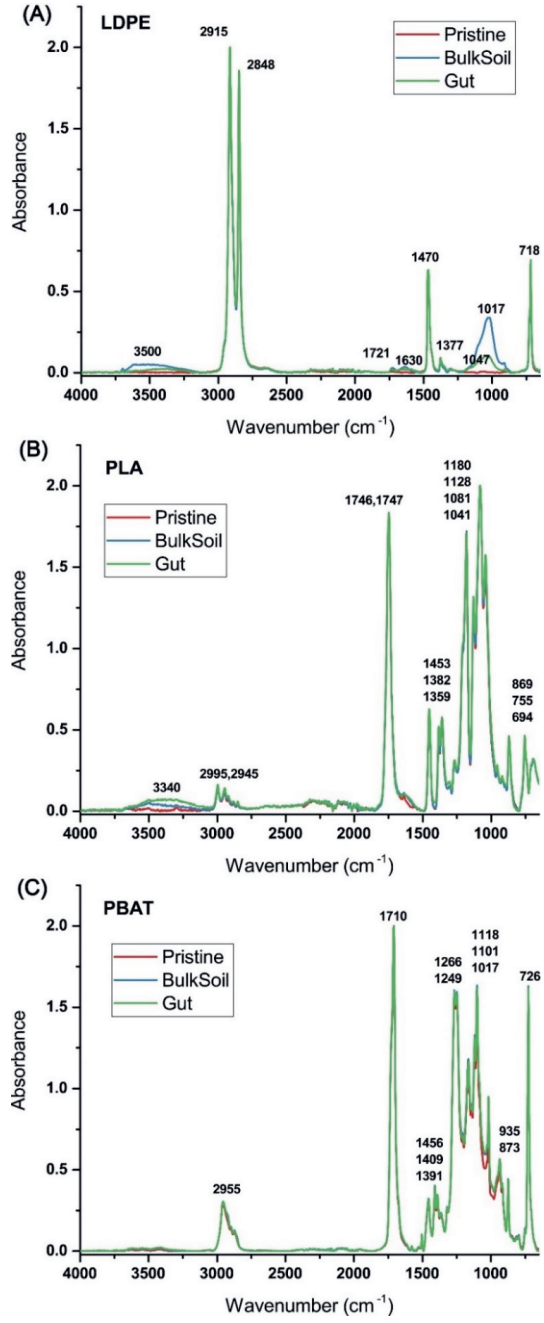

Figure S2.6 Infrared spectra of (A) LDPE, (B) PLA and (C) PBAT microplastics in different samples in Experiment 1.

3. Fate of microplastics during the aging of earthworm casts: immobilization and degradation

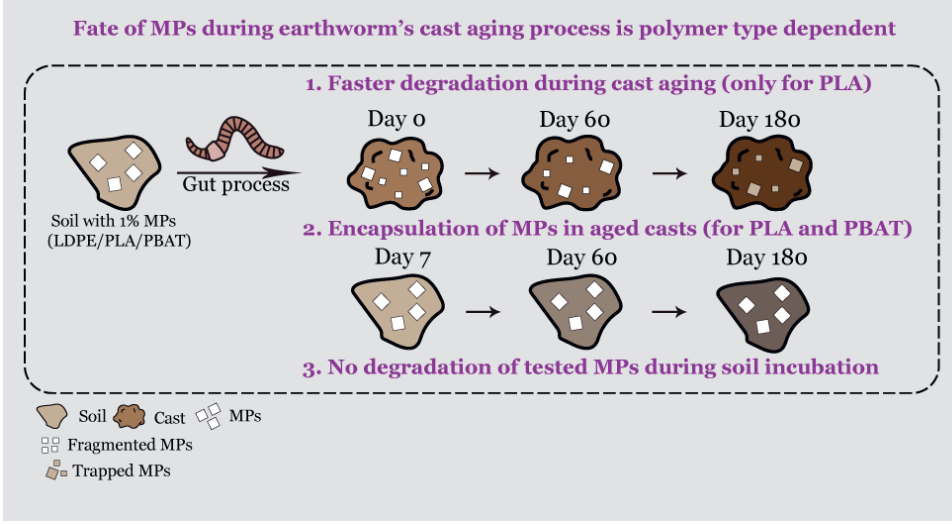

Based on:

Meng, K., Van der Zee, M., Munhoz, D. R., Lwanga, E. H. & Geissen, V. Fate of microplastics during the aging of earthworm casts: immobilization and degradation. (To be submitted)

Abstract

Revealing the fate of microplastics (MPs) in soils is crucial for assessing their potential risks and providing information to guide countermeasures. Here, the fate of low-density polyethylene (LDPE), polylactic acid (PLA) and polybutylene adipate terephthalate (PBAT) MPs during earthworm's cast aging process was explored under controlled lab conditions at a microcosm scale. MPs (residual polymers) were extracted and quantified by two approaches: 1) density separation followed by gravimetric quantification (for all MPs). 2) Soxhlet extraction followed by proton nuclear magnetic resonance quantification (for residual PLA and PBAT polymers). We tracked the MPs' concentrations, size distributions, molecular weight distributions, chemical composition, and thermodynamic properties during the 180-day aging. Results show that the fate of MPs during the cast aging process depends on polymer types. LDPE MPs stayed almost unaffected, while two phenomena were observed for biodegradable MPs: one is faster degradation than in the soil (for PLA MPs only); The other is immobilization of MPs in aged casts, which led to declined recovery performance by the density separation method. Our findings underlined the importance of combining different approaches to quantify and characterize MPs in complicated matrices. Following the gut, the earthworm's cast is another microenvironment where the degradation of certain polymers could be enhanced. However, the potential release of gut-generated secondary MPs after cast disintegration and polymer-specific degradation remain as challenges for MPs bioremediation with earthworms in soils.

3.1 Introduction

The presence of microplastics (MPs) has been widely reported in different environmental matrices (Wang et al., 2021), and the soil ecosystem has lately received increasing attention as it represents a major sink for MPs (Guo et al., 2020). Understanding the fate of MPs during various soil biological processes is the foundation for assessing their potential risks to the soil ecosystem, providing key information to guide soil restoration, hazard prevention and other countermeasures. It has been reported that MPs could be transported by soil macrofauna-related activities, including ingestion, excretion, etc.(Huerta Lwanga et al., 2017a; Heinze et al., 2021). And the drilling, rasping, and grinding activities of soil macrofauna could lead to MPs fragmentation and even certain levels of degradation (Wang et al., 2022; Adhikari et al., 2023; Meng et al., 2023a; Rambacher et al., 2023). The byproducts of these biological processes, such as smaller-sized particles and metabolites of biodegradation could be uptaken by edible plants(Luo et al., 2022) or create nutrient hotspot that affect the soil microbial community (Song et al., 2023).

The interactions between MPs and soil invertebrates, especially earthworms, have been investigated recently (Huerta Lwanga et al., 2016, 2017b; Wang et al., 2022; Adhikari et al., 2023; Ju et al., 2023; Meng et al., 2023a). Most studies have focused on the transport, ingestion, and casting processes. Little information is available about the fate of MPs during the aging of the earthworm's cast, which is crucial for completing a holistic picture of MPs' journey during the soil–earthworm gut–cast–soil cycle. Studies on earthworm ecology have reported that the half-life of earthworm casts deposited on the soil surface could last from 2 months to > 1 year, depending on the ecosystem type (Decaëns, 2000; Bottinelli et al., 2020). These casts will eventually disintegrate and become part of the soil due to natural weathering and animal activities. Considering the large amounts of casts earthworms produce under field conditions (Blouin et al., 2013), the incorporation of aged casts back into the soil can be a significant input of nutrients, microbes, and gut-processed and aged contaminants. The earthworm cast differs from the soil since significant microbiological processes occur during the aging process, which synchronizes with drastic changes in the physiochemical properties as well as microbial community composition (Mariani et al., 2007; Aira et al., 2019). Therefore, it is highly possible that MPs in the aging cast would experience varied changes compared to the soil.

Our previous work shed light on the physical fragmentation and chemical depolymerization of MPs derived from certain polymer types, i.e. low-density polyethylene (LDPE), polylactic acid (PLA) and polybutylene adipate terephthalate (PBAT) in the earthworm gut (Meng et al., 2023a). On this basis, we also raised the question of the potential of using earthworms for the bioremediation of MPs-contaminated soils. However, the fate of gut-processed MPs in the cast remains unknown, which is not only of great environmental significance but also relevant for evaluating the feasibility and potential consequences of the proposed bioremediation strategy.

In the current study, we present one of the first attempts to reveal the fate of MPs (both non-biodegradable and biodegradable) during the cast aging process, with more focus on biodegradable MPs since they are being promoted to replace non-biodegradable plastics in

agricultural production. The study was carried out under controlled lab conditions at a microcosm scale which simulates the aging of earthworm casts deposited on the soil surface. MPs (residual polymers), when applicable, were recovered and quantified by two extraction–quantification approaches based on different principles to ensure reliable MPs contents. The physicochemical properties of MPs during the cast aging process were characterized by multiple techniques to help explain the potential mechanisms associated with the fate of MPs. Our hypotheses are that i) the fate of MPs during the cast aging process could be polymer type dependent. ii) Biodegradable MPs could undergo a secondary degradation in the cast following the primary degradation caused by the gut process.

3.2 Materials and methods

3.2.1 Materials and experimental design

MPs-free soil was collected from the field at Unifarm, Wageningen University & Research (the Netherlands). The collected soil was air-dried before the removal of plant residues and impurities. The soil was sieved through a 2 mm mesh size before use. The soil was comprised of 3.2% clay, 50.0 % silt, 46.8% sand (sandy loam), with 3.8% organic matter (loss on ignition) and a pH of 6.2 (water extraction). *Lumbricus terrestris*, a widespread anecic species that typically produces its casts on the soil surface, was selected for the experiment. Adult worms with a clear clitellum and similar body weights (4.03 ± 0.12 g, n = 48) were selected for the experiment. All worms were purged in the dark for 48 h prior to the experiment.

The following three polymers from different categories were used for the experiment: 1), fossil-based non-biodegradable LDPE (Dow™ LDPE 310E), 2) bio-based compostable PLA (NatureWorks® Ingeo™ Biopolymer 2003D), and 3) fossil-based biodegradable (in soil) PBAT (Ecoflex® F Blend C1200). Pellets (clean and additive-free) were soaked in liquid nitrogen for 10 seconds before being fed into an ultra-centrifugal mill (ZM200, Retsch GmbH) together with liquid nitrogen. A ring sieve with a trapezoid hole size of 1.5 mm was used for the cryogenic fragmentation at 14,000 rpm. Fragments passing through the ring sieve were collected and screened with metal sieves (212 µm and 350 µm). The fraction remaining between the two sieves was collected for the experiment. The produced MPs showed different size distribution patterns due to distinctive polymer properties (Fig S3.1). The average sizes of prepared pristine MPs were 419 ± 160 µm for LDPE, 465 ± 107 µm for PLA, and 338 ± 215 µm for PBAT. On this basis, four treatments were established for the experiment: Control (MPs-free soil), LDPE, PLA, and PBAT (soil spiked with 1% of corresponding MPs, dw/dw).

3.2.2 Cast production

For the ease of generating and collecting uniform casts, glass Petri Dishes (⌀120 mm × 20 mm) were used as cast production units (CPUs, Photo S3.1). 50 g of clean soil or MPs-containing soil were thoroughly mixed in sealed glass jars and then transferred into the

CPUs. The soil moisture was adjusted to 25% with distilled water. In total, 24 units were established (6 units per treatment). All CPUs were pre-incubated for 7 days in the dark at 16 °C. Approximately 3.0 g of soil was collected from each CPU as soil incubated for 7 days (S7) before 2 worms were added into each CPU. The initial weight of worms in each unit was 8.05 ± 0.24 g (n = 24) and there was no significant difference between treatments ($p > 0.05$, one-way ANOVA). The cast production was carried out at 16 °C in the dark for 6 days. Every 24 h, freshly produced casts (< 1 day old) were carefully collected and weighed. Special attention was paid during the cast collection so that the intactness of the cast was maintained. Most fresh casts were immediately transferred into the cast aging units (CAUs) while a small portion was directly sampled as fresh casts (C0). As a result, the C0 samples were pooled from the 6-day cast production. After 6 days, worms were collected, rinsed with distilled water, and dried with paper tissue before recording their final weights (containing gut contents). Collected worms were kept at –20 °C for other purposes.

3.2.3 Cast aging

The aging of cast was carried out in straight specimen containers (30 mL, polypropylene) (CAUs, Photo S3.1). The CAUs were filled with 20 g of dry clean soil and a piece of cotton gauze was carefully placed on top of the soil. The water content was adjusted to 25% with distilled water. The cotton gauze was used to help separate aged casts from the soil during sampling. All CAUs were pre-incubated at 16 °C in the dark for 7 days before use. After being filled with fresh casts, the CAUs were covered with lid and sealed with parafilm to avoid excessive evaporation while keeping air exchange. For each treatment, the cast aging was performed for 15 days (C15), 60 days (C60) and 180 days (C180). While for each time point, 6 units were established with at least 3 g casts each. MPs were also incubated in the soil for 60 days (S60) and 180 days (S180) under the same settings to function as a reference for the potential MPs content changes during the cast aging process. In summary, 7 niches were defined in the experiment, which are S7, S60, S180, C0, C15, C60 and C180.

3.2.4 Sampling and extraction of microplastics

Samples (soil and cast) were collected with metal tweezers and spatula and a subset (~1.5 g) was immediately stored in Eppendorf microcentrifuge tubes (2 mL) at –80 °C (for the extraction of nucleic acids for other purposes). The rest was divided into two portions: one was kept at –20 °C for freeze drying and subsequent Soxhlet extraction, while the other was dried in the oven at 40 °C for 48 h for the extraction with density solutions.

MPs were firstly determined in all samples following a density separation method (hereafter abbreviated as DS) as described by Meng et al.(2023a). To ensure minimal influence caused by the extraction process, samples were not grinded or crushed before extraction to avoid man-made fragmentation of MPs and digestion was not applied since biodegradable plastics can be fragile against common digestion reagents. Detailed extraction procedures are available in Text S3.1. Briefly, 70% ethanol solution (density: ~0.88 g cm^{-3}) and distilled water (density: ~1.0 g cm^{-3}) were used for extracting LDPE MPs. For PLA and PBAT MPs, distilled water and sodium dihydrogen phosphate (NaH_2PO_4)

solution (density: ~1.30 g cm^{-3}) were used. The spike–recovery rate of this method verified with soil is 103.9 ± 4.6% for LDPE MPs, 102.2 ± 2.1% for PLA MPs and 104.0 ± 2.9% for PBAT MPs respectively (Meng et al., 2023a). However, after noticing the difficulty of extracting MPs from aged casts (Text S3.2), we guaranteed higher recovery performance by conducting additional extraction for aged samples (S60, S180, C15, C60, and C180). We used an unsaturated sodium chloride (NaCl) solution (density ~1.13 g cm^{-3}) for LDPE MPs, and a NaH_2PO_4 solution with an increased density (~1.36 g cm^{-3}) for both PLA and PBAT MPs. The content of MPs (C_{MP}) quantified by the DS method was calculated as follows:

(Eq 1):

$$C_{MP} = \frac{m_r}{m_s} \cdot 100\%$$

where m_r is the mass of the recovered MPs or polymers, and m_s is the mass of sample.

3.2.5 Identification of microplastics with LDIR

A Lazer Direct Infrared Chemical Imaging system (LDIR) was used to identify and distinguish recovered MPs from impurities and measure the particle size (i.e. diameter and area). Recoveries from section 3.2.4 were re-suspended with 0.5 mL 96% ethanol solution and treated with an ultrasonic bath for up to 30 s. The suspension was carefully transferred onto an infrared-reflective glass slide (7.5 × 2.5 cm; MirrIR, Kevley Technologies) using Pasteur pipets. Particle aggregates, whichever were visually distinguishable, were dispersed manually using a dissecting needle. Air dried slides were analyzed on the Agilent 8700 LDIR with the 'Particle Analysis' method. As the LDIR uses a quantum cascading laser (QCL) IR source (wavenumber 1800–900 cm^{-1}) and works in a transflectence mode, IR spectra obtained by LDIR can be different from ATR-FTIR or micro-FTIR depending on the particle size and shape. To ensure the accuracy of MPs identification, the spectra of pristine LDPE, PLA and PBAT MPs with different sizes were obtained by LDIR and added to the library. Representative spectra are available in Fig S3.2. Tests with pristine MPs showed that by setting the hit quality score at > 0.8 a recovery rate of 94.75% for LDPE, 98.02% for PBAT, and 98.73% for PLA could be achieved. Therefore, only matches with a hit quality score > 0.8 were considered valid and used to generate the MPs size distribution. For S7, C0, C60 and C180, recoveries from two independent replicates were measured on LDIR, and the MPs size distribution was pooled from the duplicate measurements.

3.2.6 Extraction of PLA and PBAT with Soxhlet extraction and quantification by q–^{1}HNMR

The contents of residual PLA and PBAT were also quantified following a novel approach (Nelson et al., 2020), where the Soxhlet extraction and quantitative proton nuclear magnetic resonance (q–^{1}HNMR) spectroscopy were combined to quantify residual PLA and PBAT in soils (hereafter abbreviated as Sox-NMR). Since this study is the first to apply such a technique to assess MPs in earthworm cast, a few modifications were made to suit

our set-up. Briefly, freeze-dried samples were gently crushed with glass rods and accurately weighed samples (~1.5 g) were transferred into extraction thimbles (⌀19 mm × 90 mm). Soxhlet extraction was carried out in extractors (30 mL) and heated in water bath. The procedures were as follows: impurities were first reduced by washing with 50 mL methanol (99.9%, HPLC grade) for 45 min. Then 50 mL of chloroform (99+%)–methanol mixture (9:1, v/v) was used to extract polymers for 70 min. After evaporation, solvent reconstitution was performed with 3 mL internal standard solution composed of deuterated chloroform (99.8% atom D) with a known amount of 1,4-dimethoxybenzene (DMB, internal standard). Extracts were fully dissolved in the internal standard solution in an ultrasonic bath, and stored in chromatography vials (4 mL, amber glass) at 4 °C before being transferred to NMR tubes for further analysis. NMR experiments were conducted on a standard-bore 700 MHz NMR spectrometer (Bruker), equipped with a 5 mm broadband inverse (BBI) probe. 1D 1H experiment with 30-degree flip angle was performed on each sample at 300 K. The number of scans was 128 in each experiment, with an inter-scan delay of 15 s. Acquisition time was 4 s. Spectra were processed and analyzed using MestReNova software.

For PBAT quantification (Fig S3.3), peaks at 8.09 ppm (4 aryl protons in the terephthalate monomer in PBAT, $I_{T\ 8.09\ ppm}$), 6.84 ppm (4 aryl protons in DMB, $I_{DMB\ 6.84\ ppm}$), 4.40 ppm (4 alpha protons of butanediol adjacent to terephthalate in PBAT, $I_{BT\ 4.40\ ppm}$), 4.12 ppm (4 alpha protons of butanediol adjacent to adipate in PBAT, $I_{BA\ 4.12\ ppm}$) and 3.78 ppm (6 protons of methyl group in DMB, $I_{DMB\ 3.78\ ppm}$) were manually integrated. The faction of butanediol–terephthalate repeat unit (BT, f_{BT}) and butanediol–adipate repeat unit (BA, f_{BA}) in the PBAT were calculated as follows:

(Eq 2):

$$f_{BT} = \frac{I_{BT\ 4.40\ ppm}}{I_{BT\ 4.40\ ppm} + I_{BA\ 4.12\ ppm}}$$

(Eq 3):

$$f_{BA} = \frac{I_{BA\ 4.12\ ppm}}{I_{BT\ 4.40\ ppm} + I_{BA\ 4.12\ ppm}}$$

The average PBAT molecular weight ($\overline{M_{PBAT}}$) is calculated as follows:

(Eq 4):

$$\overline{M_{PBAT}} = f_{BT} \cdot M_{BT} + f_{BA} \cdot M_{BA}$$

where M_{BT} and M_{BA} are the molecular weights of repeat unit BT (220.22 g mol^{-1}) and repeat unit BA (200.23 g mol^{-1}) in PBAT. The mass of residual PBAT polymers in the final extract was calculated as follows:

(Eq 5):

$$m_{PBAT} = \frac{I_{T\ 8.09\ ppm}}{I_{DMB\ 6.84\ ppm}} \cdot \frac{N_{T\ 8.09\ ppm}}{N_{DMB\ 6.84\ ppm} \cdot f_{BT}} \cdot \frac{\overline{M_{PBAT}}}{M_{DMB}} \cdot m_{DMB}$$

Where $N_{T\ 8.09\ ppm}$ is the number of protons belonging to the peak at 8.09 ppm, and $N_{DMB\ 6.84\ ppm}$ is the number of protons belonging to the peak at 6.84 ppm. M_{DMB} is the molecular weight of DMB (138.17 g mol^{-1}), and m_{DMB} (mg) is the mass of DMB in the 3

mL final extract.

For PLA quantification (Fig S3.3), peaks at 6.84 ppm (4 aryl protons in DMB, $I_{DMB\ 6.84\ ppm}$), 5.17 ppm (1 proton of –CH in PLA, $I_{PLA\ 5.17\ ppm}$) and 3.78 ppm (6 protons of methyl group in DMB, $I_{DMB\ 3.78\ ppm}$) were manually integrated. The mass of PLA (m_{PLA}) was calculated as follows:

(Eq 6):

$$m_{PLA} = \frac{I_{PLA\ 5.17\ ppm}}{I_{DMB\ 6.84\ ppm}} \cdot \frac{N_{PLA\ 5.17\ ppm}}{N_{DMB\ 6.84\ ppm}} \cdot \frac{M_{PLA}}{M_{DMB}} \cdot m_{DMB}$$

where M_{PLA} is the molecular weight of repeat unit of PLA (72.06 g mol^{-1}), $N_{PLA\ 5.17\ ppm}$ is the number of protons belonging to the peak at 5.17 ppm. The contents of PLA and PBAT in soils and casts were calculated by substituting m_{PLA} and m_{PBAT} into m_r in equation 1.

A spike–recovery test for PLA and PBAT MPs using MPs-free fresh casts was first conducted to validate the applicability of this method on the earthworm cast. The recovery rates for PLA were 89.2 ± 2.9% (nominal concentration at ~1%, w/w) to 91.3 ± 7.7% (nominal concentration at ~0.1%, w/w), and 93.0 ± 1.4% (nominal concentration at ~1%, w/w) to 89.8 ± 6.2% (nominal concentration at ~0.1%, w/w) for PBAT (Table S3.1). The background noise from the matrixes (MPs-free soil and casts) was negligible (Fig S3.3).

3.2.7 Characterization of microplastics

All pristine and recovered MPs were subjected to a cleaning procedure (Text S3.3) before further analyses. For PLA and PBAT, the weight-average molecular weight (M_w), number-average molecular weight (M_n), Z-average molecular weight (M_z), and polydispersity index (PDI = M_w/M_n) were generated from the molecular weight distributions (MWDs) measured by Gel Permeation Chromatography (GPC). The GPC measurements are described in Text S3.4. PLA and PBAT MPs recovered by the DS method from S7, C0, C15, C60, and C180 were measured to study the changes in their molecular weights during the cast aging process. In addition, the extracts of C0 and C180 by the Soxhlet extraction were dried and subjected to GPC analysis, by which we aimed to verify whether PLA and PBAT MPs recovered by different methods possess different molecular weights.

The thermodynamic properties of recovered MPs, e.g., crystallinity and melting temperature (T_m) were measured with a differential scanning calorimetry (DSC) (Perkin Elmer DSC 8000) which was cooled by a liquid nitrogen cooling system. Large volume (60 µL) stainless steel cups were used to hold the sample and used as a reference. Samples were taken as they were and placed into a stainless-steel cup and then hermetically sealed. Samples were first held at 0 °C for 3 min and heated to 250 °C at a rate of 10 °C min^{-1}. The degree of crystallinity (X) was calculated as follows:

(Eq 7)

$$X = \frac{\Delta H_m - \Delta H_{cc}}{\Delta H_0} \times 100\%$$

where ΔH_m is the melting enthalpy (J g^{-1}), ΔH_{cc} is the cold crystallization enthalpy (J g^{-1}), and the ΔH_0 is the theoretical melting enthalpy of a 100% crystallized material (J g^{-1}). The ΔH_0 equals to 293 J g^{-1} for LDPE (Poh et al., 2022), 93 J g^{-1} for PLA (Greco and Ferrari, 2021), and 114 J g^{-1} for PBAT (Bianchi et al., 2023).

Chemical compositions were measured with a Fourier transform infrared spectroscopy with an attenuated total reflectance accessory (FTIR-ATR, Agilent Cary 630). The spectra were measured within a range of 650 to 4000 cm^{-1}, with 32 scans for the background and 64 scans for the samples. A resolution of 2 cm^{-1} was applied. Samples were measured in duplicate to generate an average spectrum. For PLA and PBAT, the MPs recovered by the DS method were also characterized by ^{1}H–NMR with the same settings mentioned above.

3.2.8 Statistical analysis

The normality of data was tested with the Shapiro–Wilk test. Data following normal distribution were subjected to a one-way analysis of variance (ANOVA) test to study significant differences between values of different treatments. Levene's test was used to test the homogeneity of variance. Duncan's test (for equal variance) and Games-Howell test (for unequal variance) were utilized to conduct the post hoc test. Data not following normal distribution was subjected to a non-parametric test to study if the distributions were different between treatments. The significant level was set as 0.05.

3.3 Results and discussion

3.3.1 Effects of microplastics on the earthworm's growth and cast production

No mortality was observed during the 6-day cast production. Although gut purging was not conducted after the cast production—worms were dissected for other purposes—it is still possible to calculate a gross growth rate assuming that earthworms with similar body weights share similar mass of gut contents (Fig 3.1A), especially when the initial earthworm body weights were highly uniform (CV = 0.03). By the end of the cast production, the average final body weights increased by 34.3–39.0%, and there was no significant difference between the growth rates in different treatments ($p > 0.05$, ANOVA). The average cast productivity was 0.47–0.51 g g^{-1} worm d^{-1} for different treatments and not significantly affected by the MPs addition (Fig 3.1B). Earthworms in general survive well under low to moderate dosages of MPs, a finding also reported by other studies (Adhikari et al., 2023; Holzinger et al., 2023; Meng et al., 2023a). The daily cast production seemed to show a trend where the cast production was slightly higher on day 6, especially for MPs-spiked treatments (Fig 3.1C). However, such difference was not significant ($p > 0.05$, Kruskal–Wallis test). In a previous study, researchers found that the pre-acclimation of earthworms led to slightly higher cast production during the first 7 days of exposure to pesticide Epoxiconazole (Givaudan et al., 2014). Such phenomenon might also be accountable for our experiment, where the acclimation of earthworms to new experimental

units and MPs led to higher cast production in the late stage.

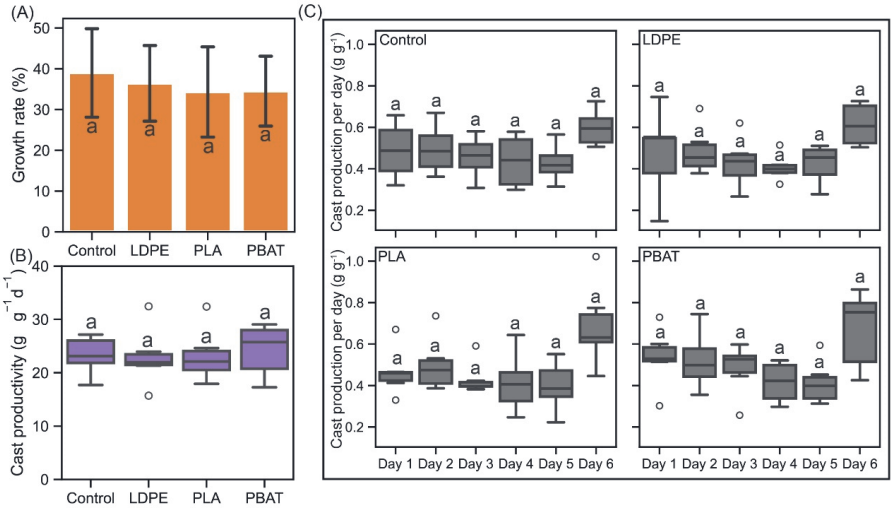

Figure 3.1 (A) Growth rates after the 6-day cast production (calculated without gut purging). Error bars represent standard deviations (n = 6), significant difference was tested with one-way ANOVA and labeled with letters. (B) Total cast productivity of earthworms in different treatments (n = 6), tested with one-way ANOVA and labeled with letters. (C) Cast production rate recorded per day, significant difference was tested with Kruskal–Wallis test and labelled letters (n = 6).

3.3.2 Microplastic concentrations during the soil incubation and the cast aging process

MPs contents quantified by the DS method during the soil incubation (Fig 3.2, A, C & E) showed a shared pattern where MP contents slightly increased with increasing incubation time, and the contents in S180 were significantly higher than S7 for all plastic types ($p < 0.05$, one-way ANOVA). The contents of PLA and PBAT were also quantified by the Sox-NMR method (Fig 3.2, A&C). In general, results by the Sox-NMR method were slightly lower than corresponding values by the DS method (on average 70–90% of the latter, Table S3.2). Such pattern was likely to be associated with the different spike–recovery rates of different methods (89–93% for Sox-NMR and 102–104% for DS). There was no significant difference between MP contents (Sox-NMR results) incubated for different periods in soil ($p > 0.05$, one-way ANOVA). For C0, the MP contents quantified by the DS method were 0.98 ± 0.24% (LDPE), 0.86 ± 0.09% (PLA) and 0.87 ± 0.14% (PBAT), and the corresponding Sox-NMR results were 0.93 ± 0.22% and 0.88 ± 0.11%, respectively. Comparing S7 and C0, neither method showed enrichment or depletion of MPs after the gut passage ($p > 0.05$, Student's t-test).

Despite the slightly different MP contents obtained for the same niche by the tested

methods, both showed that MP contents did not decrease after the 180-day incubation in the tested soil. Several reasons might explain the slightly higher MP contents in S180 than

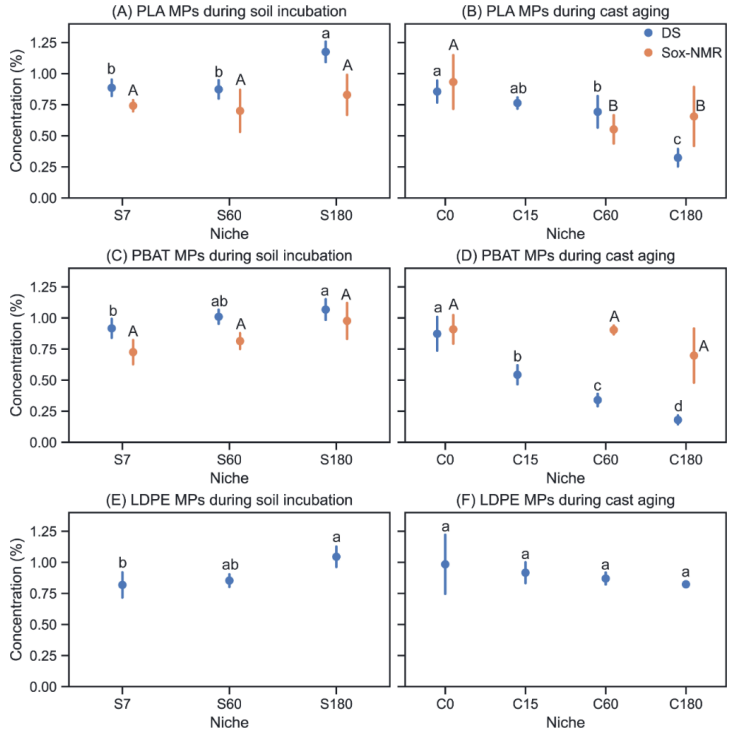

Figure 3.2 Microplastic concentrations in different niches quantified by the DS method (blue) and the Sox-NMR method (orange). (A, C, E) microplastic concentrations in soils incubated for 7 (S7), 60 (S60) and 180 (S180) days. (B, D, F) microplastic concentrations in casts aged for 0 (C0), 15 (C15), 60 (C60) and 180 (C180) days. Data displayed as mean ± standard deviations. Significant differences between different niches were compared within the same quantification method and labeled with lowercase letters (for DS) and uppercase letters (for Sox-NMR), respectively (one-way ANOVA). Graphs are based on n = 5–7 for S7 and C0, n = 3–4 for S60, S180, C15, C60 and C180 (DS method); And n = 3 for S7, S60 and S180, n = 4–6 for C0, C60 and C180 (Sox-NMR method).

S7 and S60 by the DS method. One possible reason could be the forming of biofilms and organic matter on the MP surface, which increased the mass of the final recovery. Another possible reason could be the permeation of water molecules into the polymer bulk, which is especially possible for the case of PLA and PBAT due to their higher hydrophilicities. Previous studies have shown that PLA could absorb considerable amounts of water when exposed to moist environments (Von Burkersroda et al., 2002). For example, one study reported that PLA could absorb water that take up 16% (w/w) of the initial mass (Moliner et al., 2020). Currently, PLA, PBAT, and their blends are promoted as biodegradable plastics for agricultural production. Although their biodegradability has indeed been

validated under certain conditions (Zumstein et al., 2018), many studies under realistic soil conditions have shown that products (commercial or lab-prepared, films or others) made from these polymers can also last longer than expected in soils (Sintim et al., 2020; Liao and Chen, 2021; Meng et al., 2023b; Slezak et al., 2023), which suggests that the biodegradability of a polymer not only depends on the intrinsic property, but also on the soil environment it is exposed to (Han et al., 2021).

Both methods showed that the tested MPs did not accumulate in the fresh cast. Studies where earthworms were supplied with MP-spiked litter besides the clean soil have reported that MPs were enriched in the casts (Huerta Lwanga et al., 2016; Adhikari et al., 2023). On the other hand, another study using similar feeding strategies to our study—providing earthworms with MP-spiked soil—reported no bioaccumulation of MPs in the cast (Rezaei Rashti et al., 2023). Earthworms could actively ingest sands to facilitate the fragmentation of leaf litter (Schulmann and Tiunov, 1999), hence MPs spiked in the litter could serve as substitutes for the sands, which are actively selected. The diet also plays a role since leaf litter is rich in organic matter while soil in general contains much less. Curry and Schimidt (2007) summarized that earthworm assimilation efficiencies of soils are usually < 2.5%, while earthworm assimilation efficiencies of leaf litter can reach 30–70% depending on the earthworm species and leaf types. These together could highlight the influence of diet and experimental settings on MP concentrations in the casts.

Even though both methods showed an identical trend in S7 and C0, divergent patterns were observed for aged casts (Fig 3.2, B&D). DS results showed that the MP contents in the cast declined significantly after 60 days for PLA and after 15 days for PBAT, whereas the contents of LDPE MPs remained stable throughout the 180-day aging process. For PLA, the MP contents in the cast decreased from 0.86 ± 0.09% on day 0 to 0.69 ± 0.13% on day 60 and finally reached 0.32 ± 0.07% by day 180 ($p < 0.05$, one-way ANOVA). For PBAT, the MP content decreased only after 15 days from 0.87 ± 0.14% to 0.54 ± 0.08%, which was followed by a further reduction to 0.18 ± 0.04% by day 180 ($p < 0.05$, one-way ANOVA). For LDPE, there seemed to be a declination with increasing aging time, but such difference was not significant ($p > 0.05$, one-way ANOVA). The Sox-NMR results showed that the PLA concentrations in C60 (0.55 ± 0.11%) and C180 (0.66 ± 0.24%) were significantly lower than that in C0 (0.93 ± 0.22%) ($p < 0.05$, one-way ANOVA). However, such reduction was not as evident as the values reported by the DS method. For PBAT, the Sox-NMR results of C0 and C60 were 0.88 ± 0.11% and 0.88 ± 0.04%, respectively. Despite a slight reduction in the average value, the MP content of C180 (0.69 ± 0.21%) was not statistically different from C0 and C60 ($p > 0.05$, one-way ANOVA), which conflicts with the findings by the DS method. Therefore, the size distributions, chemical compositions, molecular weight changes and thermodynamic properties of MPs during the cast aging process were studied to fill the gap between the two methods.

3.3.3 Size distributions of recoverable microplastics during the cast aging process

The size distributions of MPs recovered by the DS method are shown in Fig 3.3. The size

distributions of the two independent measurements are highly consistent (Fig S3.4). For LDPE MPs, the first quartile (Q1), median (Q2) and third quartile (Q3) of the distribution in general stayed stable from S7 to C180, except a minor shifting in C60 where the Q1 and median of C60 slightly declined to 74 µm and 312 µm, respectively.

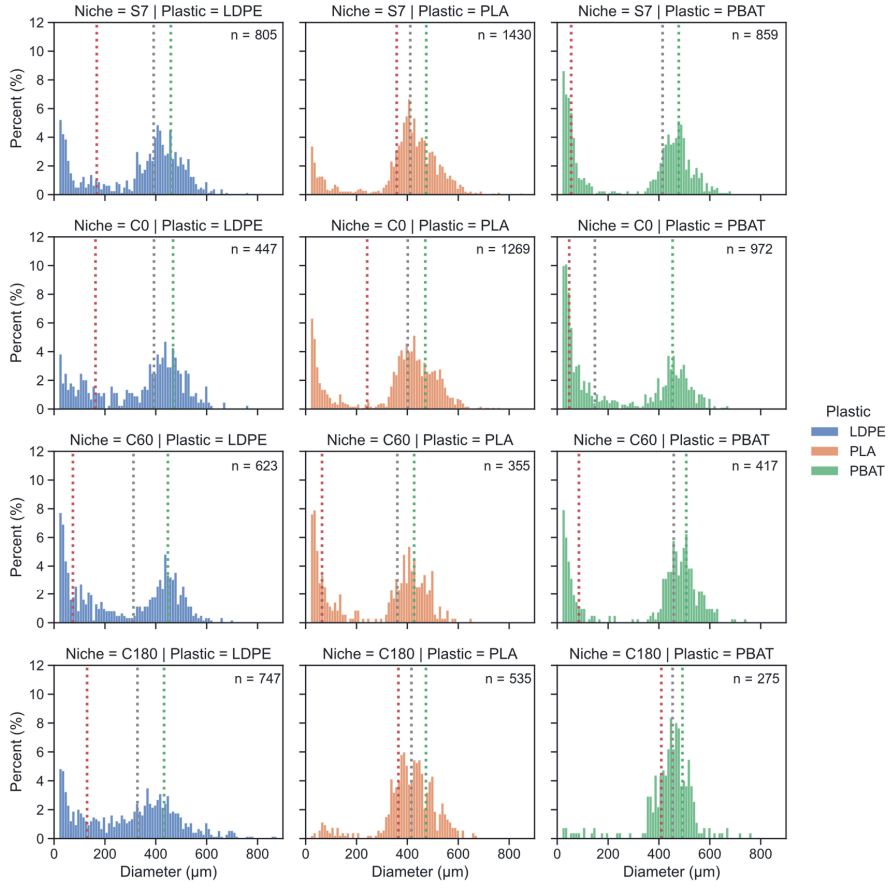

Figure 3.3 Size distributions of microplastics recovered from different niches (S7, C0, C60 and C180) by the DS method. Graphs in the same column are from the same treatment (plastic type), graphs in the same row are from the same niche. Red, grey, and green vertical dot lines in each graph show the 25% (Q1), 50% (Q2/median) and 75% (Q3) quantile of the distribution. All distributions were pooled (n particles) from two independent measurements.

The Q1, median and Q3 of PLA MPs size distribution in S7 were 358 µm, 412 µm and 474 µm, respectively. After the gut process, the Q1 of C0 significantly declined to 242 µm, while the median and Q3 stayed almost unchanged (402 µm and 470 µm). After 60 days of aging the Q1 of C60 declined drastically to 65 µm, accompanied by the shifting of median and Q3 to smaller sizes (361 µm and 427 µm). C180 denoted a noteworthy pattern, where the Q1, median, and Q3 recovered to 365 µm, 416 µm, and 473 µm, respectively. Tracking PLA

MPs size distributions in different niches, we found significantly more small-sized particles (< 150 µm) in C0, and this trend was further enhanced for C60. However, the small particles (< 150 µm) finally disappeared in C180.

For PBAT MPs, the Q1, median and Q3 of the size distribution in S7 were 55 µm, 415 µm and 478 µm, respectively. After the gut process, the Q1 and Q3 of C0 slightly declined to 47 µm and 454 µm, whereas the median of C0 significantly declined to 148 µm. The size distributions of recoverable PBAT MPs shifted to bigger sizes during the cast aging process. With the increase of aging time, Q1, median and Q3 shifted to 85 µm, 458 µm and 508 µm for C60 and 409 µm, 454 µm and 493 µm for C180. To summarize, we recovered much more small-sized PBAT MPs in the fresh cast compared to S7. However, during the aging of the cast, the small-sized MPs (< 150 µm) gradually disappeared in the size distribution.

3.3.4 Characterization of recoverable microplastics

Comparing pristine MPs, MPs recovered from S7 and aged casts, we did not find significant changes in the IR spectra (Fig 3.4). Some new peaks with low intensities around 1600–1700 cm^{-1} and 950–1150 cm^{-1} were observed in S7, C0 and C180 for LDPE MPs (Fig S3.5), which were corresponding to the C=O stretching and C–O–C stretching, respectively. These peaks were likely caused by the traced amount of organic matter residues on the MP surface. For PLA and PBAT MPs, no observable changes in the functional groups were found.

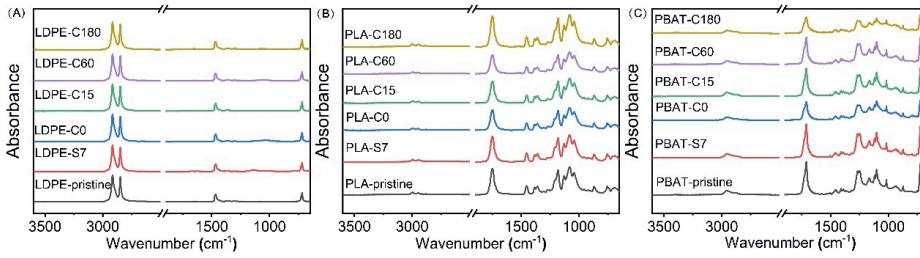

Figure 3.4 ATR-FTIR spectra of microplastics recovered from different niches by the DS method. The spectra of pristine samples were also provided as reference.

The molecular weight distributions of MPs recovered by the DS method were similar in different niches, a pattern found for both PLA and PBAT (Fig 3.5, A&C). The corresponding PDIs for PLA MPs and PBAT MPs were within the range of 1.8–2.2 and 2.0–2.3, respectively. The average molecular weights (M_n, M_w, M_z) also showed negligible difference between different niches (Table 3.1). The molecular weight distributions of PLA and PBAT recovered by Soxhlet extraction were also determined (Fig 3.5, B&D). As the Soxhlet extraction also recovered a certain level of impurities from the cast, and the peaks associated with impurities overlapped the area where small PLA and PBAT molecules might occur (retention volume 19–23 mL, Fig S3.6–S3.7), the molecular weights of PLA and PBAT fraction < 10,000 Da could not be calculated. Nevertheless, the chromatograms of the RI signal detector indicated that the ratio of PLA and PBAT molecules < 10,000 Da was negligible (Fig S3.8–S3.9). The average molecular weights (M_w) of C0 and C180 were

153 ± 4 kDa and 147 ± 1 kDa for PLA, and 60 ± 0 kDA and 60 ± 1 kDa for PBAT. In general, the GPC results of PLA and PBAT showed that recoveries from C0 and C180 by Soxhlet extraction presented almost the same molecular weight distribution.

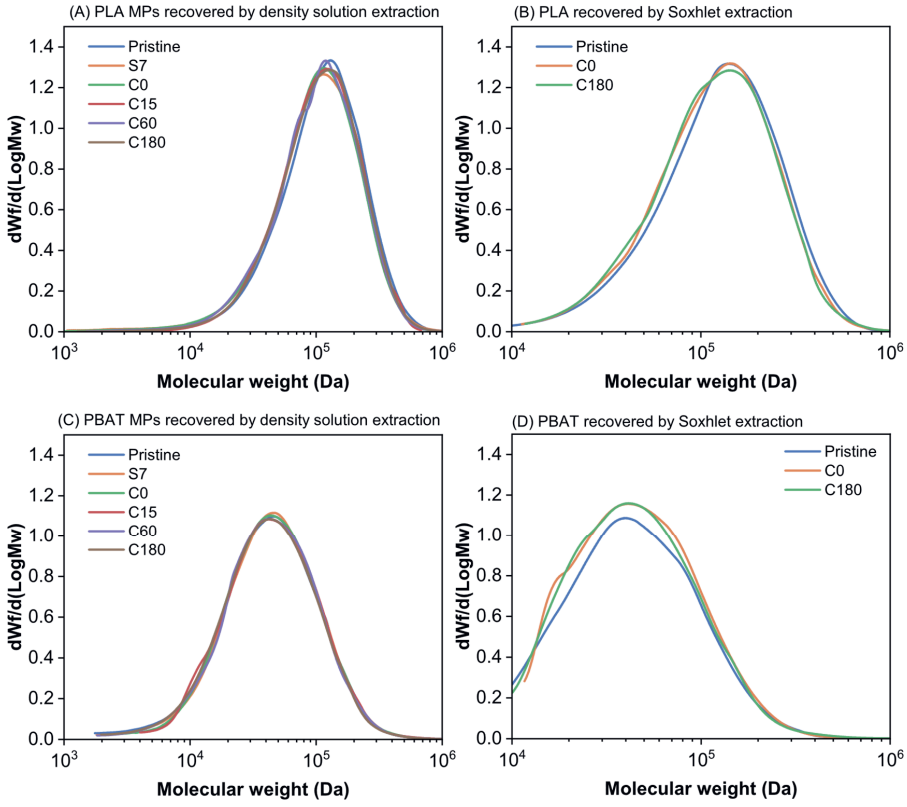

Figure 3.5 Molecular weight distributions of PLA and PBAT recovered by different methods. (A&C), PLA and PBAT MPs recovered by the DS method. (B&D), PLA and PBAT polymers recovered by the Soxhlet extraction. For samples recovered by Soxhlet extraction, data < 10,000 Da were not available due to the overlap of small PLA and PBAT molecules with impurities.

The thermodynamic properties of MPs characterized by DSC are shown in Table 3.2. For LDPE and PLA MPs, we did not find evident changes in the T_m and crystallinity between pristine MPs and MPs recovered from S7 or casts of different aging stages. The crystallinity of pristine PBAT MPs was around 24%, while for PBAT MPs recovered from S7 or casts of different aging stages, the crystallinities were slightly lower (14–19%). Comparing casts of different aging stages, we did not find a clear trend of crystallinity changes during the cast aging process for all MPs. There were some differences in the T_m of PBAT MPs, e.g., the T_m of C0 was much lower than others. However, as the melting peak of PBAT is usually flat and broad (multiple peaks could occur), such differences may not necessarily represent exact changes in the thermodynamic properties.

Table 3.1 Number average molecular weight (Mn, kDA), weight average molecular weight (Mw, kDA) and Z average molecular weight (Mz, kDA) of PLA and PBAT MPs recovered by the DS method. Results displayed as mean ± standard deviation (duplicate measurements).

Plastic	Niche	M_n (kDa)	M_w (kDa)	M_z (kDa)
PLA	Pristine	69 ± 14	141 ± 1	218 ± 0
	S7	60 ± 2	133 ± 1	211 ± 3
	C0	72 ± 18	131 ± 2	203 ± 5
	C15	74 ± 6	133 ± 1	204 ± 7
	C60	68 ± 1	132 ± 1	205 ± 1
	C180	72 ± 2	136 ± 1	212 ± 4
PBAT	Pristine	28 ± 1	62 ± 0	138 ± 4
	S7	28 ± 1	62 ± 0	130 ± 4
	C0	31 ± 1	63 ± 0	136 ± 4
	C15	31 ± 1	63 ± 0	131 ± 4
	C60	30 ± 1	62 ± 0	130 ± 11
	C180	26 ± 2	60 ± 1	126 ± 2

3.3.5 Fate of microplastics during earthworm's cast aging process

Zooming into the transition from S7 to C0, we found that PLA and PBAT MPs underwent some fragmentation (Fig 3.3), while their chemical compositions (Fig 3.4), molecular weights (Table 3.1), thermodynamic properties (Table 3.2), and concentrations in the niche did not change significantly. By contrast, LDPE MPs remained unaffected. Our previous study focusing on the gut environment of earthworms has found that PLA and PBAT MPs size distributions shifted to smaller sizes in the earthworm's gut, and PLA recovered from the gut contents even experienced slight depolymerization after a 35-day incubation (Meng et al., 2023a). Even though we did not find evident reduction in the molecular weights of PLA and PBAT in C0 in the current study, such discrepancy might be explained by the different incubation times (up to 6 days vs. up to 35 days) and target niches (gut vs. cast) applied in different experiments. Nevertheless, the results of both experiments implied that PLA and PBAT MPs could be fragmented during the passage through the earthworm's gut in a short time span (< 1 d), while a longer exposure is needed before depolymerization could happen in the gut. Fragmentation of MPs by the earthworm's gut activity has also been reported by others. PLA MPs could break down in the gut of *Eisenia fetida* (Wang et al., 2022), and PBAT MPs degraded to some extent in the gut of *Lumbricus terrestris* (Adhikari et al., 2023). Although we had found much more small-sized LDPE MPs in the earthworm's gut compared to the bulk soil in the previous work (Meng et al., 2023a), the size distribution of LDPE MPs in C0 did not differ significantly from S7 in the current study. Considering the different experimental settings in the two experiments, two reasons might explain the uncertain result for LDPE MPs. Firstly, it is possible that an adaptation period is needed before earthworms could establish the ability to break up LDPE MPs. It has been

reported that non-biodegradable MPs were more difficult to be broken up by the earthworm's intestine than bio-based MPs (Wang et al., 2022). Therefore, a longer acclimation to LDPE-spiked soil might lead to the establishment of stronger abrasion effects in the earthworm's gizzard. Secondly, there is also a possibility that LDPE MPs with different sizes have different elimination half-lifes from the gut. It might take longer for the fragmented small particles to be transported through the gut and excreted. Unfortunately, as the earthworms were dissected for other purposes, we were not able to verify this hypothesis.

Table 3.2 Melting point (T_m), melting enthalpy (ΔH_m) and crystallinity (X) of microplastics recovered from different niches by the DS method. Data for PBAT–C180 was not available due to insufficient samples.

Niche	LDPE			PLA			PBAT		
	T_m (°C)	ΔH_m (J g−1)	X (%)	T_m (°C)	ΔH_m (J g−1)	X (%)	T_m (°C)	ΔH_m (J g−1)	X (%)
pristine	114	127	43	153	36	39	128	27	24
S7	114	121	41	153	36	39	124	22	19
C0	115	127	43	152	35	37	107	22	19
C15	115	125	43	151	31	33	121	16	14
C60	115	126	43	152	34	36	124	20	18
C180	115	126	43	150	33	35	N.A.	N.A.	N.A.

Two phenomena can be summarized for the fate of the tested MPs during the cast aging process. The first is the faster degradation in the cast compared to soil, which was observed only for PLA MPs in the first 60 days. Based on the contents quantified by two different methods (Fig 3.2B), we speculate that PLA MPs underwent some degradation during the cast aging process (approx. 30–63% of concentration reduction in 60–180 days), whereas PLA MPs incubated in the soil did not show any concentration reduction by the tested methods after 180 days (Fig 3.2A). The molecular weight distributions of PLA recovered by both methods did not show significant changes during the cast aging process (Fig 3.5 & Table 3.1), indicating that PLA degradation in the cast followed a "surface erosion" mechanism, where the rate of water permeation (into the bulk material) does not exceed the rate of degradation on the material surface (Von Burkersroda et al., 2002; Haider et al., 2019). Therefore, the remaining materials stay unaffected. Such speculation was also supported by the fact that the ATR-FTIR spectra (Fig 3.3B) and ^{1}HNMR spectra (Fig S3.10) of PLA in aged casts did not differ from the fresh cast and the pristine sample. Furthermore, the size distribution of PLA MPs significantly shifted to smaller sizes from C0 to C60 (Fig 3.3), coinciding with the concentration reduction determined by both methods (Fig 3.2B). Therefore, it is highly possible that PLA MPs underwent further fragmentation during the degradation in the first 60 days. The release of smaller particles during plastic degradation has also been reported by many other studies (Sintim et al., 2019; Wei et al., 2021; Griffin-LaHue et al., 2022; Wohlleben et al., 2023; Zhang et al., 2023).

The second phenomenon is the immobilization of MPs in aged casts than soils, which was observed during C60–C180 for PLA MPs and C0–C180 for PBAT MPs (potentially also true for LDPE MPs, but the trend was not significant). Such phenomenon was characterized by

1) the contradictory trends of MPs concentrations determined by different methods (Fig 3.2), where the DS method could recover much fewer MPs (residual polymers) compared to the Sox-NMR method. 2) The molecular weight distributions and chemical compositions of extracts by both methods are the same (Fig 3.4 & Fig S3.11), and 3) the decrease of small-sized particles (< 150 μm) with increasing aging time. The particle area-weighted distribution (Fig S3.12) of PLA and PBAT MPs could to some extent reflect the contributions of MPs with different sizes to the total mass of the recoveries, if disregarding the thickness of the particles (unavailable by LDIR). The small-sized particles accounted for considerable proportions in the particle number-based distribution but had negligible mass. Therefore, the difference in MPs concentrations by different methods during C60–C180 for PLA and C0–C180 for PBAT indicated a general reduction in the recovery performance of PLA and PBAT MPs by the DS method. One possible explanation for this could be that PLA and PBAT MPs experienced fragmentation during the cast aging process, leading to the generation of particles < 5 μm, which could no longer be recovered as the pore size of the membrane filter used during extraction was 5 μm. Another possibility could be that the special physicochemical properties of the cast and cast aging process led to stronger binding effects between MPs and the cast. The earthworm's cast has lower porosity and more stable microaggregates compared to soil (Jouquet et al., 2008), which are also less water-soluble than natural soil aggregates (Schrader and Zhang, 1997). Furthermore, the drying and aging of casts can facilitate a close bonding of microbial polysaccharides and other organic compounds to clay, stabilizing the new microaggregates (Shipitalo and Protz, 1989). Therefore, MPs were likely to be trapped by the microstructures and microorganism-derived adhesives during the cast aging process, especially for PLA and PBAT due to their higher hydrophilicities. Consequently, recovering PLA and PBAT MPs by the DS method represented a challenge, more pronounced for smaller MPs.

3.3.6 Environmental implications

A major highlight of the current study is that MPs were recovered by different methods, when applicable (i.e., PLA and PBAT). The DS and Soxhlet extraction methods recovered MPs in different forms (particles vs. residual polymers), allowing the quantification and characterization of MPs from varied aspects. One key feature of the DS method is that MPs are recovered in their original forms (i.e., shapes, size, color) disregarding the potential influences caused by sonication, shaking, digestion and other procedures during the extraction. The mass, particle number, particle size, and shape of the recovered MPs could be obtained, which are relevant for evaluating the fate and potential risks of MPs on the soil ecosystem. However, several key limitations are brought in by this approach. For example, the pore size of the membrane filter sets a physical threshold for the size of MPs to be recovered, and impurities with similar densities to the target MPs are inevitable in the recoveries. Even though the Soxhlet extraction method destroys the macroscopic characteristics of MPs, e.g., size and shape, this approach can be highly polymer-specific and provide more accurate quantitative results. The findings of the current study underlined the importance of combining different extraction and quantification methods

in MPs-related studies, especially for complicated environmental matrices.

Our study also showed that the fate of MPs during the aging of the cast is polymer type dependent. Non-biodegradable LDPE MPs stayed almost unaffected. PLA MPs experienced substantial concentration reduction during the cast aging process, indicating further degradation following the initial fragmentation and depolymerization in the earthworm's gut. PBAT MPs were fragmented in the gut but did not experience substantial degradation in the cast. In addition, both biodegradable MPs were strongly immobilized in the cast during aging, hampering the recovery by the DS method, especially for small-sized particles. Collectively, our studies demonstrated that the earthworm's gut-related processes (gut passage, casting) and cast aging possess the potential for the in-situ bioremediation of MPs derived from certain polymers (e.g. PLA). However, considering the simultaneous stabilizing effect which closely traps MPs in the cast and the relatively low degradation rate of MPs in the cast, the potential release of secondary MPs with smaller sizes back to the soil after cast disintegration is not impossible. Our findings may provide pivotal information for drawing a holistic picture of how earthworm–MPs interactions affect the fate of MPs in the soil ecosystem.

Acknowledgement

We are thankful for the financial support from the China Scholarship Council (CSC: 201904910443) and the European Commission Horizon 2020 project MINAGRIS (No. 101000407). We would also like to acknowledge the financial support from the European Union's Horizon 2020 research and innovation programme under the Marie Skłodowska-Curie grant agreement No 955334. We would like to thank Yanzhang Luo (Magnefy, WUR) for help with the NMR analysis and method establishment, Evelien Maaskant (Wageningen Food & Biobased Research) for help with the interpretation of the quantitative NMR data, Frits Gillissen (Aquatic Ecology and Water Quality Management Group, WUR) for helping establish the Soxhlet extraction platform, Wouter Teunissen (Wageningen Food & Biobased Research) for the GPC analysis, Herman de Beukelaer (Wageningen Food & Biobased Research) for the DSC analysis.

Supplementary Materials

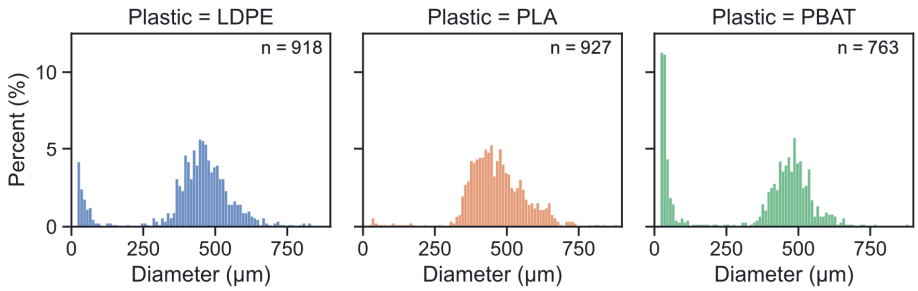

Figure S3.1 Distribution of different pristine microplastics produced by cryogenic fragmentation. Due to different polymer properties, different size distribution patterns were observed. The size of microplastics was determined by Agilent LDIR 8700.

Photo S3.1 The cast production unit (left) and the cast ageing units (right)

Text S3.1 Extraction protocol for recovering MPs from soils and earthworm casts

The current protocol was adapted from our previously established extraction protocol for LDPE, PLA and PBAT MPs from soil and fresh casts reported elsewhere (Meng et al., 2023a).

Oven-dried samples (approx. 0.5-2.5 g, depending on the extraction units) were weighed into a 10 mL glass centrifuge tube (for sample amount around 0.5 g) or 50 mL PP centrifuge tubes (for sample amount 2.0-2.5 g) and mixed with the first-step solution at a ratio of 1:16 (w/v). For C0 and S7 samples, the first-step solution varies according to the polymer type. 70% (v/v) ethanol solution (density ~0.88 g cm^{-3}) was used for LDPE (density ~0.92 g cm^{-3}), while distilled water (density 1.0 g cm^{-3}) was used for PBAT (density ~1.26 g cm^{-3}) and PLA (density ~1.24 g cm^{-3}). The solid-liquid mixture was:

1. thoroughly mixed on a vortex shaker until all aggregates were broken
2. treated with an ultrasonic bath for 10 min
3. shaken on a vertical shaker for 20 min (70 rpm).

After shaking, residues in the cap and on the inner wall of the tube were carefully rinsed back into the tube with the same solution. Then the mixture was centrifuged at 3,000 rpm for 10 min. After centrifugation, the supernatant was discarded, and the precipitate was extracted again following the above procedures with the second-step solution. The second-step solution also varies according to the polymer type. Distilled water was used for LDPE, while sodium dihydrogen phosphate (NaH_2PO_4) solution (density ~1.30 g cm^{-3}) was used for PBAT and PLA. After the second centrifugation, the supernatant was filtered through a Whatman® Cyclopore® polycarbonate membrane filter (pore size 5 μm, diameter 25 mm) using a vacuum filtration unit. The filtration column was rinsed with distilled water three times and one last time with 70% (v/v) ethanol solution to guarantee that everything in the column was collected onto the filter. The filtration column was covered with aluminum foil during filtration to avoid contamination from the lab environment. The polycarbonate filter was then gently recovered with tweezers and deposited in an empty glass scintillation vial with known weight. The bottleneck of the filtration column was washed out with 96% (v/v) ethanol solution into the scintillation vial, which was treated with an ultrasonic bath to release microplastics from the filter. The filter was rinsed and removed from the vials. The scintillation vials were dried in the oven at 50 °C. Finally, the weights of the vials containing dried particles were recorded.

Meng, K.; Lwanga, E. H.; van der Zee, M.; Munhoz, D. R.; Geissen, V. Fragmentation and Depolymerization of Microplastics in the Earthworm Gut: A Potential for Microplastic Bioremediation? *J Hazard Mater* **2023**, *447*.

Text S3.2 Additional extraction for aged soils and casts

During the MPs extraction, we observed a sharp decrease in the recovery of all types of MPs for aged cast samples (C15, C60, and C180). Hence, we speculated that the aging of MPs in the environmental matrix might have led to the increase in their bulk densities. After gradually increasing the densities of the extraction solutions, we found that for LDPE MPs an unsaturated sodium chloride (NaCl) solution (density ~1.13 g cm^{-3}) could achieve a "complete" extraction (no more MPs floating in the supernatant). For PLA and PBAT MPs, the NaH_2PO_4 solution with an increased density (~1.36 g cm^{-3}) can guarantee that no more MPs float in the supernatant.

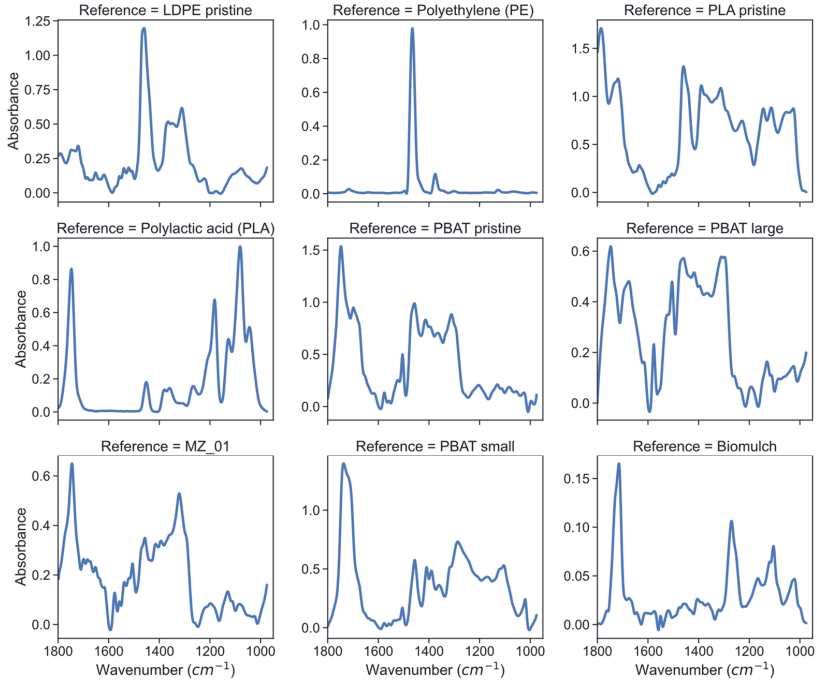

Figure S3.2 Representative spectra of references corresponding to LDPE, PLA and PBAT in the customized library. Explanations on the references are as follows: ***LDPE pristine*** shows a typical spectrum of produced LDPE MPs (125–500 µm) on LDIR. ***Polyethylene (PE)*** shows a typical spectrum of small LDPE MPs (< 125 µm), which is similar to the ATR-FTIR signal. ***PLA pristine*** shows a typical spectrum of produced PLA MPs (125–500 µm) on LDIR. ***Polylactic acid (PLA)*** shows a typical spectrum of small PLA MPs (< 125 µm), which is similar to the ATR-FTIR signal. ***PBAT pristine*** shows a typical spectrum of produced PBAT MPs (125–500 µm) on LDIR. ***PBAT large*** shows a typical spectrum of produced PBAT MPs (> 500 µm) on LDIR. ***PBAT small*** shows a typical spectrum of produced PBAT MPs (< 125 µm), which is similar to the ATR-FTIR signal. ***MZ_01*** shows a typical spectrum of plastic film made of Ecoflex® C1200. ***Biomulch*** shows a typical spectrum of a commercial biodegradable mulch film made from 75–90% PBAT.

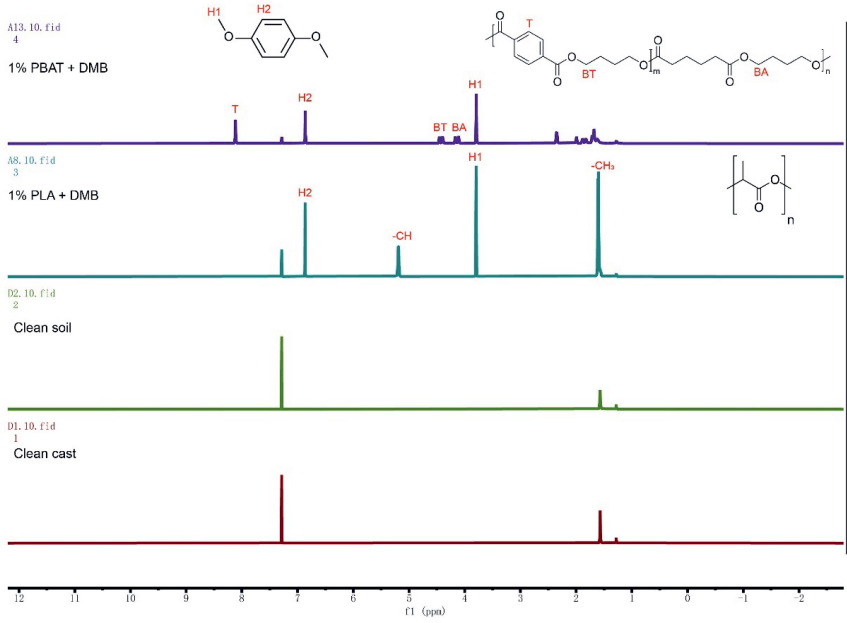

Figure S3.3 Representative NMR spectra of extracts from different samples. ***Clean cast***: extract from MP-free cast aged for 0 day. ***Clean soil***: extract from MP-free soil aged for 7 days. ***1% PLA + DMB***: extract from clean cast spiked with 1% PLA MPs, DMB was added as internal standard. ***1% PBAT + DMB***: extract from clean cast spiked with 1% PBAT MPs, DMB was added as internal standard. Proton peaks selected for integral, and calculation were labelled with red signs and shown in the chemical structures.

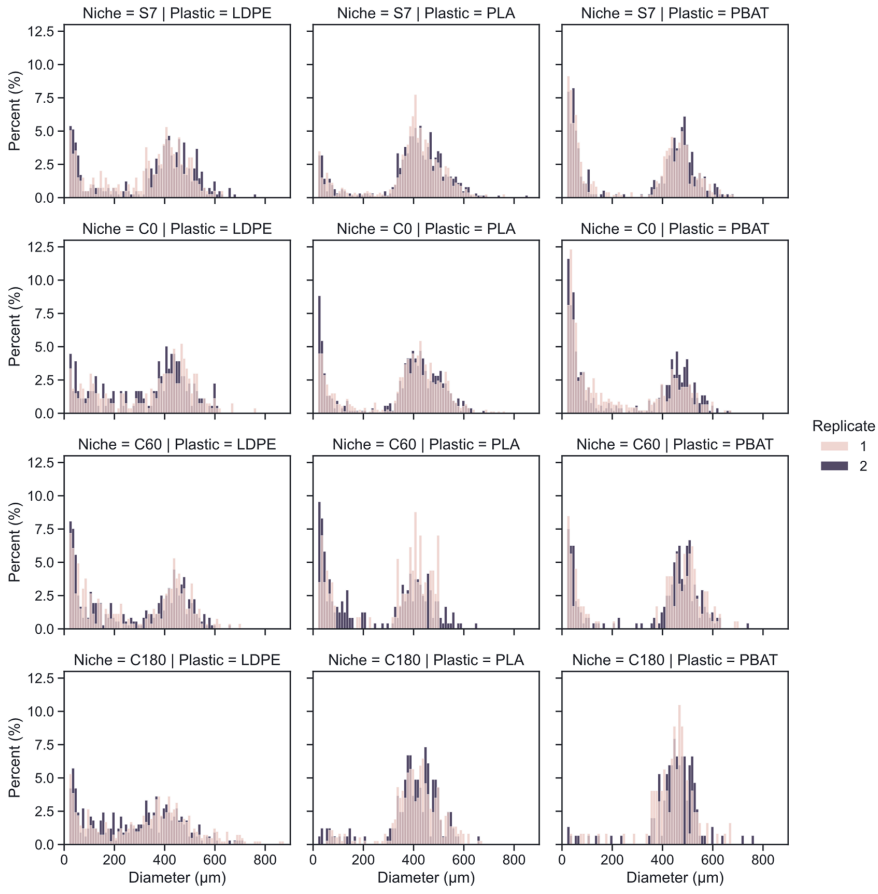

Figure S3.4 Size distributions of microplastics recovered from different niches (S7, C0, C60 and C180) by the DS method. Graphs in the same column are from the same treatment (plastic type), graphs in the same row are from the same niche. For each graph, size distributions of two independent measurements (replicates) are displayed.

Table S3.1 Recovery rates of PLA and PBAT microplastics from earthworm casts by the Sox-NMR method

Code	Sample	Cast (g)	Spiked (mg)	DMB (mg)	D-chloroform (mL)	IS volume (mL)	Recovered (mg)	Recovery rate (%)
A1	Blank-1	1.61000	0	49.85	25	3	0	0
A2	Blank-2	1.58500	0	49.85	25	3	0	0
A3	Blank-3	1.78300	0	49.85	25	3	0	0
A4	PLA-low-1	1.50240	1.85	98.20	50	3	1.57	84.6
A5	PLA-low-2	1.52512	1.50	98.20	50	3	1.34	89.6
A6	PLA-low-3	1.51404	1.48	98.20	50	3	1.48	99.7
A7	PLA-high-1	1.52694	19.36	98.20	50	3	17.48	90.3
A8	PLA-high-2	1.53108	19.77	98.20	50	3	18.09	91.5
A9	PLA-high-3	1.52408	21.27	98.20	50	3	18.27	85.9
A10	PBAT-low-1	1.51844	1.82	98.20	50	3	1.65	90.9
A11	PBAT-low-2	1.52004	1.63	98.20	50	3	1.35	83.1
A12	PBAT-low-3	1.51192	1.39	98.20	50	3	1.33	95.4
A13	PBAT-high-1	1.50480	20.03	98.20	50	3	18.56	92.7
A14	PBAT-high-2	1.51905	20.69	98.20	50	3	19.00	91.8
A15	PBAT-high-3	1.51256	21.03	98.20	50	3	19.88	94.5

*Blank treatments are clean casts without addition of MPs

**PLA-low and PBAT-low treatments have a nominal spike concentration at ~0.1%, w/w

***PLA-high and PBAT-high treatments have a nominal spike concentration at ~1%, w/w

Text S3.3 Cleaning procedures of microplastics

1 Microplastics were mixed with 10 mL of 2% SDS solution (Sodium dodecyl sulfate) in a 20 mL glass vial.

2 The suspension was treated with an ultrasonic bath for 1 h.

3 The suspension was filtrated through a Cyclopore polycarbonate membrane filter (5 μm, 25 mm, Whatman). The glass column was washed with distilled water 5 times (10 mL each time), then with 70% ethanol to remove all particles from the inner wall.

4 The filter membrane was transferred into a 50 mL centrifuge tube (plastic) and particles on the filter were rinsed off with 45 mL distilled water.

5 The centrifuge tube was treated with an ultrasonic bath for another 30 min.

6 Second filtration onto a new filter membrane.

7 Rinse the glass column 5 times with distilled water (10 mL each time) and one last time with 70% ethanol.

8 Transfer the filter into a glass vial and rinse everything off with 70% ethanol.

9 Dry in the oven at 40 °C.

Text S3.4 GPC analysis PLA and PBAT samples.

The settings are as follows, an OmniSEC Reveal GPC (model CHR6000) provided with an OmniSEC Resolve (model 7100) Triple Detector Array (RALLS and LALLS light scattering detectors, Refractive Index detector, and Viscometer detector) was used. The selected effluent was 1,1,1,3,3,3-hexafluor-2-propanol (HFIP) + 0.02M KTFA, at a flow of 0.7 mL min^{-1}. Columns used are a PSS PFG analytical linear M and guard column, molecular range ~ 300 – $2{\cdot}10^6$ D (PMMA in HFIP) at an oven temperature of 35 °C. Accurately weighed samples were dissolved overnight in 1.0 mL effluent in 1.5 mL GLC vials (or in 3.0 mL effluent in 4 mL glass vials for samples recovered by Soxhlet extraction). Concentrations were 3 to 4 mg mL^{-1} of polymer (accurate weight of sample and liquid). Filtering is done before measuring through 0.45 μm PTFE syringe filters. The (standard) injection volume was 100 μL. All measurements were performed in duplicate.

Table S3.2 Concentrations of PLA and PBAT microplastics quantified by the DS and Sox-NMR methods. The ratio of the two methods were calculated and displayed as percentages.

Plastic	Niche	DS method		Sox-NMR		Sox-NMR/DS (%)
		Concentration (%)	SD	Concentration (%)	SD	
PLA	S7	0.89	0.07	0.74	0.05	83
PLA	S60	0.87	0.07	0.7	0.17	80
PLA	S180	1.18	0.08	0.83	0.16	70
PLA	C0	0.86	0.09	0.93	0.22	108
PLA	C15	0.76	0.05	N.A.	N.A.	N.A.
PLA	C60	0.69	0.13	0.55	0.11	80
PLA	C180	0.32	0.07	0.66	0.24	206
PBAT	S7	0.92	0.08	0.71	0.1	77
PBAT	S60	1.01	0.06	0.8	0.07	79
PBAT	S180	1.07	0.08	0.96	0.14	90
PBAT	C0	0.87	0.14	0.88	0.11	101
PBAT	C15	0.54	0.08	N.A.	N.A.	N.A.
PBAT	C60	0.34	0.05	0.88	0.04	259
PBAT	C180	0.18	0.04	0.69	0.21	383

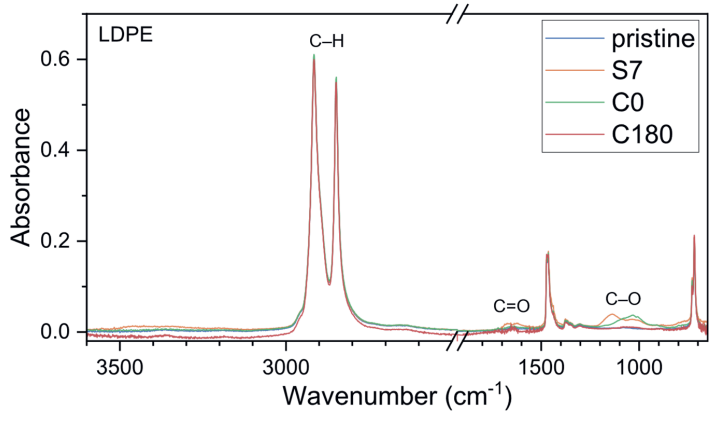

Figure S3.5 Infrared spectra of pristine LDPE MPs and LDPE MPs recovered from S7, C0, and C180 by the DS method.

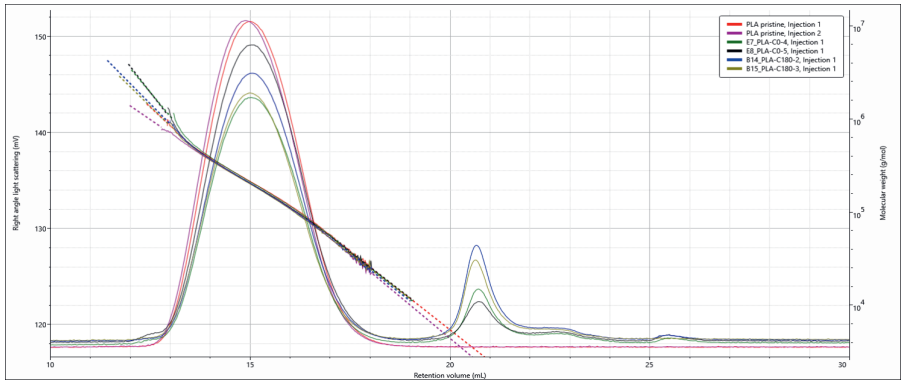

Figure S3.6 Chromatograms of RALLS signal of PLA samples. Pristine PLA, and extracts from C0 and C180 by Soxhlet extraction were measured twice. The fraction 13–18 mL is the main body of PLA, 23–25 mL was DMB, and the fraction 19–23 mL was impurities and potentially small PLA molecules, and 25–27 mL was unknown impurities from the cast.

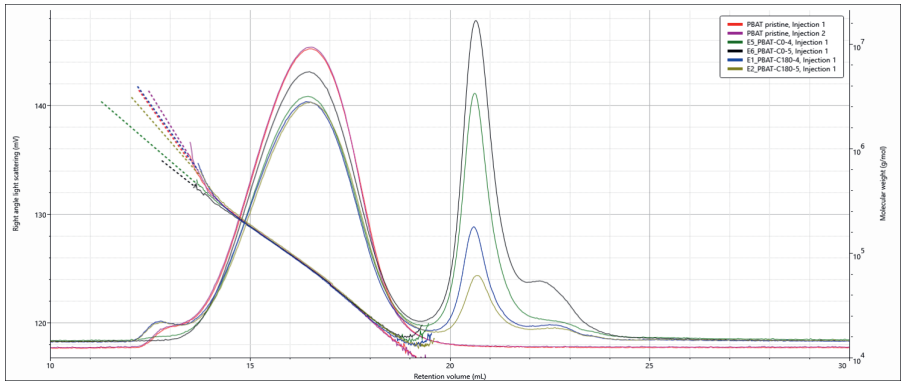

Figure S3.7 Chromatograms of RALLS signal of PBAT samples. Pristine PBAT, and extracts from C0 and C180 by Soxhlet extraction were measured twice. The fraction 12–19 mL is the main body of PBAT, the fraction 19–23 mL was impurities and potentially small PBAT molecules, and the fraction 23–25 mL was DMB.

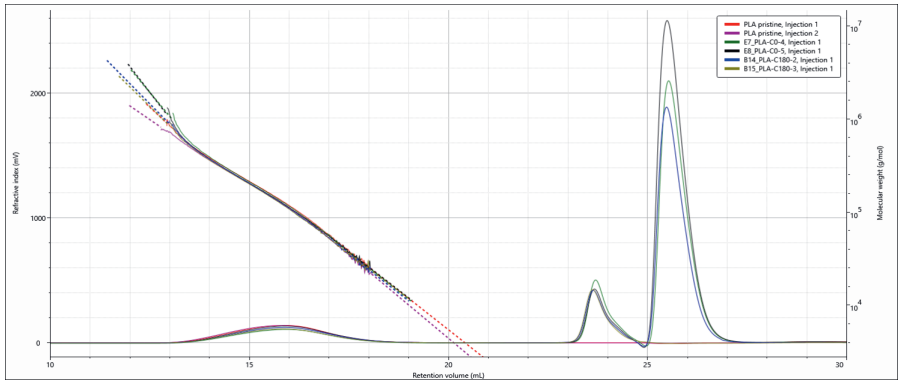

Figure S3.8 Chromatograms of RI signal of PLA samples. Pristine PLA, and extracts from C0 and C180 by Soxhlet extraction were measured twice. The fraction 13–18 mL is the main body of PLA, 23–25 mL was DMB, and the fraction 20–22 mL was impurities and potentially small PLA molecules, and 25–27 mL was unknown impurities from the cast.

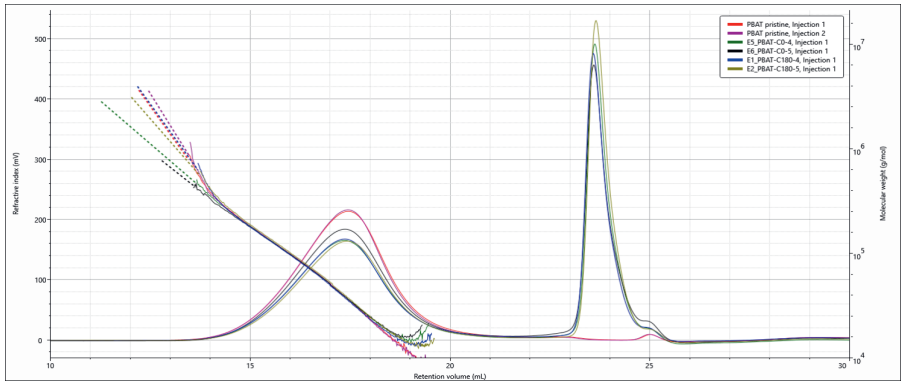

Figure S3.9 Chromatograms of RI signal of PBAT samples. Pristine PBAT, and extracts from C0 and C180 by Soxhlet extraction were measured twice. The fraction 12–19 mL is the main body of PBAT, the fraction 20–23 mL was impurities and potentially small PBAT molecules, and the fraction 23–25 mL was DMB.

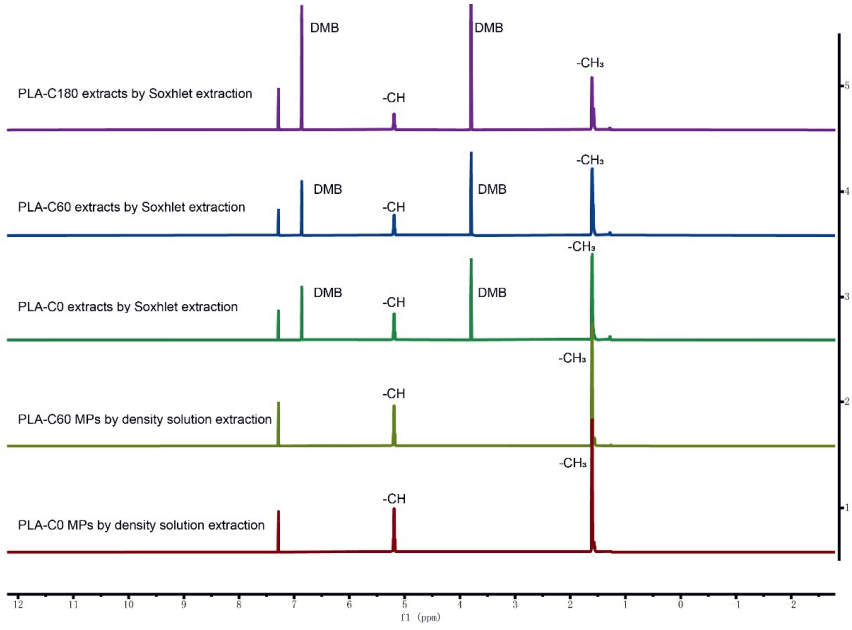

Figure S3.10 ^{1}HNMR spectra of PLA recovered by the DS method and Soxhlet extraction. The occurrence of new proton peaks was not detected.

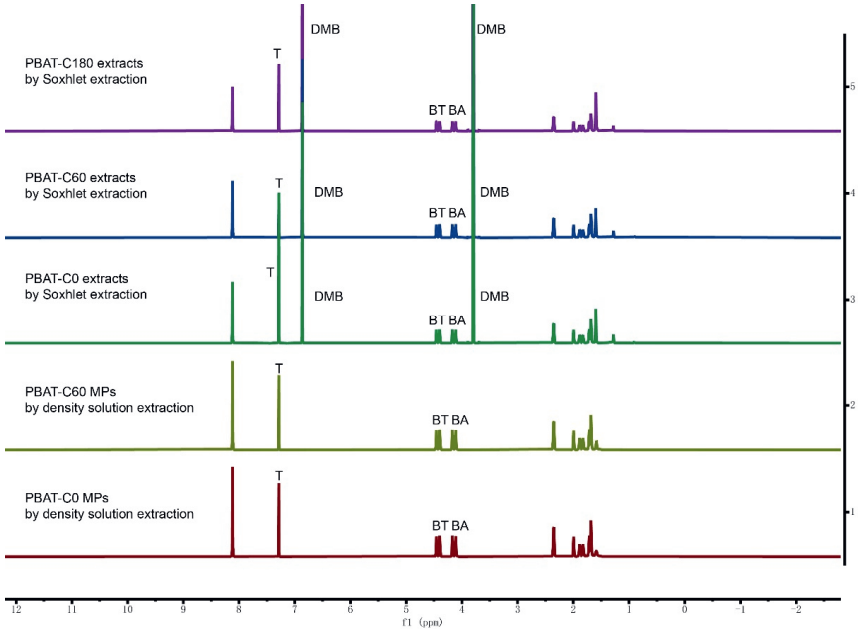

Figure S3.11 ^{1}HNMR spectra of PBAT recovered by the DS method and Soxhlet extraction. The occurrence of new proton peaks was not detected.

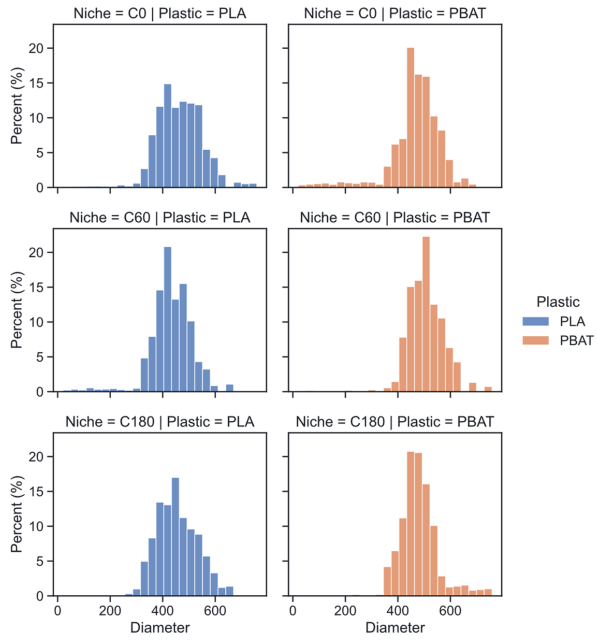

Figure S3.12 Particle area-weighted distribution of PLA and PBAT MPs recovered from C0–C180 by the DS method. Distributions here were generated from the same data displayed in Fig 3.3 with introducing the weight of particle area to the size distributions. The area-weighed distribution is proportional to the mass distribution if disregarding the thickness of the MPs, which is not available by the LDIR.

4. Microplastics exert minor influence on bacterial community succession during the aging of earthworm (*Lumbricus terrestris*) casts

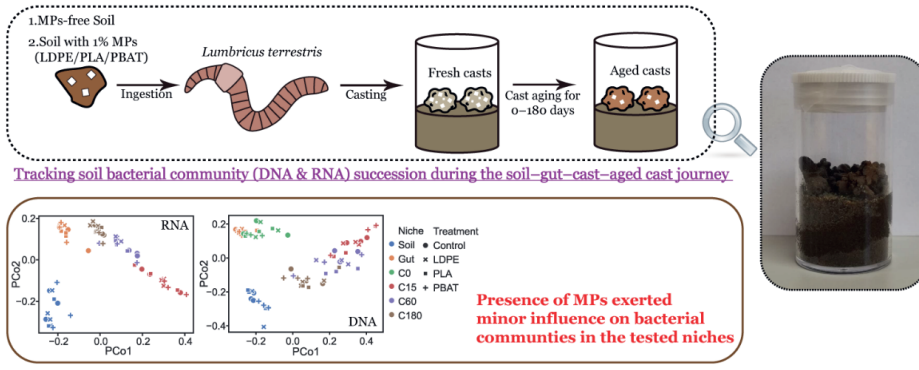

Based on:

Meng, K., Harkes, P., Lwanga, E. H. & Geissen, V. Microplastics exert minor influence on bacterial community succession during the aging of earthworm (*Lumbricus terrestris*) casts. (*Soil Biology and Biochemistry, in revision*)

Abstract

Microplastics (MPs) contamination of soils can affect the structure and function of soil microbiome. Earthworm's ingestion, digestion, and casting activities play a key role in shaping the soil microbiome. However, MPs' effects on earthworm's gut and cast microbiomes are poorly explored. Here, we investigated the influence of MPs (1% in soil, w/w) on the physicochemical properties and bacterial communities of soil during the gut passage and the aging of casts of *Lumbricus terrestris*. MPs associated with agricultural film production were selected, i.e., low density polyethylene (LDPE), polylactic acid (PLA) and polybutylene adipate terephthalate (PBAT). Different niches, e.g., pre-ingestion soil (Soil), gut content (Gut) and casts aged for 0–180 days (C0–C180) were studied. Results show that MPs enhanced the gut passage-derived differences between Soil and C0, in terms of pH, ammonium, nitrate and nitrite, and dissolved organic carbon. But such effects mostly faded out after the 180-day aging. The composition, alpha and beta diversity of both total (DNA) and active (RNA) bacterial communities were shaped by its niche (Soil, Gut, C0, etc.), rather than the presence/absence or the types of MPs. Nevertheless, a few biomarkers indicative of PBAT were identified, and the functional prediction (FAPROTAX) for the active community showed that bacterial communities under PBAT treatment were associated with higher potential for aliphatic and aromatic hydrocarbon degradation. In addition, we identified a soil-related core community and a gut-related core community, which might have neutralized MPs' effects and maintained the main structure and function of bacterial communities during the Soil–Gut–Cast transition. Our findings indicate that the tested MPs exerted minor influence on the bacterial communities during the cast aging process, MPs in aged casts might not add additional influence on the soil microbial community when they are finally incorporated into the soil. Future studies testing different soil types, polymer types, earthworm species, and field conditions are recommended to help enhance current knowledge on the influence of MPs on earthworms' cast microbiome.

4.1 Introduction

Microplastics (MPs) varying in the size, shape, color, polymer type, etc., have been found in almost all parts on the Earth, even in the Arctic and Antarctica (Aves et al., 2022; Bergmann et al., 2022). Since the first report where MPs were found on UK beaches (Thompson et al., 2004), intensive research has been done in the aquatic ecosystem. More recently, MPs in the terrestrial ecosystem have also gained increasing research attention.

Plastic debris, including but not limited to MPs, can affect the soil microbial community composition and function (Meng et al., 2019; Ng et al., 2021), potentially via changing the soil properties and biophysical environment (De Souza Machado et al., 2018; Qi et al., 2020), creating soil hotspots where the carbon and nutrient turnovers are enhanced (Zhou et al., 2021), releasing labile compounds that favor the growth of certain groups of microbes (Meng et al., 2023b), etc. Recent studies have also reported that "soil plastisphere"—the microenvironment directly under the influence of plastic debris—can function as hotspots of antibiotic resistance genes and potential pathogens (Zhu et al., 2022; Rillig et al., 2023). It has been reported that MPs also potentially affect the soil geochemical cycles by shaping the microbial community. For example, high dosage of polyethylene MPs (5%, w/w) was found to affect the emission of N_2O in fertilized soils by affecting the abundance of key bacterial taxa (Ren et al., 2020). Another study found that hydrogen production from isopod guts was stimulated by polylactic acid (PLA) MPs but inhibited by polyethylene terephthalate (PET) and polystyrene (PS) MPs (Hink et al., 2023).

Earthworms play a vital role in shaping the microbiome compositions and ecological functions of soils (Phillips et al., 2019). The earthworms' gut-related processes including ingestion, digestion and casting can stimulate a subset of the ingested soil microorganisms, leading to changes in element cycles in soils (Drake and Horn, 2007). The presence of MPs in the earthworms' cast has been reported (Huerta Lwanga et al., 2017b), inciting research interests on MPs influence on the gut microbiome of earthworms. Studies involving MPs of different polymer types, sizes, and shapes have found that MPs in general showed negligible influence on the earthworm's gut microbiome (Cheng et al., 2021; Yu et al., 2022; Adhikari et al., 2023; Tang et al., 2023). By contrast, others have reported that MPs derived from certain polymers (e.g., PS) could affect the occurrence of antibiotic resistance genes in the earthworm's gut (Xu and Yu, 2021) and potentially cause gut bacterial translocation (Li et al., 2022). Most existing studies only reported the response of the total microbial community (DNA) to MPs, which may not necessarily reflect the real effects caused by MPs. Studies targeting both the total and active community could provide more comprehensive profiling of the microbial community–MPs interplay.

In contrast with the soil and earthworm gut, the earthworm's cast is an overlooked niche when studying MPs' influence on the soil microbiome. Earthworm casts are mostly more fertile than the bulk soil (Van Groenigen et al., 2019), and once deposited back to the soil the earthworm cast can undergo drastic aging which leads to significant changes in its microbial composition and physicochemical properties (Aira et al., 2005). Existing information show that the bacterial community composition of cast is likely to show a time-

and nutrient-dependent succession during aging (Aira et al., 2019). Aged casts will eventually be incorporated back to the soil due to natural weathering or animal activities. The release of nutrients and microbial community back to the soil can exert certain influence on the soil microbiome. A recent work studying the microbiome in aged casts of *Lumbricus terrestris* has reported that the legacy of earthworm gut transitions on the soil microbiome could last beyond 168 days (Yang et al., 2024). Although there have been studies on the influence of MPs on earthworm's gut microbiome, there is little information about MPs' influence on the earthworm's cast microbiome during the aging process.

In the current study, we aimed to (i) explore the potential influence of MPs on the physicochemical properties of the earthworm's cast. (ii) reveal the influence of MPs on the bacterial communities residing in the earthworm's gut and casts of different aging stages. By employing MPs derived from polymers commonly used to produce non-biodegradable and biodegradable agricultural mulch films and targeting both the total community (DNA) and the active community (RNA), we provided realistic and comprehensive information that help complete a holistic picture of MPs influence on the bacterial community succession during the soil–gut–cast journey.

4.2 Materials and methods

4.2.1 Soil, earthworms and microplastics

MPs-free soil was collected from fields at Unifarm, Wageningen University & Research (the Netherlands). The collected soil was screened with a metal sieve (2 mm) after being air dried. The soil consisted of 3.2% clay, 50.0 % silt and 46.8% sand (sandy loam). The soil pH was 6.2 (1:5, w/v, extracted with water) and contained 3.8% organic matter (loss on ignition). To simulate the aging of earthworm casts deposited on the soil surface (Photo S4.1), *Lumbricus terrestris,* a widespread anecic species, was selected for cast production. Adult worms with a clear clitellum and similar body weights were handpicked and purged in the dark for 48 h prior to the experiment (4.03 ± 0.12 g, n = 48). Three polymers that are commonly used for producing agricultural mulch films from different categories were selected for the experiment, which are fossil-based non-biodegradable low-density polyethylene (LDPE, Dow™ LDPE 310E), bio-based compostable PLA (NatureWorks® Ingeo™ Biopolymer 2003D), and fossil-based biodegradable polybutylene adipate terephthalat (PBAT, Ecoflex® F Blend C1200). MPs were lab-prepared following a cryogenic fragmentation method described by Meng et al. (2023a). MPs obtained from the cryogenic fragmentation were screened with metal sieves (212 µm and 350 µm mesh). The fraction remaining between the two sieves was collected for experiment. The final average sizes of MPs were 419 ± 160 µm for LDPE, 465 ± 107 µm for PLA and 338 ± 215 µm for PBAT. Detailed size distributions are provided in Fig S4.1.

4.2.2 Cast production and cast aging

For the ease of producing and collecting uniform casts, we carried out the cast production and aging in microcosms in the lab (Photo S4.2). Four treatments were established for the

experiment. The control treatment (Control) was established using MPs-free soil, while in LDPE, PLA and PBAT treatments, soil spiked with 1% (dw/dw) corresponding MPs was used. For each treatment, different niches were selected for detailed study, they are the pre-ingestion soil (Soil), earthworm's gut content (Gut), freshly produced cast (C0), and cast aged for 15 (C15), 60 (C60) and 180 (C180) days.

Glass Petri Dishes (⌀120 mm × 20 mm) were used as cast production units (CPUs). 50 g of dry clean soil or dry MP-spiked soil were fully mixed in a sealed glass jar and transferred into the CPU. The water content was adjusted to 25% with distilled water. Six units were prepared for each treatment (totally 24 Petri Dishes). All units were pre-incubated for 7 days and approximately 3 g of soil were collected as pre-ingestion soil (Soil) before two worms being transferred into each CPU. The cast production was carried out at 16 ºC in the dark (to get higher cast production). Every 24 h, freshly produced casts (less than 1 d old) were carefully collected. Special attention was paid during the cast collection so that the intactness of the cast was maintained. Most of the collected fresh casts were immediately transferred into the cast aging units while a small portion was directly sampled as fresh casts (C0). As a result, the C0 samples were collected across the 6-day cast production, which could ensure the representativeness for casts produced on different days. At the end of the cast production worms were collected, rinsed with distilled water, dried with paper tissue, and preserved at −20 ºC before extracting the gut content.

Cast aging was performed in straight specimen containers (30 mL, polypropylene). The containers were filled with 20 g of dry MPs-free soil and a piece of cotton gauze was carefully placed on top of the soil. The water content was then adjusted to 25% with distilled water. The purpose of covering the soil with cotton gauze was to help separate aged casts from the soil during sampling. All the containers were pre-incubated at 16 ºC in the dark for 7 days before use. After introducing the fresh casts in the containers, the containers were wrapped with parafilm to avoid excessive evaporation while keeping air exchange. For each treatment, the aging of cast was performed for 15 days (C15), 60 days (C60) and 180 days (C180). While for each time point, six units were established with approx. 3 g casts per unit.

4.2.3 Sampling

Pre-ingestion soil (Soil) was collected right before adding earthworms to the CAUs. Fresh (C0) and aged (C15, C60 and C180) casts were collected with metal tweezers and spatula, tools were cleaned and disinfected with 70% ethanol after each use. The collected soil and cast samples were divided into two portions: one portion was immediately stored in sterile Eppendorf microcentrifuge tubes (2 mL) at −80 ºC, the other portion was weighed and stored in glass vials (20 mL) and dried in the oven at 40 ºC for 48 h.

Earthworms kept at −20 ºC were slowly defrost in the biosafety cabinet. The dissection of earthworms was conducted with sterile surgical scissors and nails inside the biosafety cabinet. The cutting was carefully made from the dorsal side of the worm, and the gut content was transferred into sterile Eppendorf microcentrifuge tubes (2 mL). Collected gut contents were kept at −80 ºC for nucleic acid extraction.

4.2.4 Chemical analysis

At least 18 grams of cast (from 6 replicates, fresh weight) were produced for each niche, while the majority of the oven-dried cast samples were used for other MP-related measurements (paper in preparation). Therefore, we had to merge the replicates to get enough samples for the chemical analysis. Soil and cast pH were measured from water extracts with a ratio of 1:5 (m:v) using a pH meter (Fisherbrand™ accumet™ FE150). The moisture contents were calculated based on the gravimetric difference before and after being dried in the oven (40 °C, 48 h). Oven dried samples were gently crushed with glass rods and completely passed through the 2 mm sieve. Then samples were shaken in a ratio of 1:10 (m:v) for 2 h with a 0.01M calcium chloride solution. After centrifugation and filtration of the suspension, the concentrations of nitrate and nitrite ($N\text{-}NO_x$), ammonium ($N\text{-}NH_4$) and dissolved organic carbon (DOC) in the extract were measured using a segmented flow analyzer (SFA, Skalar San++). The detection limits for $N\text{-}NO_x$, $N\text{-}NH_4$ and DOC were 0.5 mg kg^{-1}, 1 mg kg^{-1}, and 3 mg kg^{-1} respectively.

4.2.5 Nucleic acid extraction and reverse–transcription polymerase chain reaction (RT–PCR)

The extraction of both total DNA and RNA was conducted following a lab-made protocol previously reported (Harkes et al., 2019). The protocol was scaled down proportionally to fit in the Eppendorf microcentrifuge tube (2 mL) for 250–350 mg samples. Detailed procedures are described in Text S4.1. The quantity and quality of obtained DNA and RNA were determined by NanoDrop™ One (Thermo Scientific™) and Qubit 4 Fluorometers (Thermo Scientific™), respectively. DNA was successfully extracted from all niches, however, we failed to extract enough RNA from Co. Therefore, Co was excluded from the downstream analysis to be introduced below. The final extracts were kept at –80 °C before further use.

The synthesis of complementary DNA (cDNA) from the extracted total RNA (RT–PCR) was carried out using the Maxima First Stand cDNA Synthesis Kit for RT-qPCR (Thermo Scientific™) following the user manual. The final products were kept at –80 °C before further use.

4.2.6 16S amplicon sequencing and bioinformatic analysis

The V3–V4 region of the 16S rRNA gene was amplified using the 341F (CCTAYGGGRBGCASCAG)–806R (GGACTACNNGGGTATCTAAT) primer set. Polymerase chain reaction (PCR) was carried out with 15 µL of Phusion® High-Fidelity PCR Master Mix (New England Biolabs); 0.2 µM of forward and reverse primers, and about 10 ng DNA or cDNA. Thermal cycling consisted of initial denaturation at 98 °C for 1 min, followed by 30 cycles of denaturation at 98 °C for 10 s, annealing at 50 °C for 30 s, and

elongation at 72 ºC for 30 s. The PCR products of proper size were selected through 2% agarose gel electrophoresis. The same amount of PCR products from each sample was pooled, end-repaired, A-tailed, and further ligated with Illumina adapters. Libraries were sequenced on a paired-end Illumina platform (PE250) at Novogene Co., Ltd.

Paired-end reads were assigned to samples based on their unique barcode and truncated by cutting off the barcode and primer sequence. Paired-end reads were merged using FLASH (v1.2.11, http://ccb.jhu.edu/software/FLASH/) (Magoč and Salzberg, 2011). Quality filtering on the raw tags was performed using the fastp software (version 0.23.1) to obtain high-quality clean tags (Chen et al., 2018). Chimera sequences were detected and removed with UCHIME. Denoise was performed with DADA2 to obtain initial ASVs (amplicon sequence variants). Species annotation was performed with QIIME2 software against the Silva (v138.1) database. Finally, a total of 10,046,679 sequences (avg 75,539 ± 6,152 per sample) passed all quality filters and were assigned to ASVs. Sequence data have been uploaded to NCBI Sequence Read Archive (SRA) with accession number PRJNA1063260.

4.2.7 Community analysis and statistics

Data analysis was performed on R (v4.2.3) using package "microeco" (v1.3.0) (Liu et al., 2021). ASVs not assigned in the Kingdom "k__Archaea" or "k__Bacteria" were removed. ASVs with the taxonomic assignment "mitochondria" or "chloroplast were considered as contaminants and removed. Rarefaction was not conducted as the sequencing depths of all samples have reached saturation (Fig S4.2) to retain as much information as possible (Willis, 2019). Abundance-based coverage estimator index (ACE) and Shannon index were calculated to estimate the richness and diversity of communities. Principal coordinate analysis (PCoA) based on Bray–Curtis and Unweighed Unifrac distance was performed to profile the similarity and dissimilarity between samples and tested with pairwise permutational multivariate analysis of variance (PERMANOVA). We defined a soil-related core community, the members (ASVs) of which should be present (sequence > 0) in 100% of the samples in all niches. We also defined a gut-related core community, the members (ASVs) of which should not be present (sequence = 0) in any sample in the Soil niche and occur (sequence > 0) in more than 80% of the samples in other niches. Biomarkers indicative of certain niche or treatment were explored using Linear discriminant analysis (LDA) Effect Size (LEfSE) (Segata et al., 2011). Community functional prediction was performed only for the active bacterial community (RNA) using FAPROTAX (Louca et al., 2016). The normality of data was checked with Shapiro–Wilk test. For data following normal distribution, inter-niche or inter-treatment comparison was conducted with one-way analysis of variance (ANOVA). For data not following normal distribution, Kruskal–Wallis H-test was used. Significance level was set as $\alpha = 0.05$. Data visualization was conducted on Python (v3.12.0) using the Seaborn (v0.13.1) and Matplotlib (v3.5.3) library.

4.3 Results

4.3.1 Physicochemical properties of the soil and cast

The moisture content of the cast stayed stable during the 180-day aging process (Fig 4.1E) and there was no significant difference between different treatments ($p > 0.05$). The only fluctuation was observed between C0 and C15 in LDPE, where the moisture of C15 was significantly higher than C0 ($p < 0.05$). The pH values of C0 were remarkably higher than Soil, and the addition of MPs led to higher pH values (7.35 for PBAT, 7.38 for PLA and 7.50 for LDPE) compared to Control (6.89) (Fig 4.1D). Such difference gradually disappeared from C0 to C60, however, with extended aging to 180 days, a slightly lower pH was found for PBAT (6.23) compared to other treatments (6.46–6.53).

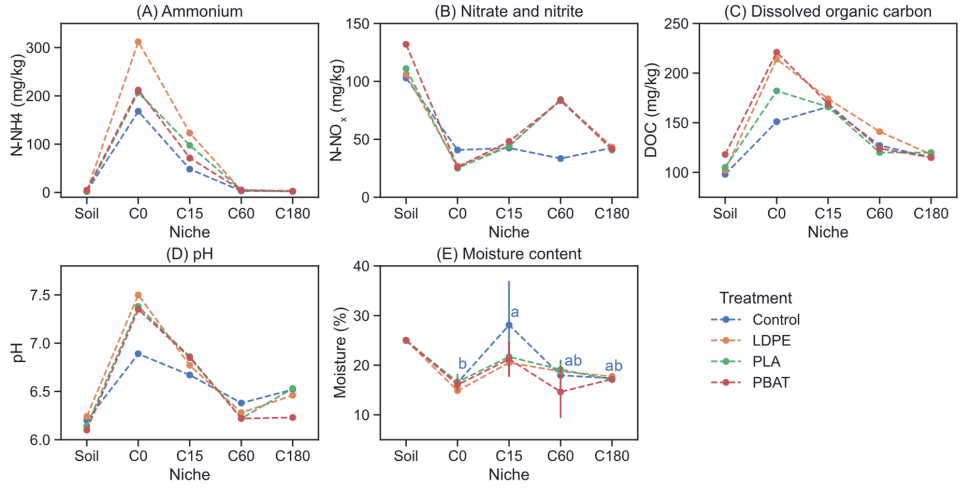

Figure 4.1 Physicochemical properties of pre-ingestion soil (Soil) and casts in different treatments. C0–C180: casts aged for 0–180 days. Significant differences between cast moisture in different niches were tested within the same treatment (one-way ANOVA) and labeled (if any) with lowercase letters. Due to insufficient sample amount, the values of pH, $N\text{-}NH_4$, $N\text{-}NO_x$ and DOC were measured by merging all replicates in the same niche.

The addition of MPs did not change the trend of $N\text{-}NH_4$ and DOC (Fig 4.1, A&C). Their contents in C0 (168–312 mg kg^{-1} for $N\text{-}NH_4$ and 151–221 mg kg^{-1} for DOC) were much higher than Soil (1.7–4.6 mg kg^{-1} for $N\text{-}NH_4$ and 98–118 mg kg^{-1} for DOC), and the contents of C0 in MPs-addition treatments (LDPE, PLA and PBAT) were 23–86% ($N\text{-}NH_4$) and 21–46% (DOC) higher than Control. During the aging process, the $N\text{-}NH_4$ and DOC contents in all treatments declined drastically to a similar level after 60 days and stayed stable from C60 to C180. The $N\text{-}NO_x$ contents substantially declined from Soil to C0 for all treatments and larger reductions were observed for MPs-addition treatments (–80% to –75%) compared to Control (–60%). The $N\text{-}NO_x$ content of Control stayed stable throughout the 180-day aging, whereas a different trend was observed for MPs-addition treatments.

The N-NO_x concentrations of LDPE, PLA and PBAT gradually increased in the first 60 days and reached ~84 mg kg^{-1}, which was more than twice of Control (33 mg kg^{-1}). From C60 to C180, the N-NO_x contents of MPs-addition treatments declined back to a level similar to Control.

4.3.2 Bacterial community compositions of different niches under different treatments

The compositions of total (DNA) and active (RNA) bacterial communities at phylum level (Fig 4.2) and genus level (Fig S4.3) were displayed. Most detected phyla were shared by both the 16S DNA sequencing and the 16S cDNA sequencing, except 6 phyla with extremely low relative abundances (Table S4.1). Principal coordinate analysis (PCoA) at ASV level (Fig 4.3, C–D) showed clear separation between communities derived from DNA and RNA (Table S4.2, Bray–Curtis: $R^2 = 0.14$, $p < 0.001$; Unweighed Unifrac: $R^2 = 0.07$, $p < 0.001$).

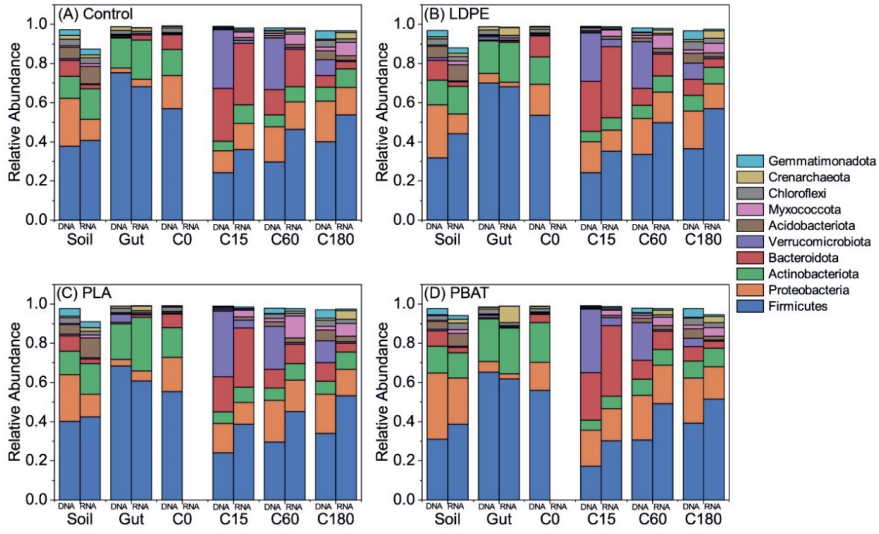

Figure 4.2 Bacterial community compositions of different niches under different treatments at phylum level. Ten phyla with the highest relative abundances are displayed. "DNA" and "RNA" represent total community and active community. C0, C15, C60 and C180 represent earthworm casts aged for 0, 15, 60 and 180 days, respectively.

In general, bacterial communities inhabiting the same niche shared similar compositions and the influence of MPs was negligible (Fig 4.2 & Fig S4.3). This is also reflected by the PCoA analysis (Fig 4.3, A–B), where both the total and active communities were clearly separated by the niche (Table S4.3, Pairwise PERMANOVA, $R^2 = 0.18–0.67$, $p < 0.001$) rather than by the treatment (Table S4.4, Pairwise PERMANOVA, $R^2 = 0.01–0.03$, $p = 0.942–0.982$).

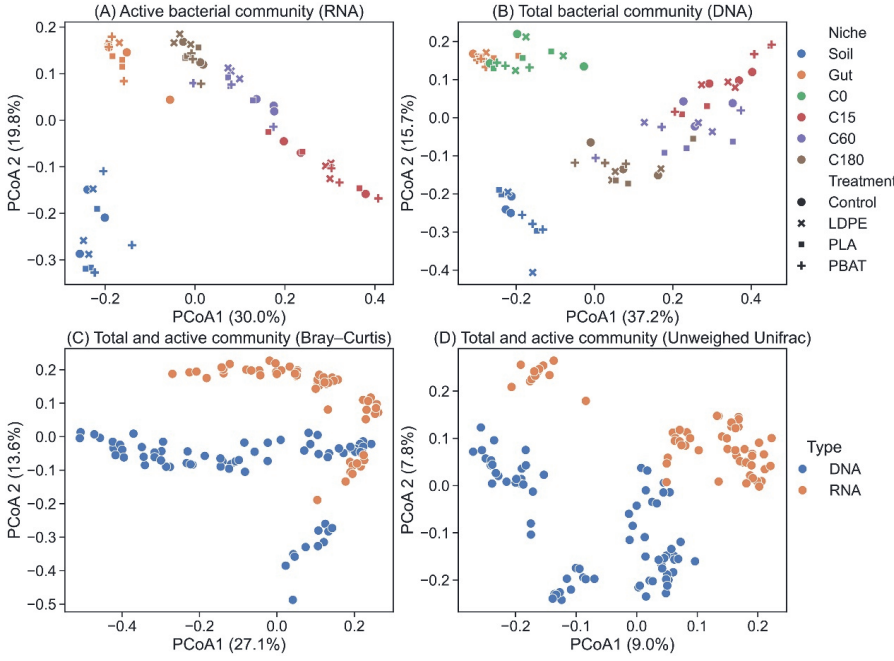

Figure 4.3 Principal coordinate analysis (PCoA) of bacterial communities at ASV level. (A) Active community (RNA) by Bray–Curtis distance. (B) total community (DNA) by Bray–Curtis distance. (C–D) Comparison between active community and total community by Bray–Curtis distance and Unweighed Unifrac distance. C0, C15, C60 and C180 represent earthworm casts aged for 0, 15, 60 and 180 days, respectively.

In Soil, phyla including Firmicutes, Proteobacteria, Actinobacteriota, Bacteroidota and Acidobacteriota dominated the community, adding up to 54.7–97.2% (DNA) and 72.1–95.8% (RNA) of the total sequences across all samples. While in the gut, the ratios of sequences belonging to Firmicutes (e.g., *Bacillus, Sporosarcina, Paenibacillus*) and Actinobacteriota increased significantly, accounting for 82.5–92.2% (DNA) and 75.2–93.0% (RNA) of the total sequences. During the cast aging process, bacterial communities in the cast developed in a clear aging time-dependent manner (Gut–C180). The relative abundances of gut-predominating phyla e.g., Firmicutes and Actinobacteriota declined sharply in the first 15 days (Gut–C15), but later increased steadily from C15 to C180. While those suppressed in the gut, such as Verrucomicrobiota and Bacteroidota experienced a boom from Gut to C15 (from 0.11% to 33.7% for Verrucomicrobiota, from 0.24% to 36.3% for Bacteroidota) and then decreased gradually from C15 to C180.

4.3.3 Bacterial community richness and diversity of different niches under different treatments

Across all samples, the total (DNA) community richness (ACE: 1317 ± 286) was significantly higher than the active (RNA) community richness (ACE: 1061 ± 141)

(Kruskal–Wallis H-test, $p < 0.001$), while the total community diversity (Shannon index) did not differ significantly from the active community. The total and active community

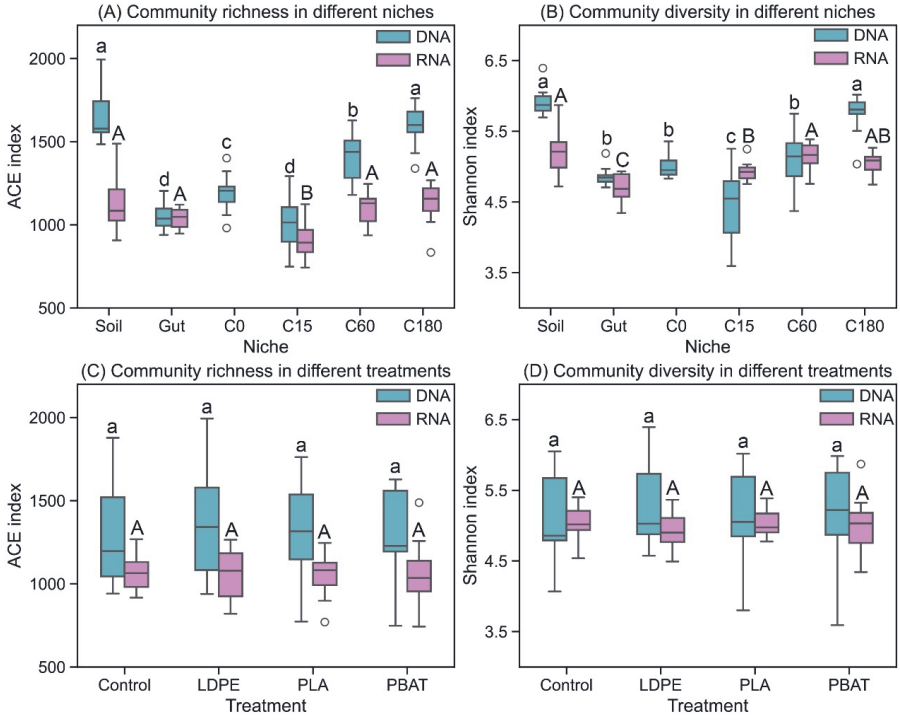

Figure 4.4 Community richness (ACE index) and diversity (Shannon index) at ASV level. (A–B) Alpha diversity indexes in different niches. (C–D) Alpha diversity indexes in different treatments. Blue and pink colors represent DNA- and RNA-based results, respectively. Significant differences tested with one-way ANOVA were labeled with lowercase and uppercase letters for DNA and RNA results, respectively. C0, C15, C60 and C180 represent earthworm casts aged for 0, 15, 60 and 180 days.

richness and diversity under different treatments were compared within each niche (Fig S4.4) and across all niches (Fig 4.4, C–D). It turned out that the alpha diversity of bacterial communities was not affected by the addition of MPs. By contrast, significant differences in richness and diversity were found between different niches within each treatment (Fig S4.5) and across all treatments (Fig 4.4, A–B). It is also obvious that the total community in general exhibited larger inter-niche differences than the active community (Fig S4.5 & Fig 4.4, A–B). The richness and diversity of the total bacterial communities decreased significantly from Soil to Gut and reached the lowest in C15 ($p < 0.05$). While from C15 to C180, the richness and diversity increased gradually and finally recovered to similar levels to Soil. By contrast, results of active community only showed that the community richness in C15 was significantly lower than other niches ($p < 0.05$), and the community diversity was lower than other niches in Gut ($p < 0.05$).

4.3.4 Core community and biomarkers for different niches and treatments

The soil-related core community which was present in all niches (Soil–C180) was identified (Fig 4.5, A–B). The total core community was comprised of 37 ASVs (Table S4.5) mostly belonging to Firmicutes (*Bacillus*, *Sporosarcina*, and *Lysinibacillus*, etc.) and Actinobacteriota (*Pseudarthrobacter*), accounting for 10.0–61.9% (average 36.0%) of the total communities in all samples. The active core community was comprised of 36 ASVs (Table S4.5) mostly belonging to Firmicutes (*Bacillus*), Crenarchaeota (*Nitrososphaeraceae*) and Actinobacteriota (*Acidothermus*, *Pseudarthrobacter*, *Gaiella*, etc.), accounting for 20.3–62.4% (average 41.8%) of the total communities in all samples. In addition, 21 ASVs were shared by both the total core community and the active core community (Table S4.5).

The gut-related core community—absent in the soil but present from Gut to C180—exhibited the contribution of the earthworm's gut bacteria to the cast bacterial community (Fig 4.5, C–D). The gut-related total core community consisted of 7 ASVs belonging to Verrucomicrobiota (*Luteolibacter*), Bacteroidota (*Flavobacterium*) and Proteobacteria (*Aeromonas* and *Pseudomonas*) (Table S4.6), accounting for 0.1–48.1% (average 13.3%) of the total sequences across different samples. The gut-related active core community consisted of 8 ASVs belonging to Bacteroidota (*Flavobacterium*) and Proteobacteria (*Aeromonas* and *Pseudomonas*) and Firmicutes (*Candidatus_Lumbricincola*), etc. (Table S4.6), accounting for 0.28–15.0% (average 3.7%) of the total sequences across different samples. ASV26 (*Flavobacterium*) and ASV67 (*Pseudomonas*) were present in both the total and active gut-related core communities.

Given the clear separation of samples by different niches on PCoA plots (Fig 4.3), thousands of ASVs were identified as biomarkers for different niches. For the ease of interpretation, biomarkers for niches were studied at phylum level. Biomarkers (LDA > 2) were successfully identified for most niches (Table S4.7). In Soil, Proteobacteria (total community) and Acidobacteriota/Gemmatimonadota/Chloroflexi (active community) were the main representative taxa. In Gut, Firmucutes and Actinobacteriota were identified as biomarkers for both the total community and active community. There were no indicative phyla for C0. Casts aged for 15 days were characterized by the flourishing of Verrucomicrobiota and Bacteroidota in both the total and active community. Mycoccota, Bdellovibrionota and Fibrobacterota were indicative phyla for the total and active community of C60, while Proteobacteria was exclusively indicative of the active community of C60. For C180 Crenarchaerota/Nitrospirota/Elusimicrobiota (in the active community) and Acidobacteriota/Gemmatimonadota/Chloroflexi (in the total community) were identified as main biomarkers.

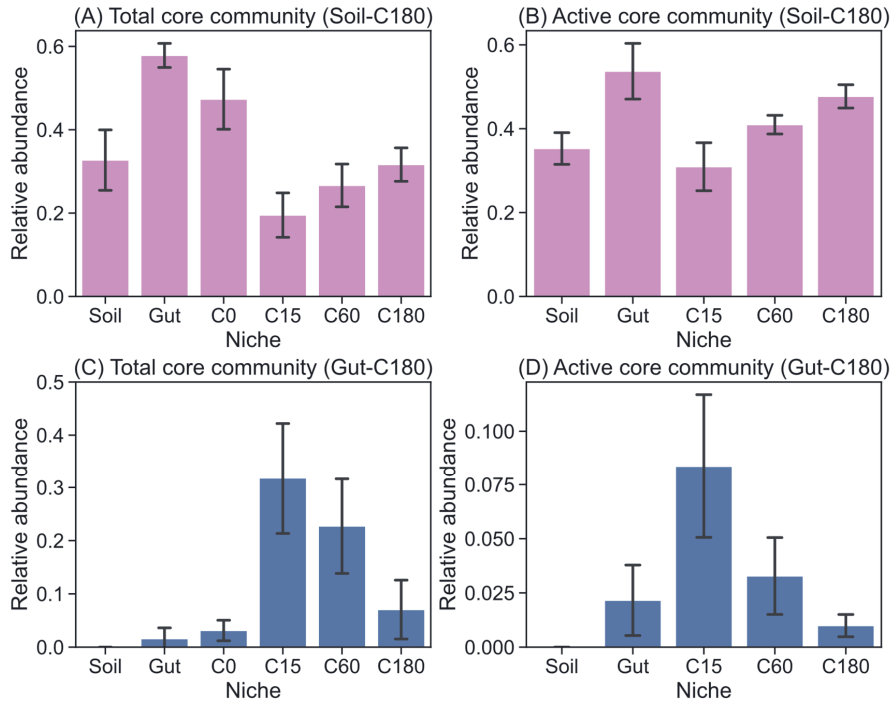

Figure 4.5 Dynamics of (A) soil-related total core community, (B) soil-related active core community, (C) gut-related total core community and (D) gut-related active core community. The taxonomic compositions of the defined core communities can be found in Table S4.5 and Table S4.6. Bars represent average relative abundances calculated from 12 samples of each niche and error bars represent standard deviations.

By contrast, only a few taxa were identified as biomarkers for MPs. Specifically, 8 genera (12 ASVs) were identified as biomarkers for PBAT in the total community and 5 genera (6 ASVs) were identified as biomarkers for PBAT in the active community (Table S4.8). Among them, 5 biomarkers belonging to Oxalobacteraceae, Comamonadaceae, *Cupriavidus* and *Bacteriovorax* were shared by both the total and active community. No biomarker was found for other treatments.

4.3.5 Functional groups of active bacterial communities in different treatments and niches.

Functional prediction was performed only for the active bacterial community (RNA) using FAPROTAX and several functions related to nitrogen cycling, degradation of hydrocarbon and energy sources were selected and displayed in Fig 4.6. We did not find any significant influence of MPs addition on functions related to nitrogen cycling. The addition of PBAT MPs significantly promoted the potential of active bacterial communities for

aromatic/aliphatic hydrocarbon degradation in most niches ($p < 0.05$, Fig 4.6, E–H), and such influence was also evident across all niches (Fig S4.6, E–H). In addition, PBAT MPs also increased the abundance of bacteria associated with aerobic chemoheterotrophy in the soil ($p < 0.05$, Fig 4.6, I).

Nevertheless, the overall results indicated that the community functions were mainly affected by the niches per se (Fig S4.7). Bacterial communities in Gut and C180 showed significantly higher potential for nitrification compared to Soil, C15 and C60 ($p < 0.05$, Fig S4.7, A). Function groups associated with denitrification and aerobic chemoheterotropy were more abundant in C15 and C60 ($p < 0.05$, Fig S4.7 C–D). Gut hosted significantly more bacteria potentially able to degrade aromatic/aliphatic hydrocarbon compounds than any other niche ($p < 0.05$, Fig S4.7, E–H). Abundances of anaerobic chemoheterotropy in different niches were as follows, C15 ≈ C60 > Gut ≈ C180 > Soil (Fig S4.7, J).

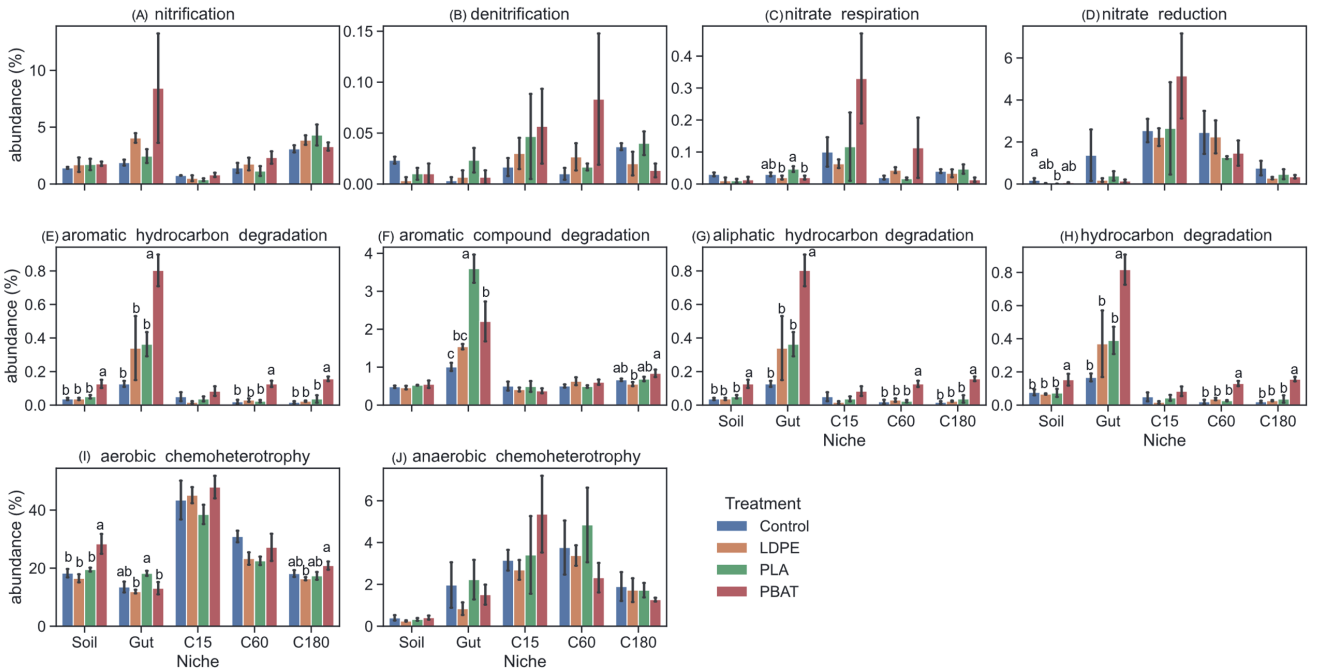

Figure 4.6 Effects of microplastic-addition on the active bacterial functional groups in different niches. (A–D) functions related to nitrogen cycling. (E–H) functions related to the degradation capacity of hydrocarbon compounds. (I–J) functions related to energy sources. Differences in abundance of bacterial functional groups between treatments were tested for each niche (one-way ANOVA) and labelled with lowercase letters. Error bars represent standard errors (n = 3).

4.4 Discussion

4.4.1 MPs affected physicochemical properties of the earthworm's cast

Our study showed that gut passage largely increased the pH, N-NH_4 and DOC contents but reduced the N-NO_x contents (Fig 4.1) in the fresh cast compared to Soil, which is consistent with previous findings (Horn et al., 2003; Van Groenigen et al., 2019; Vos et al., 2019). It has been reported that earthworm's gut contains significantly more water-soluble polysaccharides and amino acids than the surrounding soils (Drake and Horn, 2007), and earthworm's cast is characterized by higher pH, Ca^{2+}, Mg^{2+} and K^{+} contents (Jouquet et al., 2008). Although nitrate and nitrite were not measured separately, the reduction of N-NO_x and the increase of N-NH_4 in the fresh cast was evident, and such changes could be attributed the fact that the earthworm's gut is an anaerobic and reductive microenvironment ideal for the reduction of nitrate (Horn et al., 2003; Zhou et al., 2019). Although the physicochemical property values were obtained from one sample merged from replicates, the sheer difference between the MP-addition treatments and Control was evident, considering the detection limit of applied analytical methods. It seems that the presence of MPs could enhance the effect of gut process on soils, leading to an even higher increase in the pH, N-NH_4 contents and DOC contents, and a larger decrease in the N-NO_x contents.

The sharp reduction of N-NH_4 and DOC contents from C0 to C60 in our study was in consistent with previous findings (Decaëns, 2000; Aira et al., 2005; N. Bottinelli et al., 2020). The development of N-NO_x contents in Control was also similar to previous field observations (Decaëns, 2000). During the aging of cast, MPs did not show much influence on the development of DOC, N-NH_4 and pH, except that the pH of PBAT did not increase from C60 to C180 as happened to other treatments. Possibly, PBAT MPs experienced some hydrolysis, and the hydrolysates led to the slightly declined pH value. The different trends of N-NO_x development between Control and MPs-addition treatments might be attributed to the increased soil/cast porosity caused by MPs (Qi et al., 2020), which could enhance aeration and favor nitrification.

Little information is available for MPs' influence on the physicochemical properties of earthworm's gut content and cast; however, some studies have reported similar findings but on the soil. For example, MPs in the form of fragments and foams were reported to increase the soil pH (Zhao et al., 2021), and PE MPs were found to increase the DOC content in the soil (Liu et al., 2017). Recent study has also shown that the presence of PP MPs (> 0.5%) could accelerate soil nitrification (Guo et al., 2023). While contrasting findings were also reported, where MPs from PE were found to inhibit nitrification in the soil by directly affecting enzyme activity (Lan et al., 2024). Although the effects of MPs on soils might provide useful reference, earthworm gut and cast are more complex microenvironments. Therefore, more in-depth studies are needed to elucidate MPs' effects

on the earthworm's gut and cast physicochemical properties.

4.4.2 LDPE, PLA and PBAT microplastics pose minor influence on bacterial communities in earthworm gut and casts.

The current study provides key information that adds to the holistic picture of how MPs associated with plastic mulch films affect bacterial community compositions and functions during the earthworm's ingestion–digestion–casting process. Overall, we report that the addition of LDPE, PLA and PBAT MPs in the soil at a dosage of 1% (w/w) did not significantly shift the total (DNA) and active (RNA) community compositions in different niches (i.e., soil, gut, fresh cast, and aged cast).

The influence of MPs on soil microbiome has recently been intensively investigated. Varying the polymer types (non-biodegradable plastics, biodegradable plastics), particle sizes (nanoplastics, microplastics), soil types, dosages (environmental concentrations, high concentrations), and incubation time (short-term, long-term), among other parameters, researchers have mostly reported that MPs can exert influence on soil microbiome in different environments, e.g., crop rhizospheres (Qi et al., 2020; Meng et al., 2023), forest soil (Ng et al., 2021) and vegetable farmlands (Beriot et al., 2023). A meta-analysis based on existing literature suggested that soil biota exposed to MPs under high concentrations and for long periods are more likely to receive negative effects on the structure and function (Liu et al., 2023). Several factors, such as the relatively short incubation time (7 days), moderate dosage (1%, w/w) and the types of MPs (pure MPs free of additives), might explain why MPs addition did not exert significant influence on soil bacterial communities in our study.

However, less information is available for the influence of MPs on the earthworm's gut and cast microbiome. Several studies have reported that MPs (e.g., PS and PLA) significantly shifted the gut microbiome of *Eisenia fetida* (Xu and Yu, 2021; Li et al., 2022; Holzinger et al., 2023), while others reported that MPs showed negligible effects on the gut microbiome of *Eisenia fetida*, *Lumbricus terrestris* and *Metaphire guillelmi* (Cheng et al., 2021; Yu et al., 2022; Adhikari et al., 2023; Tang et al., 2023). Furthermore, the influence of MPs on the earthworm's cast microbiome remains largely unknown. To the best of our knowledge, the only available information is from Adhikari et al. (2023), where the authors also reported that LDPE and PBAT MPs did not significantly affect the bacterial communities in the cast of *Lumbricus terrestris* (cast aging was not performed but equivalent to 0–20 days old by our definition) using a larger experimental scale (mesocosm) and a different feeding strategy. By extending the aging process to 180 days and including both the total and active bacterial community, our study further suggests that the presence of MPs (LDPE, PLA and PBAT) in the cast might not add additional influence on the soil bacterial community when the aged casts are finally incorporated into the soil.

An interesting finding was that some functional groups relating to aromatic/aliphatic

hydrocarbon degradation and aerobic chemoheterotrophy were significantly enhanced by the presence of PBAT MPs in most niches (Fig 4.6, E–I), and several taxa were identified as PBAT biomarkers across all niches (Table S4.8). Previous studies have reported that PBAT MPs could undergo fragmentation and slight degradation during the passage through the earthworm's gut (Adhikari et al., 2023; Meng et al., 2023a). PBAT is a copolyester of adipic acid (aliphatic acid), 1,4-butanediol (aliphatic alcohol) and terephthalic acid (aromatic acid). It is therefore possible that PBAT MPs either experienced slight hydrolysis or released trace amounts of PBAT monomers and/or oligomers during the cast aging process, which stimulated the growth of bacteria capable of utilizing PBAT hydrolysates. Most PBAT biomarkers identified by LEfSE were Proteobacteria (Table S4.8), a phylum possessing large plastic-degrading potential (Zrimec et al., 2021). A few recent studies have also found that the addition of PBAT MPs in soils is associated with the increase of Proteobacteria abundance (Liu et al., 2022; Chen et al., 2024; Han et al., 2024). In addition, one of the PBAT biomarkers identified in our study, ASV443 (f__Comamonadaceae), was previously reported as a potential PBAT degrader (Han et al., 2021). Although the relative abundances of these PBAT biomarkers were not high—on average accounting for 1.4% and 0.52% of the total (DNA) and active (RNA) community—a slight change in certain microbes is also capable of changing the functions of the microbiome.

4.4.3 Earthworm's gut process has dominating influence on the composition and function of bacterial communities in the cast.

The digestion–casting–aging processes exerted decisive influence on the bacterial communities in different niches (Fig 4.3, A–B; Fig 4.4, A–C). The digestion process (Soil–Gut) is accompanied by significant enzymatic activity in the gut, where ingested microorganism may perish or flourish according to their physiological requirements (Manuel Aira et al., 2022). This explains why the community diversity declined in Gut compared to Soil (Fig 4.4). Significant enrichment of Firmicutes and Actinobacteriota occurred in Gut (Fig 4.2), making them the biomarkers for Gut. This could be attributed to a few reasons. First, most microorganisms belonging to Firmicutes and Actinobacteriota can produce endospores or spores that help survive the digestion process. Second, the earthworm's gut is a microaerophilic or even anaerobic microenvironment (Drake and Horn, 2007), therefore, facultative and/or obligate anaerobic microorganisms from phyla Firmicutes and Actinobacteriota can better survive in the gut.

During the aging of cast (C0–C180), the richness and diversity of bacterial communities in the cast first experienced a decline until C15 then gradually increase to a level similar to Soil (Fig 4.4, A–B), indicating a potential dividing of the cast aging process into 0–15 days and 15–180 days. As biomarkers of C15 (Table S4.7), Verrucomicrobiota carries genes capable of degrading stable polysaccharide (Orellana et al., 2022) and Bacteroidota is specialized in the degradation of complex organic matter, especially in the form of

polysaccharide (Wolińska et al., 2017). Their flourishing in C15 could be related to the adequate carbon pool in C0 and C15 (Fig 4.1C). The biomarkers of C60 and C180, by contrast, were mainly oligotrophic bacteria such as Acidobacteriota, Chloroflexi and Myxococcota etc. The dividing of cast aging process (0–15 days and 15–180 days) coincided with the dynamics of measured cast physicochemical properties, where C15 being seen as a transition point from fast to slow in terms of the changes of N-NH_4, DOC and pH (Fig 4.1). Our findings were in consistent with the previous report by (Aira et al., 2019), where the bacterial communities in the cast of *Aporrectodea caliginosa* were grouped into 0–7 days and 15–60 days.

We identified a soil-related core bacterial community which exists and functions across all niches (Soil–C180) where drastic biochemical processes occur (Fig 4.5, A–B, Table S4.5). The identified soil-related core bacterial community accounted for considerable ratios of the total and active community and was mainly comprised of Firmicutes, Actinobacteriota, which were also biomarkers for Gut. The stability of this core community might have guaranteed the resistance of the whole community to the disturbance caused by contaminants. Such hypothesis has been demonstrated by a previous work where keystone taxa shared by soil and earthworm gut helped resist chlordane stress (Zhu et al., 2021).

In addition, the influence of earthworm gut bacteria on the cast bacterial community was revealed (Fig 4.5, C–D, Table S4.6). Among others, the *Candidatus_lumbricincola* was an eye-catching genus, which was firstly detected in the gut of earthworm family Lumbricidae (Nechitaylo et al., 2009). Classic views are that the microbial composition of the earthworm gut reflects that of ingested soil or plant residues (Curry and Schmidt, 2007a), this is to some extent echoed by the soil-related core community discussed in the previous paragraph. However, the contribution of bacteria exclusively inhabiting the earthworm gut to the cast bacterial community was also evident.

4.4.4 Conclusion and prospects

Our research presents one of the first attempts to provide a holistic picture of MPs' effects on bacterial communities during the earthworm's ingestion–digestion–casting process. The observed alteration in the physicochemical properties indicate that the tested MPs (LDPE, PLA and PBAT) could enlarge the difference in pH, ammonium, nitrate/nitrite, and DOC contents caused by the gut passage between the pre-ingestion soil and the fresh cast, while such effects gradually disappeared during the aging of cast. It was also found that the bacterial community composition (both DNA and RNA) and the richness and diversity were decisively shaped by the niche, instead of the addition of the tested MPs. The soil-related core community and gut-related community identified in our research both significantly contributed to the main body of the cast microbiome, which was likely to have buffered the effects caused by MPs. Nevertheless, biomarkers were identified for PBAT and PBAT exerted some influence on the predicted community function. In general, our findings indicate that MPs containing cast might not add additional influence on the soil microbial community when they are finally incorporated into the soil. However, there is still a lack of knowledge on how MPs affect the microbiome composition and function in

the earthworm's cast. Future research focusing on the community metabolic activity and enzymatic activity in the earthworm's gut and cast, as has been explored in the soil (Song et al., 2023; Lan et al., 2024), shall provide more explicit knowledge on MPs' influence on these niches. In addition, the influence of MPs might be limited to only the small sphere surrounding the particles. More in-depth knowledge might be obtained by zooming into the MPs hotspots (Zhou et al., 2021) or define the target niche at the level of (micro)plastisphere (Rillig et al., 2023). Finally, as the current study was conducted in a microcosm system, long-term field-scale studies are needed to generate more comprehensive and realistic information by testing the combinations of different earthworm species, soil types and MPs.

Acknowledgement

We are thankful for the financial support from the China Scholarship Council (CSC: 201904910443) and the European Commission Horizon 2020 project MINAGRIS (No. 101000407). We would like to thank Harm Gooren for the soil texture analysis.

Supplementary Materials

Photo S4.1 Photos showing the earthworm's surface casting activity. (Shot at Wageningen University Campus)

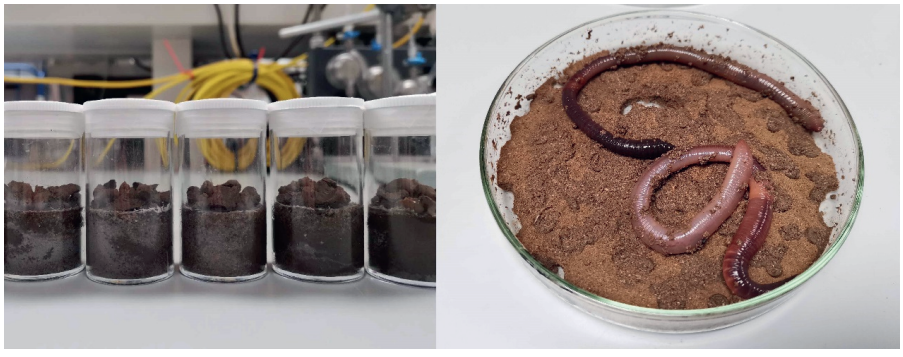

Photo S4.2 Photos showing the cast production units (right) and cast ageing units (left).

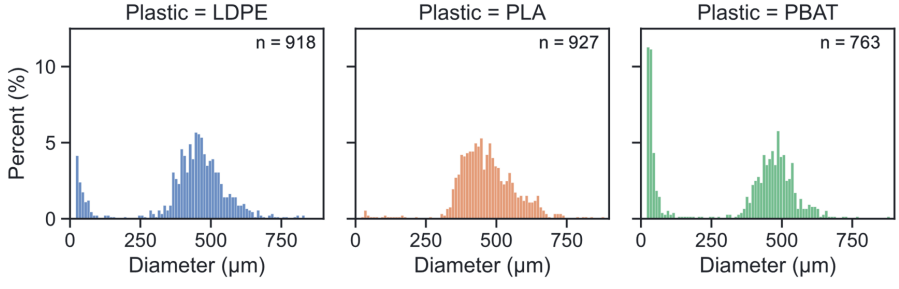

Figure S4.1 Size distributions of prepared microplastics for the experiment. The size of microplastics were generated on Lazer Direct Infrared Chemical Imaging system (LDIR 8700, Agilent). Size distributions were generated from n particles.

Text S4.1 Protocol for the extraction of total DNA and RNA from soils, gut contents and casts

1. Weigh 350 mg of sample and 200 mg of Carbid powder into a round bottom microcentrifuge tube (2 mL).

2. Add 320 µL of bead solution (S0: 181 mM disodium phosphate, 121 mM guanidinium thiocyanate), 35 µL of lysis buffer (S1: 150 mM sodium chloride, 4% (w/v) sodium dodecyl sulfate, 0.5 M Tris) and 100 µL of S2 (120 mM Aluminum ammonium sulfate dodecahydrate solution) into the tube.

3. Add 450 µL of phenol:chloroform:isoamyl alcohol (25:24:1, pH 8.0) and mix the tube manually to disintegrate the biphasic layer.

4. Vortex the tube for 10 min horizontally at max speed (2850 rpm), preferably at 4 °C.

5. Incubate the tubes horizontally at −20 °C for 10 min. Then repeat step 4 and continue with step 6.

6. Centrifuge the tubes at 10,000×g (4 °C) for 10 min to separate the soil particles from the lysate.

7. Transfer 200 µL of supernatant (avoid phenol layer) into a new 1.5 mL centrifuge tube and add 100 µL of ice-cold precipitation solution (S3: 22 mM citric acid, 5 M sodium chloride, 29 mM tri-sodium citrate dihydrate) and incubate at 2–8 °C for 10 min.

8. Centrifuge the tubes at 10,000×g for 10 min to separate the precipitate from the nucleic acids.

9. Transfer 250 µL of supernatant into a new 1.5 mL centrifuge tube containing 320 µL of isopropanol at room temperature. Gently mix by hand for 5 s and centrifuge at 10,000×g for 10 min.

10. Discard the isopropanol and air dry the pellet for 8 minutes at room temperature.

11. Add 70 µL of binding solution (S4: 5M guanidinium thiocyanate and 30mM Tris-HCl (pH: 6.5) with 9% (v/v) isopropanol) at room temperature to the pellet and vortex to re-dissolve the pellet.

12. Transfer all liquid from step 11 to a silica spin filter (in a 2.0 mL round bottom collection tube) and spin at 10,000×g for 30 s. This step is to load nucleic acids onto the column.

13. Discard the flow-through and wash the column 4 times with 250 µL of washing solution (S5: (10mM Tris-HCl, pH 6.5), 100mM sodium chloride, and absolute ethanol at final concentration of 60% (v/v)). Stop spinning when it reaches 10,000×g. Then do another dry run (10,000×g, 4 °C, 5 min) to make sure all washing solution is removed.

14. Air dry the filter column for 8 min and transfer the filter column to a clean 1.5 mL centrifuge tube.

15. Add 50 µL of elution buffer (S6: 10mM Tris-HCl, pH 8.0) to the filter and spin for 30 s at 10,000×g.

16. The final elute containing total DNA and RNA is preserve at −80 °C.

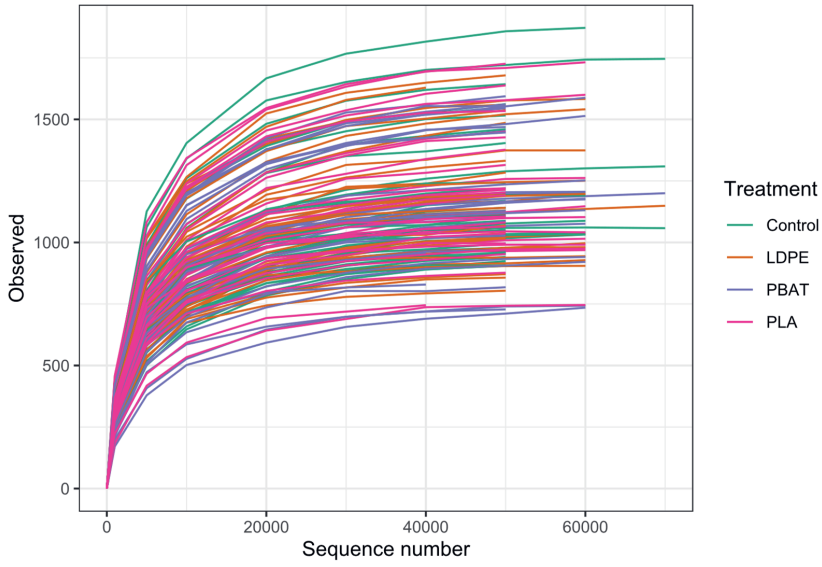

Figure S4.2 Rarefaction curves for all samples.

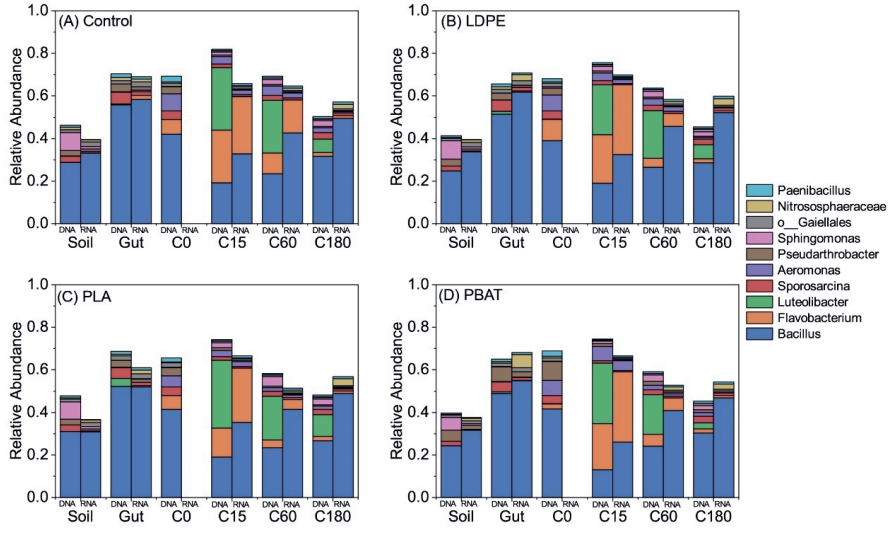

Figure S4.3 Bacterial community compositions of different treatments and niches at genus level. Ten genera with the highest relative abundances are displayed. "DNA" and "RNA" represent total community and active community. C0, C15, C60 and C180 represent earthworm casts aged for 0, 15, 60 and 180 days.

Table S4.1 Phyla not shared by the total community (DNA) and active community (RNA).

Taxa	DNA	RNA
k__Bacteria|p__Deferribacterota	Yes	No
k__Bacteria|p__Halanaerobiaeota	Yes	No
k__Archaea|p__Euryarchaeota	Yes	No
k__Bacteria|p__Entotheonellaeota	No	Yes
k__Bacteria|p__GAL15	Yes	No
k__Bacteria|p__Caldatribacteriota	Yes	No

Table S4.2 Pairwise permutational analysis of variance (PERMANOVA) for DNA and RNA derived communities by Bray–Curtis distance and Unweighed Unifrac distance.

Groups	measure	F	R^2	p.value	p.adjusted	Significance
DNA vs RNA	bray	20.69	0.14	0.001	0.001	***
DNA vs RNA	unwei_unifrac	10.28	0.07	0.001	0.001	***

Table S4.3 Pairwise permutational analysis of variance (PERMANOVA) for different niches in the DNA and RNA based PCoA profile.

Profile type	Groups	measure	F	R^2	p.value	p.adjusted	Significance
DNA	Soil vs Gut	bray	24.36	0.53	0.001	0.001	***
	Soil vs Co	bray	18.66	0.46	0.001	0.001	***
	Soil vs C15	bray	34.66	0.61	0.001	0.001	***
	Soil vs C60	bray	26.56	0.55	0.001	0.001	***
	Soil vs C180	bray	19.99	0.48	0.001	0.001	***
	Gut vs Co	bray	8.95	0.29	0.001	0.001	***
	Gut vs C15	bray	44.82	0.67	0.001	0.001	***
	Gut vs C60	bray	36.16	0.62	0.001	0.001	***
	Gut vs C180	bray	27.37	0.55	0.001	0.001	***
	Co vs C15	bray	27.95	0.56	0.001	0.001	***
	Co vs C60	bray	24.03	0.52	0.001	0.001	***
	Co vs C180	bray	19.87	0.47	0.001	0.001	***
	C15 vs C60	bray	7.03	0.24	0.001	0.001	***
	C15 vs C180	bray	19.92	0.48	0.001	0.001	***
	C60 vs C180	bray	7.10	0.24	0.001	0.001	***
RNA	Soil vs Gut	bray	20.55	0.48	0.001	0.001	***
	Soil vs C15	bray	27.11	0.55	0.001	0.001	***
	Soil vs C60	bray	21.07	0.49	0.001	0.001	***
	Soil vs C180	bray	21.54	0.49	0.001	0.001	***
	Gut vs C15	bray	29.73	0.57	0.001	0.001	***
	Gut vs C60	bray	18.99	0.46	0.001	0.001	***
	Gut vs C180	bray	15.10	0.41	0.001	0.001	***
	C15 vs C60	bray	10.47	0.32	0.001	0.001	***
	C15 vs C180	bray	20.83	0.49	0.001	0.001	***
	C60 vs C180	bray	4.95	0.18	0.001	0.001	***

Table S4.4 Pairwise permutational analysis of variance (PERMANOVA) for different treatments in DNA and RNA based PCoA profile.

Profile type	Groups	measure	F	R^2	p.value	p.adjusted	Significance
DNA	Control vs LDPE	bray	0.34	0.01	0.971	0.982	
	Control vs PLA	bray	0.44	0.01	0.907	0.982	
	Control vs PBAT	bray	0.87	0.03	0.473	0.946	
	LDPE vs PLA	bray	0.30	0.01	0.982	0.982	
	LDPE vs PBAT	bray	0.79	0.02	0.422	0.946	
	PLA vs PBAT	bray	0.93	0.03	0.418	0.946	
RNA	Control vs LDPE	bray	0.37	0.01	0.971	0.982	
	Control vs PLA	bray	0.44	0.01	0.907	0.982	
	Control vs PBAT	bray	0.87	0.03	0.473	0.946	
	LDPE vs PLA	bray	0.34	0.01	0.982	0.982	
	LDPE vs PBAT	bray	0.95	0.03	0.422	0.946	
	PLA vs PBAT	bray	0.93	0.03	0.418	0.946	

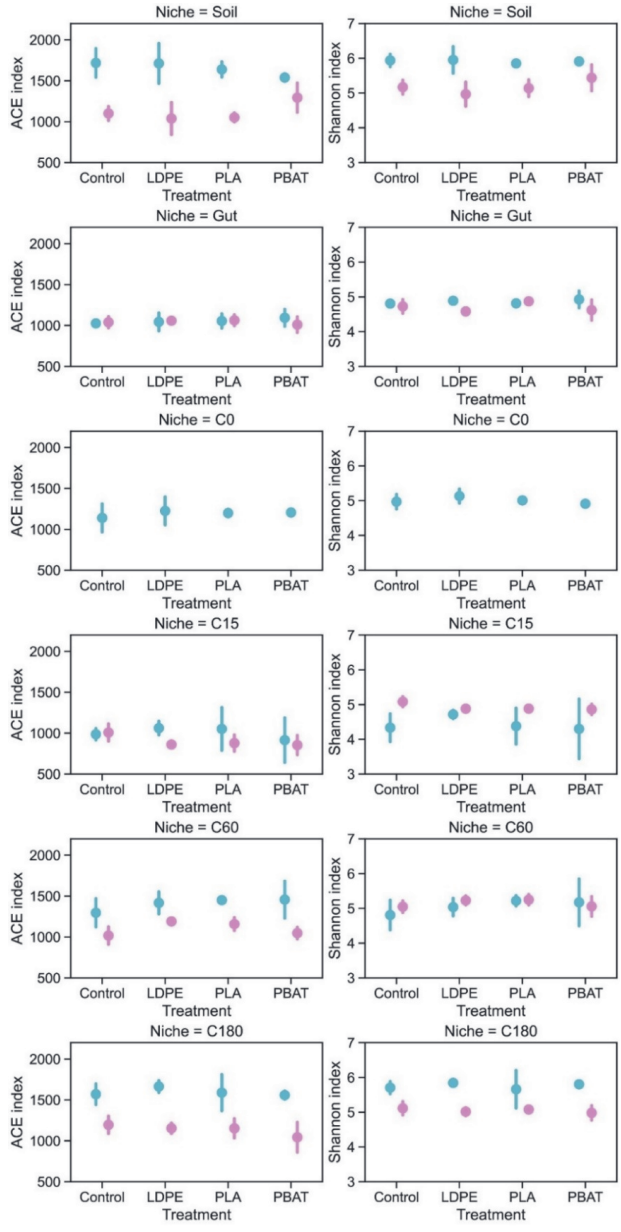

Figure S4.4 Influence of different microplastics on the community richness (ACE index) and diversity (Shannon index) for each niche at ASV level. Blue and pink colors represent DNA– and RNA–based results, respectively. Significant differences tested with one-way ANOVA were labeled with lowercase and uppercase letters (if any) for DNA and RNA, respectively.

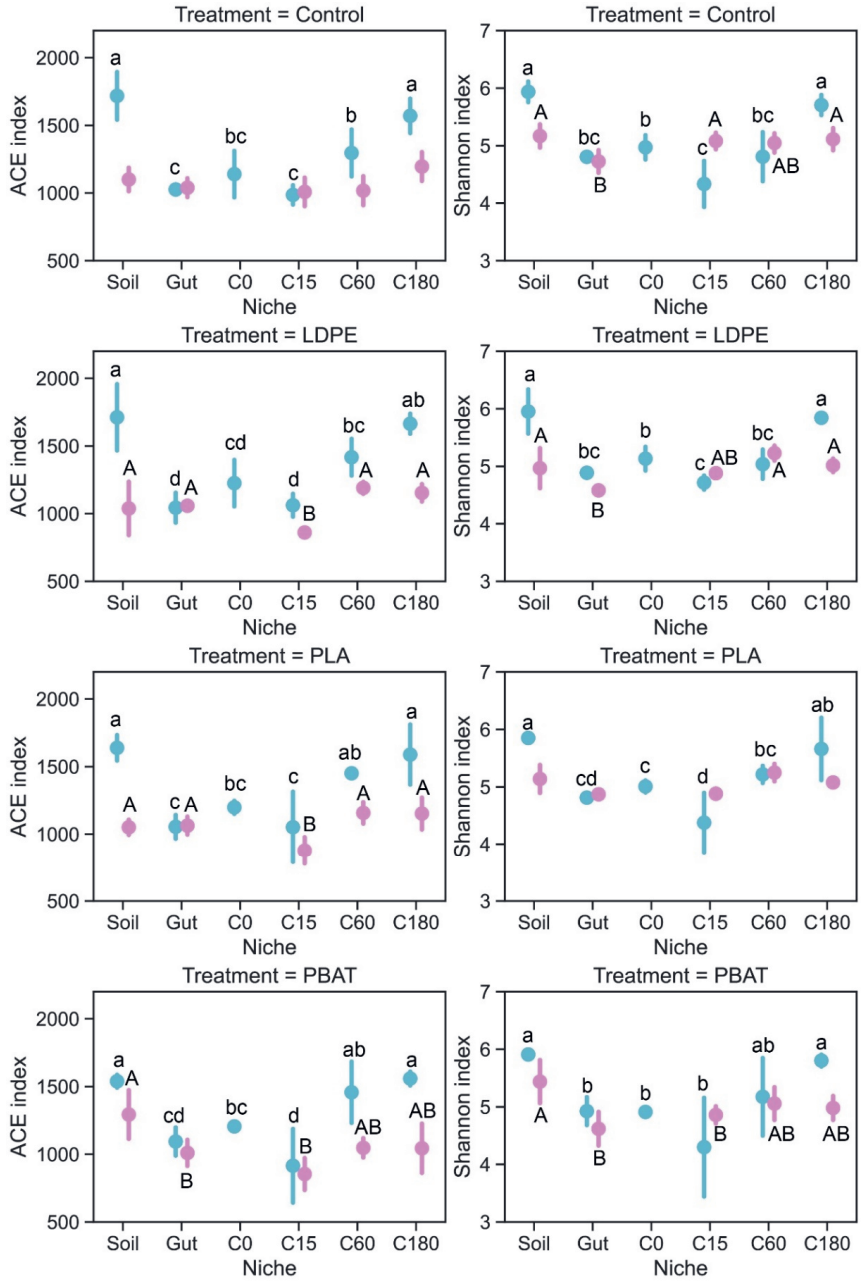

Figure S4.5 Community richness (ACE index) and diversity (Shannon index) of different niches for each treatment at ASV level. Blue and pink colors represent DNA– and RNA–based results, respectively. Significant differences tested with one-way ANOVA were labeled (if any) with lowercase and uppercase letters for DNA and RNA, respectively.

Table S4.5 Core community that was present in all niches (Soil–C180) during the experiment. ASVs marked in red are shared by both the total core community and the active core community.

Total core community (DNA)			Active core community (RNA)		
ASV	**Phylum**	**Genus**	**ASV**	**Phylum**	**Genus**
ASV0	Firmicutes	*Bacillus*	ASV0	Firmicutes	*Bacillus*
ASV1	Firmicutes	*Bacillus*	ASV1	Firmicutes	*Bacillus*
ASV3	Firmicutes	*Bacillus*	ASV3	Firmicutes	*Bacillus*
ASV4	Firmicutes	*Bacillus*	ASV4	Firmicutes	*Bacillus*
ASV5	Firmicutes	*Bacillus*	ASV5	Firmicutes	*Bacillus*
ASV6	Firmicutes	*Bacillus*	ASV6	Firmicutes	*Bacillus*
ASV7	Actinobacteriota	*Pseudarthrobacter*	ASV7	Actinobacteriota	*Pseudarthrobacter*
ASV8	Firmicutes	*Sporosarcina*	ASV9	Firmicutes	*Bacillus*
ASV9	Firmicutes	*Bacillus*	ASV10	Crenarchaeota	*Nitrososphaeraceae*
ASV10	Crenarchaeota	*Nitrososphaeraceae*	ASV12	Firmicutes	*Bacillus*
ASV12	Firmicutes	*Bacillus*	ASV16	Firmicutes	*Bacillus*
ASV15	Actinobacteriota	f__Micrococcaceae	ASV20	Actinobacteriota	*Acidothermus*
ASV16	Firmicutes	*Bacillus*	ASV24	Firmicutes	*Bacillus*
ASV19	Firmicutes	*Bacillus*	ASV29	Firmicutes	*Bacillus*
ASV20	Actinobacteriota	*Acidothermus*	ASV30	Firmicutes	*Bacillus*
ASV21	Firmicutes	*Bacillus*	ASV32	Firmicutes	*Bacillus*
ASV25	Firmicutes	*Bacillus*	ASV38	Firmicutes	*Bacillus*
ASV27	Firmicutes	*Bacillus*	ASV43	Chloroflexi	JG30-KF-AS9
ASV31	Firmicutes	f__Planococcaceae	ASV44	Actinobacteriota	*Gaiella*
ASV32	Firmicutes	*Bacillus*	ASV47	Firmicutes	*Bacillus*
ASV36	Firmicutes	*Lysinibacillus*	ASV49	Firmicutes	*Lysinibacillus*
ASV38	Firmicutes	*Bacillus*	ASV53	Actinobacteriota	o__Gaiellales
ASV43	Chloroflexi	JG30-KF-AS9	ASV57	Actinobacteriota	*Conexibacter*
ASV44	Actinobacteriota	*Gaiella*	ASV63	Firmicutes	*Bacillus*
ASV46	Firmicutes	*Sporosarcina*	ASV64	Actinobacteriota	*Gaiella*
ASV49	Firmicutes	*Lysinibacillus*	ASV92	Firmicutes	*Bacillus*
ASV50	Firmicutes	*Ammoniphilus*	ASV104	Firmicutes	*Bacillus*
ASV52	Firmicutes	*Lysinibacillus*	ASV108	Firmicutes	*Bacillus*
ASV53	Actinobacteriota	o__Gaiellales	ASV114	Actinobacteriota	*Nakamurella*
ASV56	Firmicutes	*Sporosarcina*	ASV141	Actinobacteriota	*Gaiella*
ASV64	Actinobacteriota	*Gaiella*	ASV146	Firmicutes	*Bacillus*
ASV70	Firmicutes	*Tuberibacillus*	ASV156	Actinobacteriota	*Acidothermus*
ASV77	Firmicutes	*Bacillus*	ASV174	Actinobacteriota	IMCC26256
ASV118	Firmicutes	*Bacillus*	ASV187	Actinobacteriota	*Conexibacter*
ASV142	Bacteroidota	*Bacteroidetes_vadinHA17*	ASV209	Actinobacteriota	o__Gaiellales
ASV169	Actinobacteriota	*Gaiella*	ASV211	Myxococcota	*bacteriap25*
ASV240	Actinobacteriota	f__Micromonosporaceae			

Table S4.6 Core community that was absent in the soil but present in > 80% of the samples from Gut to C180. (ASVs in red are shared by both the total core community and the active core community.

Total core community (DNA)			Active core community (RNA)		
ASV	**Phylum**	**Genus**	**ASV**	**Phylum**	**Genus**
ASV2	Verrucomicrobiota	*Luteolibacter*	ASV14	Proteobacteria	*Aeromonas*
ASV11	Bacteroidota	*Flavobacterium*	ASV22	Bacteroidota	*Flavobacterium*
ASV13	Bacteroidota	*Flavobacterium*	ASV23	Proteobacteria	*Aeromonas*
ASV26	Bacteroidota	*Flavobacterium*	ASV26	Bacteroidota	*Flavobacterium*
ASV40	Verrucomicrobiota	*Luteolibacter*	ASV34	Firmicutes	*Candidatus_Lumbricincola*
ASV55	Proteobacteria	*Aeromonas*	ASV67	Proteobacteria	*Pseudomonas*
ASV67	Proteobacteria	*Pseudomonas*	ASV133	Actinobacteriota	*Terrabacter*
			ASV474	Bdellovibrionota	OM27_clade

Table S4.7 Biomarkers of different niches at Phylum level across all treatments by LEfSE. Only taxa with LDA values > 2 are displayed.

Type	Taxa	Group	LDA	P.adj
DNA	k__Bacteria|p__Proteobacteria	Soil	5.06	< 0.001
	k__Bacteria|p__Armatimonadota	Soil	3.12	< 0.001
	k__Bacteria|p__Cyanobacteria	Soil	3.07	< 0.001
	k__Bacteria|p__SAR324_clade(Marine_group_B)	Soil	2.42	< 0.001
	k__Bacteria|p__WS4	Soil	2.11	< 0.001
	k__Bacteria|p__Latescibacterota	Soil	2.10	< 0.001
	k__Bacteria|p__Firmicutes	Gut	5.38	< 0.001
	k__Bacteria|p__Actinobacteriota	Gut	4.81	< 0.001
	k__Archaea|p__Crenarchaeota	Gut	3.78	< 0.001
	k__Archaea|p__Halobacterota	Gut	2.42	< 0.001
	k__Bacteria|p__Sumerlaeota	Gut	2.12	0.005
	k__Bacteria|p__Verrucomicrobiota	C15	5.18	< 0.001
	k__Bacteria|p__Bacteroidota	C15	5.07	< 0.001
	k__Bacteria|p__Bdellovibrionota	C60	3.46	< 0.001
	k__Bacteria|p__Planctomycetota	C60	3.26	< 0.001
	k__Bacteria|p__Fibrobacterota	C60	2.21	< 0.001
	k__Bacteria|p__Acidobacteriota	C180	4.38	< 0.001
	k__Bacteria|p__Gemmatimonadota	C180	4.32	< 0.001
	k__Bacteria|p__Chloroflexi	C180	4.17	< 0.001
	k__Bacteria|p__Myxococcota	C180	3.86	< 0.001
	k__Bacteria|k__Bacteria	C180	3.24	< 0.001
	k__Bacteria|p__Patescibacteria	C180	3.19	< 0.001
	k__Bacteria|p__Nitrospirota	C180	3.19	< 0.001
	k__Bacteria|p__Desulfobacterota	C180	3.10	< 0.001
	k__Bacteria|p__Elusimicrobiota	C180	2.97	< 0.001
	k__Archaea|p__Nanoarchaeota	C180	2.11	< 0.001
RNA	k__Bacteria|p__Acidobacteriota	Soil	4.62	< 0.001
	k__Bacteria|k__Bacteria	Soil	4.53	< 0.001
	k__Bacteria|p__Gemmatimonadota	Soil	4.12	< 0.001
	k__Bacteria|p__Chloroflexi	Soil	4.01	< 0.001
	k__Bacteria|p__Planctomycetota	Soil	3.63	< 0.001
	k__Bacteria|p__Armatimonadota	Soil	3.29	< 0.001
	k__Bacteria|p__Cyanobacteria	Soil	3.28	< 0.001
	k__Bacteria|p__Desulfobacterota	Soil	2.89	< 0.001
	k__Bacteria|p__SAR324_clade(Marine_group_B)	Soil	2.27	< 0.001
	k__Bacteria|p__Latescibacterota	Soil	2.23	< 0.001
	k__Bacteria|p__DTB120	Soil	2.09	< 0.001
	k__Bacteria|p__Firmicutes	Gut	5.17	< 0.001

	k__Bacteria|p__Actinobacteriota	Gut	4.89	< 0.001
	k__Archaea|p__Halobacterota	Gut	2.52	< 0.001
	k__Bacteria|p__Sumerlaeota	Gut	2.37	< 0.001

(Continued from the table above)

Type	Taxa	Group	LDA	P.adj
RNA	k__Bacteria|p__Bacteroidota	C15	5.21	< 0.001
	k__Bacteria|p__Verrucomicrobiota	C15	4.22	< 0.001
	k__Bacteria|p__Proteobacteria	C60	4.80	< 0.001
	k__Bacteria|p__Myxococcota	C60	4.49	< 0.001
	k__Bacteria|p__Bdellovibrionota	C60	3.60	< 0.001
	k__Bacteria|p__Fibrobacterota	C60	2.43	< 0.001
	k__Archaea|p__Crenarchaeota	C180	4.24	< 0.001
	k__Bacteria|p__Nitrospirota	C180	2.98	< 0.001
	k__Bacteria|p__Elusimicrobiota	C180	2.66	< 0.001

Table S4.8 PBAT biomarkers at ASV level across all niches by LEfSE. Only taxa with LDA values > 2 are displayed. PBAT biomarkers shared by the total community and active community were marked in red.

Type	Taxa	Group	LDA	P.adj	Average abundance (%) *
DNA	p__Proteobacteria|f__Oxalobacteraceae|ASV157	PBAT	3.34	< 0.001	0.41
	p__Proteobacteria|g__Noviherbaspirillum|ASV349	PBAT	2.98	< 0.001	0.19
	p__Proteobacteria|f__Oxalobacteraceae|ASV412	PBAT	2.78	0.002	0.12
	p__Proteobacteriaf__Oxalobacteraceae|ASV479	PBAT	2.70	0.009	0.10
	p__Proteobacteria|f__Oxalobacteraceae|ASV642	PBAT	2.67	< 0.001	0.09
	p__Proteobacteria|g__Cupriavidus|ASV609	PBAT	2.67	< 0.001	0.09
	p__Bdellovibrionota|g__Bacteriovorax|ASV601	PBAT	2.56	0.004	0.07
	p__Actinobacteriota|g__Rhodococcus|ASV212	PBAT	2.55	0.038	0.08
	p__Proteobacteria|g__Noviherbaspirillum|ASV864	PBAT	2.47	0.009	0.05
	p__Proteobacteria|g__Caulobacter|ASV667	PBAT	2.42	0.038	0.06
	p__Proteobacteria|f__Comamonadaceae|ASV443	PBAT	2.38	< 0.001	0.05
	p__Proteobacteria|g__Caenimonas|ASV600	PBAT	2.36	0.004	0.05
RNA	p__Proteobacteria|f__Comamonadaceae|ASV443	PBAT	2.96	0.001	0.17
	p__Proteobacteria|f__Oxalobacteraceae|ASV157	PBAT	2.91	< 0.001	0.14
	p__Proteobacteria|f__Oxalobacteraceae|ASV412	PBAT	2.70	< 0.001	0.10
	p__Proteobacteria|g__Cupriavidus|ASV609	PBAT	2.36	0.003	0.05
	p__Bdellovibrionota|g__Bacteriovorax|ASV601	PBAT	2.09	0.008	0.03
	p__Proteobacteria|g__Noviherbaspirillum|ASV1080	PBAT	2.05	0.045	0.02

*Average abundance calculated from all samples with PBAT addition

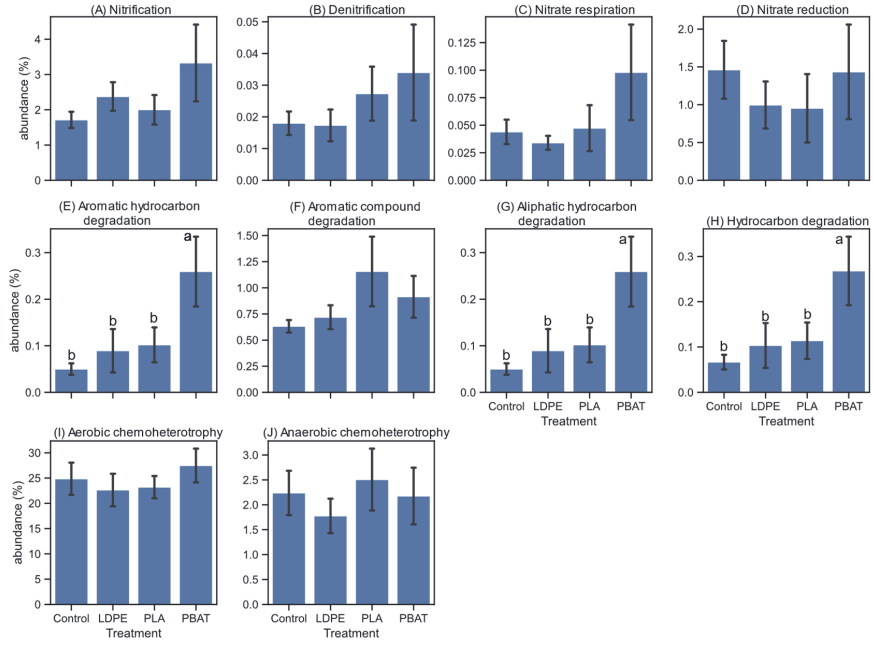

Figure S4.6 Effects of microplastic-addition on the overall active bacterial functional groups across all niches. Differences in abundance of bacterial functional groups between treatments were tested (one-way ANOVA) and labelled with lowercase letters. Error bars represent standard errors (n = 15).

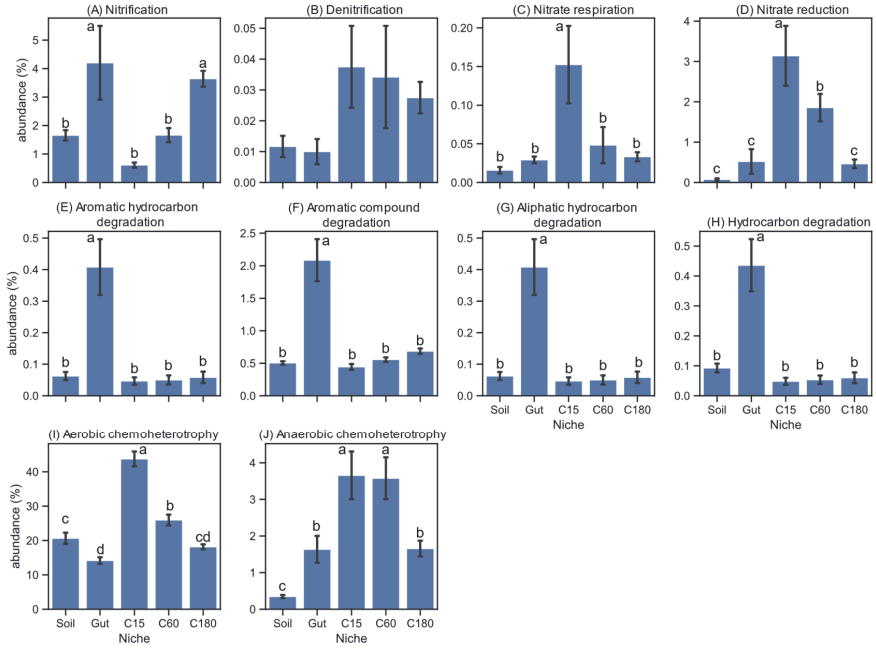

Figure S4.7 Effects of niches on the overall active bacterial functional groups across different treatments. Differences in abundance of bacterial functional groups between niches were tested (one-way ANOVA) and labelled with lowercase letters. Error bars represent standard errors (n = 12).

5. Synthesis

5.1 Major findings of the thesis

There are increasing concerns over the potential risks caused by the occurrence and accumulation of microplastics (MPs) in soils, as well as the potential accumulation of MPs derived from biodegradable plastics due to their unclear degradation performance in different environments. Given the relatively moderate contamination levels of MPs in soils (4.5–55.5 mg kg^{-1}) (Scheurer and Bigalke, 2018; Büks and Kaupenjohann, 2020), and the difficulties of massively recovering MPs from the soil, the current PhD thesis explored the potential of in-situ bioremediation of MPs contaminated soils by earthworms. For the ease of quantifying and characterizing MPs in the soil, earthworm gut and casts, and to present our findings based on a contamination level that could reflect the potentially high "future concentration", we used a 1% (w/w) spiking rate throughout the thesis. To simulate a realistic contamination pattern that could represent the current soils and the future soils, three polymers that are either widely used to produce agricultural mulch films, i.e. low-density polyethylene (LDPE) or actively promoted to produce biodegradable mulch films, i.e. polylactic acid (PLA) and polybutylene adipate terephthalate (PBAT) were tested in the thesis. A widespread anecic earthworm *Lumbricus terrestris* was used as a model species due to its relatively large body size, high stress tolerance and wide range of feeding sources. The main findings of each objective are summarized below.

5.1.1 Fragmentation and depolymerization of microplastics in the earthworm gut: A potential for microplastic bioremediation? (Chapter 2)

In chapter 2, we presented a preliminary exploration on the physical and chemical changes of MPs during the passage through the earthworm gut in a Petri Dish system and a mesocosm system. In the Petris Dish experiment, *L. terrestris* was exposed to moist MPs only (100% MPs) for 4 days at 16 °C. In the mesocosm experiment, *L. terrestris* was incubated in 1.5 kg MP-free soil or MPs-spiked soil (1%, w/w) for 35 days at 16 °C. The sizes of MPs used in the experiments were 362 ± 119 μm for LDPE, 300 ± 167 μm for PLA, and 234 ± 139 μm for PBAT. Our findings are as follows,

1. By comparing the MPs size distributions in the earthworm crop and gizzard with pre-ingestion pure MPs (Petri Dish experiment) we confirmed that the ingestion of MPs by *L. terrestris* was not particle size dependent, which served as an important basis for other findings in this chapter.
2. We found that the mortality rate was high (30–80%) after the 4-day incubation in Petri Dishes while no mortality was recorded in the mesocosm experiment.
3. By comparing the MPs size distributions in the bulk soil with different parts of the gut

(mesocosm), and by comparing the MPs size distributions in the gut with pre-ingestion MPs (Petri Dish), the fragmentation of LDPE MPs in the gizzard facilitated by soil was observed, featured by the significantly increased proportion of small-sized (20-113 μm) MPs in the size distribution from the bulk soil to the gut (from 8.4% to 18.8%). PLA and PBAT MPs could be fragmented by gizzard without the facilitation of soil, the proportions of small-sized (20-113 μm) PLA and PBAT MPs in the gut were 55.5% and 108.2% higher in the gut than in respective pristine distributions.

4. Substantial depolymerization of PLA (weight-average molar mass reduced by 17.7% with clear shift in the molecular weight distribution) and suspected depolymerization of PBAT were observed in the worm gut, while no change in the molar weight distribution was observed for PLA and PBAT MPs in the bulk soil after 49 days.
5. The earthworm's gut could function as a microenvironment where ingested MPs are subjected to a certain level physical and chemical deterioration.

5.1.2 Fate of microplastics during the earthworm's cast aging process: immobilization and degradation (Chapter 3)

The findings in chapter 2 naturally led to the question of what happens to MPs during the cast aging process once they are excreted back to the environment. The answer to this question provides key knowledge not only for assessing the potential risks of MPs, but also for evaluating the feasibility of bioremediation of MPs by earthworms. Therefore, chapter 3 presents a comprehensive picture about the fate of MPs during the earthworm's cast aging process. The experiment was carried out using a microcosm system that mimics aging of earthworm casts deposited on the soil surface for up to 180 days (0, 15, 60 and 180 days).

To obtain reliable MPs contents in the soil and cast, we applied two extraction–quantification approaches based on different principles for PLA MPs and PBAT MPs: 1) the density separation + gravimetric quantification approach (DS). 2) the Soxhlet extraction + quantitative proton nuclear magnetic resonance approach (Sox-NMR). In addition, the physicochemical properties of MPs were characterized by multiple techniques. Our findings are as follows,

1. The DS approach and Sox-NMR approach generated identical trends of MPs contents for soil samples and fresh casts. While for PLA and PBAT MPs in aged casts, the DS approach reported significantly lower values compared to Sox-NMR. We suspected that such phenomenon was caused by the immobilization effect of cast aging on biodegradable MPs.
2. The fragmentation of PLA MPs and PBAT MPs in the gut was also observed in the microcosm experiment within a short time span (<1 d).
3. During the 180-day incubation, LDPE and PBAT MPs did not show observable degradation in the soil or the cast. PLA MPs did not degrade in the soil but underwent certain levels of degradation during cast aging (polymer contents declined by 30–63%

in 60–180 days).

4. We speculate that the degradation mechanism of PLA MPs during cast aging is surface erosion and fragmentation of PLA MPs occurred during the degradation process.

5.1.3 Microplastics exert minor influence on bacterial community succession during the aging of earthworm (*Lumbricus terrestris*) cast (Chapter 4)

Another import aspect from which we can evaluate the strategy—bioremediating MPs contaminated soils with earthworms—is to study the microbial responses to MPs. The changes in the microbial community composition and function could help explain the mechanisms of the potential MPs degradation in the gut and cast, and help assessing the potential influence of MPs on the soil microbiome. Therefore chapter 4 studied the influence of MPs on the physiochemical properties of earthworm casts, and on bacterial communities in different niches during the soil–gut–cast journey based on the experiment performed in Chapter 3. The bacterial communities were investigated by 16S rRNA sequencing and 16S cDNA sequencing so that we could get the information on the total bacterial community and the active community. Our main findings are as follows:

1. The tested MPs (LDPE, PLA and PBAT) could enlarge the difference in pH, ammonium, nitrate/nitrite, and DOC contents caused by the gut passage between the pre-ingestion soil and the fresh cast, while such effects gradually disappeared during the aging of cast.
2. It was also found that the bacterial community composition (both DNA and RNA) and the richness and diversity were decisively shaped by the niche, instead of the addition of the tested MPs.
3. The soil-related core community and gut-related community identified in our research both significantly contributed to the main body of the cast microbiome, which was likely to have buffered the effects caused by MPs.
4. Biomarkers were identified only for PBAT and the presence of PBAT exerted some influence on the predicted community function, such as the increased metabolization potential for aliphatic and aromatic hydrocarbon and enhanced aerobic chemoheterotrophy capacity.

5.2 General discussion

Overview of the proposed strategy "*mitigating microplastics contamination in soils with earthworms*"

Earthworms are important soil engineers that maintain soil fertility, optimize soil structure, stimulate microbial activities in soils, and adjust soil nutrient cycles. This PhD project was inspired by early studies on two topics, (1) where the role of earthworms played in easing stress caused by pollutants in the soil ecosystem was reported. (2) where the interactions between different earthworm species and different types and dosages of MPs were reported. After rounds of intensive and inspiring discussions with Dr. Violette Geissen and Dr. Esperanza Huerta Lwanga, we agreed to launch this PhD project as one of the first attempts to explore the potential of earthworms to mitigate MPs contamination in soils. Here, a comprehensive overview of the proposed bioremediation is provided.

Resistance of earthworms to MPs-contaminated soils

Throughout the thesis, earthworms (*Lumbricus terrestris*) were exposed to MPs in two scenarios. One scenario is being incubated in or fed with MPs-spiked soil at a dosage of 1% (w/w). The other scenario is being solely exposed to MPs in the Petri Dish. We observed high mortality (30–80%) in the second scenario within 4 days, probably because the ingestion of pure MPs caused severe damage to the earthworm's intestine. By contrast, we did not record any mortality for experiments carried out in the soil under the dosage of 1%. The current global contamination level of MPs may not be high, one review in 2020 provided an estimation of 4.5 mg kg^{-1} in soils (Büks and Kaupenjohann, 2020). While if zooming into a smaller scale, the effective input concentration could reach 0.36% (w/w) for fields where plastic agricultural tools are applied (Meng et al., 2023b). Ecotoxicity study on *Eisenia fetida* has shown that earthworms only showed clear avoidance behavior against MPs at a dosage of >4% (w/w) and the reproduction rate was not affected under 5.3% (w/w) (Ding et al., 2021). Some researchers even reported that the presence of PLA MPs at the dosage of 1% and 2.5% even increased the reproduction of *Eisenia fetida* (Holzinger et al., 2023).

Of course, the effects of MPs on earthworms does not only depend on the dosage. The polymer type also plays a role. For example, Ding et al. (2021) found that biodegradable PLA MPs showed less toxicity compared to PE. This might also be true in our case as the mortalities of earthworms exposed to sole MPs were as follows: 30% for PBAT, 40% for PLA and 80% for LDPE. In addition, the effect of the particle size should also be taken into consideration. Let us imagine a scenario, where in treatment A the soil is spiked with 1% MPs with an average size of 10 μm, and in treatment B the soil was spiked with 1% MPs with an average size of 500 μm. Despite the same mass-based concentration, the item numbers of MPs in the soil might be different by several orders of magnitude, leading to a huge difference in the exposure probability. What's more, the toxic effects of MPs can also vary depending on the particle sizes. For example, Xu and Yu (2021) has found that the micron-size MPs (10 and 100 μm) exhibited higher toxicity to earthworms than nano-size (100 nm). The MPs used in our studies were cryogenically prepared in the lab and all

covered a wide size distribution (20–900 μm, measured with LDIR), which could represent a mixture of MPs with different sizes. In conclusion, our findings together with most existing findings suggest that earthworms are resistant to moderate–high levels of MPs contamination in the soil.

Effects of earthworm gut processes on MPs

Chapter 2 and 3 both covered the physicochemical changes of MPs caused by the earthworms. Chapter 2 focused on the ingestion and digestion processes, where the crop, gizzard, and different parts of the gut were individually studied. Chapter 3, on the other hand, focused on the casting and cast aging process, where the fate of MPs during the cast aging process for up to 180 days was revealed. Even though chapter 2 and 3 vary in targeted processes and experimental settings, the findings of both could draw a relatively comprehensive picture showing the changes of MPs during the Soil–Gut–Cast journey.

The findings in the gut (chapter 2) and in fresh casts (chapter 3) showed that PLA and PBAT MPs could be fragmented by the earthworm's ingestion and digestion behaviors, leading to higher ratios of small-sized MPs in the gut/cast. The Petri Dish experiment (chapter 2) further proved that the observed changes in size distribution inside the worm were not caused by size-dependent ingestion. While the fragmentation of LDPE MPs was observed in the gut in the mesocosm experiment in chapter 2, the size distribution of LDPE MPs in the fresh cast did not differ significantly from the pre-ingestion soil in chapter 3. Considering the different experimental settings in the two chapters, several reasons might have caused the uncertain result. First, it is possible that an adaptation period is needed before earthworms could establish the ability to break up LDPE MPs. The incubation was 35 days in mesocosm in chapter 2 and 6 days in Petri Dish in chapter 3, respectively. It was reported that compared to non-biodegradable MPs (e.g. PET), PLA MPs were easier to be broken up by the earthworm's intestine (Wang et al., 2022). Second, there is also a possibility that LDPE MPs with different sizes have different elimination half lifes from the gut. It might take longer time for the small particles to be transported through the gut, a mechanism like the gel permeation chromatography (GPC), where smaller molecules came out late in the separation process. The potential fragmentation of MPs by earthworms could also be inferred from findings reported elsewhere. For example, Huerta Lwanga et al. (2016) found that LDPE MPs with a diameter <50 μm enriched in the cast. In another study, the generation of nanoplastics in the gut of *Eisenia fetida* was reported (Kwak and An, 2021). In general, our studies and other studies show that the earthworm's gut process could lead to the physical fragmentation of ingested MPs, and such effect is polymer type dependent.

Earthworm gut processes can also lead to polymer type- and time- dependent chemical changes to the ingested MPs. For LDPE and PBAT MPs, we characterized the changes in functional groups with ATR-FTIR (for gut and fresh cast), and changes in crystallinity and thermodynamic properties with DSC (for fresh cast). For PBAT MPs, the chemical composition was additionally examined by NMR (for fresh cast) and the molecular weight distribution was determined by GPC (for gut and fresh cast). The contents of PBAT and LDPE MPs in the pre-ingestion soil, gut content and fresh cast were quantified with at least one approach, and we did not find significant changes between different niches. Therefore,

our findings show that earthworm gut processes did not facilitate the degradation of LDPE and PBAT MPs. By contrast, the chemical properties of PLA MPs were affected by the gut processes. In the mesocosm experiment in chapter 2, PLA MPs recovered from the gut contents showed a lower weight-average molecular weight compared to pre-ingestion soil (17.7% reduction), and the molecular weight distribution clearly shifted to the lower-molecular weight region. The infrared spectra also exhibited some changes in the range of 3200–3600 cm^{-1}, indicating the forming of alcohol group in the material. Both evidences suggest that PLA MPs underwent a certain level of depolymerization in the earthworm's gut. Such phenomenon could be assigned to the "bulk erosion" mechanism, which occurs when the permeation of water molecules exceeds the hydrolysis of materials from the surface (Haider et al., 2019). At the early stage of PLA "bulk erosion", the molecular weight of the bulk material declines but the mass of materials stays unchanged (Von Burkersroda et al., 2002). The observations for PLA MPs in the earthworm gut fit well in the "bulk erosion" mechanism. There is currently little information on the degradation of MPs in the earthworm gut. A recent study reported that PBAT MPs in the gut of *Lumbricus terrestris* showed some chemical changes under Raman spectroscopy inspection (Adhikari et al., 2023).

It is, however, noteworthy that the reduction of average molecular weight and the changes in functional groups were not observed for PLA MPs recovered from the fresh cast in chapter 3 and for PLA MPs recovered from the gut in Petri Dish experiment in chapter 2. Such discrepancy might imply that (1) the effect of gut process on PLA MPs replies on the microbial activities in ingested soil and (2) the depolymerization of PLA MPs in the gut takes place at a relatively slow rate, which is not evident in a short incubation period.

Effects of earthworm cast aging on MPs

The effects of earthworm cast aging on MPs were mainly explored in chapter 3. In general, two phenomena can be summarized from the results.

The first phenomenon is the faster degradation of MPs in the cast compared to the soil, which was confirmed only for PLA MPs. By applying two extraction–quantification approaches, the substantial reduction of PLA MPs contents in aged casts was observed while the contents of PLA MPs incubated in the soil did not show any reduction after 180 days. However, we did not find the generation of new peaks or peak shifting in the IR spectra and ^{1}H–NMR spectra for PLA MPs aged in the cast, indicating that the chemical properties of PLA MPs did not show substantial changes. The shifting in the size distribution from day 0 to day 60, nevertheless, might indicate that PLA MPs experienced further fragmentation during the degradation in the cast. All these findings point to the "surface erosion" mechanism of polyesters, where the permeation of water molecules into the bulk does not exceed the rate of hydrolysis happening on the material surface (Haider et al., 2019). PLA degradation under the "surface erosion" mechanism is characterized by the reduction in mass while the properties of remaining parts stay unchanged (Von Burkersroda et al., 2002). The results in chapter 4 as well as previous studies have shown that the aging of the earthworm cast is accompanied by drastic changes in the pH, dissolved organic carbon contents and bacterial community composition (Decaëns, 2000; Aira et al., 2005; Bottinelli et al., 2020). Therefore, we propose that following the gut, the earthworm

cast is another microenvironment where the degradation of PLA MPs could be enhanced.

The second phenomenon is the immobilization of MPs in the cast, which was observed during C60–C180 for PLA MPs and C0–C180 for PBAT MPs (potentially also true for LDPE MPs, but the trend was not significant). The DS method and Sox-NMR method reported inconsistent trends of MPs concentrations during the cast aging process (C60–C180 for PLA and C0–C180 for PBAT). Specifically, the DS method reported that as the aging time increased, the contents of PLA and PBAT MPs continued to decrease. By contrast, the Sox-NMR results showed that the PLA and PBAT contents did not decline with the increasing aging time. Meanwhile, significant shifting was observed for the size distribution of MPs that can be extracted by the DS method, which was featured by the disappearance/reduction of small-sized particles (< 150 μm) in the size distribution. By comparing the ^{1}H–NMR spectra and the molecular weight distributions between recoveries of C0 and C60/C180 by both methods, we confirmed that the non-extractable part by the DS method possessed the same chemical properties with the DS-extractable part, indicating that there was a general reduction in the recovery performance of PLA and PBAT MPs by the DS method from aged casts. One possible explanation for this could be that PLA and PBAT MPs experienced fragmentation during the cast aging process, leading to the generation of particles <5 μm, which could no longer be recovered as the pore size of the membrane filter used during extraction was 5 μm. Another possibility could be that the special physicochemical properties of the cast and cast aging process led to stronger binding effects between MPs and the cast. Earthworm casts have lower porosity and more stable microaggregates compared to soil (Jouquet et al., 2008), and are also less water-soluble than natural soil aggregates (Schrader and Zhang, 1997). It was found that the drying and aging of casts could facilitate a close bonding of microbial polysaccharides and other organic compounds to clay, stabilizing the new microaggregates (Shipitalo and Protz, 1989). Therefore, it is highly possible that MPs were trapped by the microstructures and microorganism-derived adhesives during the cast aging process, especially for PLA and PBAT, due to the higher hydrophilicity. Consequently, PLA and PBAT MPs were more difficult to recover by the DS method and smaller MPs were more affected.

Response of bacterial communities in the earthworm gut and casts to ingested microplastics

Chapter 4 reported that the tested MPs exerted negligible influence on the bacterial community succession during the cast aging process. To our knowledge, this is one of the first studies which reported the responses of bacterial communities inhabiting the earthworm gut and cast to MPs. We could only find one similar study, where the influence of LDPE and PBAT MPs on the total bacterial communities in the gut and cast of *Lumbricus terrestris* was reported (Adhikari et al., 2023). Despite the fact that different experimental scales (mesocosm vs. microcosm) and feeding strategies of earthworms (litter+MPs vs. soil+MPs) were applied, Adhikari et al. (2023) also found that LDPE and PBAT MPs did not significantly affect the gut and cast bacterial communities. While by dividing the casts into different aging stages and targeting both the total (DNA) and active (RNA) community, our study focused more on the mid–long term effects of MPs on the cast microbiome and aimed to evaluate the potential effects once the casts are incorporated

back to the soil.

Our results indicate that the compositions and functions of the total (DNA) and active (RNA) bacterial community during the soil–aged cast transition were mainly shaped by the substantial biological and chemical processes that happen during ingestion, digestion and cast aging, instead of by the treatments (i.e. Control, LDPE, PLA and PBAT). Several reasons might have led to our findings.

First, the physicochemical changes of MPs during passage through the gut and the aging of cast were not drastic. The results of chapter 2 and 3 showed that the earthworm's gut process and cast aging only caused physical fragmentation of LDPE and PBAT MPs. Although the fragmentation and depolymerization of PLA MPs could happen in the gut and the degradation of PLA MPs happened during the cast aging process, the extent of degradation was not high. These findings might suggest that (1) the interactions between MPs and microorganisms were not enough to induce the biodegradation of MPs (for the case of LDPE and PBAT) or (2) the amount released carbon sources relating to MPs degradation (for the case of PLA) was not enough to affect the community composition.

Second, the digestion and cast aging processes per se are accompanied by drastic successions in the microbial community, which could largely neutralize the influence of MPs, if there is any. Our results for Control (treatment with MPs-free soil) also echoed the drastic microbiome dynamics during gut digestion and the cast aging reported by previous studies (Aira et al., 2019; Aira et al., 2022; Yang et al., 2024). In addition, we identified soil-related and gut-related core communities for both the total and active community, which were likely to maintain the stability of the community composition and function.

Finally, we treated the MPs-containing niches as a whole for community analysis. It is very likely that the influence of MPs is restricted to surface of MPs, which is defined as the "plastisphere" by previous study (Zettler et al., 2013). By zooming into the soil plastisphere (Rillig et al., 2023) or the hotspots of MPs (Zhou et al., 2021) in the studied niches, we might be able to find more significant effects of MPs on the microbial communities.

The physicochemical properties of casts of different aging stages were also studied. However, due to the insufficient sample amounts, the reported values were measured from one sample pooled from all replicates of the same niche under the same treatment. Therefore, we could not test if the differences in physicochemical properties between treatments or niches were statistically significant and perform analysis like RDA and db-RDA to further study the correlations between environmental factors and the microbial communities. Nevertheless, our results showed that gut passage largely increased the pH, $N\text{-}NH_4$ and DOC contents in the fresh cast but reduced the $N\text{-}NO_x$ contents, which is in consistent with previous findings (Horn et al., 2003; Van Groenigen et al., 2019; Vos et al., 2019). And the temporal dynamics of measured indicators during cast aging under Control treatment also echoed previous findings with different earthworm species, soil types, and regions (Decaëns, 2000; Aira et al., 2005; N. Bottinelli et al., 2020). Comparing the values of MP-addition treatments with Control, we speculate that the presence of MPs could enhance the effect of gut passage on soils, leading to an even higher increase in the pH, $N\text{-}NH_4$ contents and DOC contents, and a larger decrease in the $N\text{-}NO_x$ contents.

Feasibility of microplastic bioremediation with earthworms

Using *Lumbricus terrestris* as model species and LDPE, PLA and PBAT MPs as model MPs, our work showed that:

1. Earthworms are resistant to moderate MPs contamination in soils.
2. Earthworm gut processes can cause physical fragmentation of MPs in the ingested soil.
3. Only certain polymers (e.g., PLA) could be deteriorated by earthworm gut processes and undergo some degradation during cast aging process.
4. Excreted biodegradable MPs are closely immobilized in the cast, especially after certain periods of aging.

The fragmentation of MPs by earthworms could generate much more small-size particles. On one hand, this can increase the total surface area of the fragmented particle and accelerate the degradation if the polymer is biodegradable or relatively easy-to-degrade. On the other hand, however, for polymers that are extremely chemically inert, earthworm induced fragmentation might only increase the particle numbers and reduce the particle sizes over a longer period. The fate of fragmented MPs in the cast also depends on the polymer type. Earthworm casts could function as either microenvironments favoring the degradation of certain polymers (e.g., PLA) due to microbial activity and suitable physicochemical conditions or sinks (before cast disintegration) and potential sources (after cast disintegration) of earthworm induced secondary MPs in the soil ecosystem.

Based on these findings, we propose that earthworms possess the potential to help solve MPs contamination of certain polymer types under certain conditions. A good option can be the vermicomposting of biodegradable MPs. In this scenario, earthworms are exposed to MPs in a relatively closed bioactive environment, where MPs in the matrix could be repeatedly treated with earthworm gut processes. The reduction of MPs sizes could in return accelerate the degradation of biodegradable polymers. Another good option can be using earthworms to mitigate the accumulation of biodegradable MPs in soils. The degradation of biodegradable polymers might happen faster in the cast than in the soil. By introducing earthworms into fields where biodegradable mulch films or other biodegradable plastic products are being applied, the fragments derived from biodegradable plastics can be processed and encapsulated in the earthworm's cast via the ingestion and casting activity and experience faster degradation. However, for fields contaminated mainly with inert plastics, the introduction of earthworms may not be an appropriate solution.

5.3 Implications, limitations, and prospects

5.3.1 Are biodegradable plastics promising substitutes for the non-biodegradable plastics in agricultural production?

In this thesis, two popular biodegradable polymers (PLA and PBAT) were studied in parallel with the non-biodegradable polymer (LDPE). According to data released by European Bioplastics (2023), PLA and PBAT accounted for 31.0% and 4.6% of the global production capacity for bio-based and biodegradable plastics. In the market, biodegradable mulch films made from PLA and PBAT blends are also very popular. However, we did not observe the degradation of PLA and PBAT MPs in the soil either for 49 days in the mesocosm or for 180 days in the microcosm. Both experiments were performed at environmentally relevant temperature (16 °C) and moisture (25%). One might criticize that the results reported by our experiments only showed that PLA and PBAT did not degrade under these certain conditions, whereas the real concern is that there is no proper guidance for the application of biodegradable plastics in soils. The rate of plastic degradation depends not only on the intrinsic properties (e.g., polymer type, molecular weight, fillers, etc.), but also on the extrinsic properties such as the size, shape, availability of microbial degraders, soil type and climate, etc. (Chamas et al., 2020; Han et al., 2021). If applied in fields where the soil physicochemical properties, native microbial communities and climate do not support a good degradation rate, biodegradable plastics could also accumulate like the non-biodegradable plastics. Therefore, we strongly appeal that proper guidance and in-field pre-tests are needed before massively promoting biodegradable plastics in agricultural production. In addition, techniques facilitating the biodegradation performance of biodegradable plastics in fields should also be explored.

5.3.2 Importance of studying microplastics with multiple approaches based on different principles

A major highlight of the thesis is that MPs were recovered by different methods in chapter 3, where applicable (i.e., PLA and PBAT). The density separation and Soxhlet extraction methods recovered MPs in different forms (particles vs. polymers), allowing the subsequent quantification and characterization of MPs from different aspects. The density separation method can recover MPs in their original forms if not considering the potential influences caused by sonication, shaking and digestion etc. during the extraction. As a result, the mass, particle number, particle size, and shape of the recovered MPs could be obtained, all import properties for evaluating the fate and potential risks of MPs on the soil ecosystem. However, several key limits are brought in by this approach. For example, the pore size of the membrane filter sets a physical threshold for the size of MPs to be recovered,

and the presence of impurities with similar densities to the target MPs is inevitable in the recoveries. By contrast, the Soxhlet extraction method would destroy the macroscopic characteristics of MPs e.g., size, shape, etc. Nevertheless, such an approach could be highly polymer type-specific and provide more accurate quantitative results. The findings of the current study underlined the importance of combing different extraction and quantification methods in MPs-related studies, especially for complicated environmental matrixes.

5.3.3 Research challenges and prospects

Some limitations and challenges remain for the current thesis, based on which we propose some prospects for future studies on similar topics. First, in the initial plan for the proposed PhD project, earthworms from different ecological groups were intended to be studied. However, due to the massive workload and availability of worms, we only kept *Lumbricus terrestris* as the model species. The epigeic worms mainly live close to the soil surface and feed on manure and litter. The anecic worms build vertical tunnels and feed on litter and soil. The endogeic worms live in deeper layers and mainly feed on mineral soil. Due to different living and feeding strategies, earthworms belonging to different ecological groups might exert different effects on the ingested MPs. Classic views are that the enzymatic and microbial activities in the gut of worms belonging to different ecological groups vary. For example, some summarized that epigeic species have a broad range of enzymatic capacities, while the anecic species obtain microflora from the ingested food (Curry and Schmidt, 2007). Therefore, the effects of earthworm gut processes on ingested MPs might also depend on the worm species. We recommend doing more studies involving different earthworm species and feeding strategies in the future.

Second, the conversion of "plastic carbon" to "biomass carbon" and/or "inorganic carbon" was not investigated in the thesis. The current findings indicate that PLA could be depolymerized and degraded to some extent in the gut and cast. However, it is still unclear whether the degradation was caused by abiotic or biotic forces. It is possible that the PLA degradation was purely abiotic hydrolysis induced by the special physicochemical conditions in the gut and cast. It could also be that the PLA degradation was caused by gut and cast microorganisms that can utilize PLA. Alternatively, PLA degradation could also be triggered by the enzymes excreted by the earthworm. Future studies using stable isotopic labeling (e.g., ^{13}C) might help reveal the biochemical mechanisms of PLA degradation in the complex gut/cast environment.

Third, results of the thesis show that earthworms do not have the potential to facilitate the degradation of non-biodegradable plastics, e.g. LDPE, which has been widely used for producing agricultural films for decades. The existing MPs contamination in agriculture fields are therefore likely to be dominated by LDPE MPs. Nevertheless, the role of earthworms in stimulating and spreading soil microbiome can still be considered as a useful tool for restoring plastic contaminated soils. In the future, if degraders for inert polymers are successfully discovered and isolated, efforts could be made to explore the role of earthworms in improving the performance of functional strains in soils.

Literature cited

Adhikari, K., Astner, A.F., DeBruyn, J.M., Yu, Y., Hayes, D.G., O'Callahan, B.T., Flury, M., 2023. Earthworms Exposed to Polyethylene and Biodegradable Microplastics in Soil: Microplastic Characterization and Microbial Community Analysis. ACS Agricultural Science & Technology 3, 340–349. doi:10.1021/acsagscitech.2c00333

Adhikari, K., Pearce, C.I., Sanguinet, K.A., Bary, A.I., Chowdhury, I., Eggleston, I., Xing, B., Flury, M., 2024. Accumulation of microplastics in soil after long-term application of biosolids and atmospheric deposition. Science of The Total Environment 912, 168883. doi:10.1016/j.scitotenv.2023.168883

Aira, M., Monroy, F., Domínguez, J., 2005. Ageing effects on nitrogen dynamics and enzyme activities in casts of *Aporrectodea caliginosa* (Lumbricidae). Pedobiologia 49, 467–473. doi:10.1016/j.pedobi.2005.07.003

Aira, Manuel, Pérez-Losada, M., Crandall, K.A., Domínguez, J., 2022. Host taxonomy determines the composition, structure, and diversity of the earthworm cast microbiome under homogenous feeding conditions. FEMS Microbiology Ecology 98. doi:10.1093/femsec/fiac093

Aira, M, Perez-Losada, M., Crandall, K.A., Dominguez, J., 2022. Composition, Structure and Diversity of Soil Bacterial Communities before, during and after Transit through the Gut of the Earthworm *Aporrectodea caliginosa*. Microorganisms 10. doi:10.3390/microorganisms10051025

Aira, M., Pérez-Losada, M., Domínguez, J., 2019. Microbiome dynamics during cast ageing in the earthworm Aporrectodea caliginosa. Applied Soil Ecology 139, 56–63. doi:10.1016/j.apsoil.2019.03.019

Auta, H.S., Emenike, C.U., Fauziah, S.H., 2017. Screening of Bacillus strains isolated from mangrove ecosystems in Peninsular Malaysia for microplastic degradation. Environmental Pollution 231, 1552–1559. doi:10.1016/j.envpol.2017.09.043

Aves, A.R., Revell, L.E., Gaw, S., Ruffell, H., Schuddeboom, A., Wotherspoon, N.E., LaRue, M., McDonald, A.J., 2022. First evidence of microplastics in Antarctic snow. The Cryosphere 16, 2127–2145. doi:10.5194/tc-16-2127-2022

Barois, I., Villemin, G., Lavelle, P., Toutain, F., 1993. Transformation of the soil structure through *Pontoscolex corethrurus* (Oligochaeta) intestinal tract. Geoderma 56, 57–66. doi:10.1016/0016-7061(93)90100-Y

Bergmann, M., Collard, F., Fabres, J., Gabrielsen, G.W., Provencher, J.F., Rochman, C.M., van Sebille, E., Tekman, M.B., 2022. Plastic pollution in the Arctic. Nature Reviews Earth & Environment 3, 323–337. doi:10.1038/s43017-022-00279-8

Beriot, N., Zornoza, R., Lwanga, E.H., Zomer, P., van Schothorst, B., Ozbolat, O., Lloret, E., Ortega, R., Miralles, I., Harkes, P., van Steenbrugge, J., Geissen, V., 2023. Intensive vegetable production under plastic mulch: A field study on soil plastic and pesticide

residues and their effects on the soil microbiome. Science of The Total Environment 900, 165179. doi:10.1016/j.scitotenv.2023.165179

Bianchi, M., Dorigato, A., Morreale, M., Pegoretti, A., 2023. Evaluation of the Physical and Shape Memory Properties of Fully Biodegradable Poly(lactic acid) (PLA)/Poly(butylene adipate terephthalate) (PBAT) Blends. Polymers 15, 881. doi:10.3390/polym15040881

Blouin, M., Hodson, M.E., Delgado, E.A., Baker, G., Brussaard, L., Butt, K.R., Dai, J., Dendooven, L., Peres, G., Tondoh, J.E., Cluzeau, D., Brun, J.J., 2013. A review of earthworm impact on soil function and ecosystem services. European Journal of Soil Science. doi:10.1111/ejss.12025

Borelbach, P., Kopitzky, R., Dahringer, J., Gutmann, P., 2023. Degradation Behavior of Biodegradable Man-Made Fibers in Natural Soil and in Compost. Polymers 15, 2959. doi:10.3390/polym15132959

Bottinelli, N, Kaupenjohann, M., Märten, M., Jouquet, P., Soucémarianadin, L., Baudin, F., Tran, T.M., Rumpel, C., 2020. Age matters: Fate of soil organic matter during ageing of earthworm casts produced by the anecic earthworm *Amynthas khami*. Soil Biology and Biochemistry 148. doi:10.1016/j.soilbio.2020.107906

Bottinelli, N., Kaupenjohann, M., Märten, M., Jouquet, P., Soucémarianadin, L., Baudin, F., Tran, T.M., Rumpel, C., 2020. Age matters: Fate of soil organic matter during ageing of earthworm casts produced by the anecic earthworm *Amynthas khami*. Soil Biology and Biochemistry 148. doi:10.1016/j.soilbio.2020.107906

Brandon, A.M., Gao, S.-H., Tian, R., Ning, D., Yang, S.-S., Zhou, J., Wu, W.-M., Criddle, C.S., 2018. Biodegradation of Polyethylene and Plastic Mixtures in Mealworms (Larvae of *Tenebrio molitor*) and Effects on the Gut Microbiome. Environmental Science & Technology 52, 6526–6533. doi:10.1021/acs.est.8b02301

Büks, F., Kaupenjohann, M., 2020. Global concentrations of microplastics in soils – a review. SOIL 6, 649–662. doi:10.5194/soil-6-649-2020

Bullard, J.E., Ockelford, A., O'Brien, P., McKenna Neuman, C., 2021. Preferential transport of microplastics by wind. Atmospheric Environment 245, 118038. doi:10.1016/j.atmosenv.2020.118038

Chamas, A., Moon, H., Zheng, J., Qiu, Y., Tabassum, T., Jang, J.H., Abu-Omar, M., Scott, S.L., Suh, S., 2020. Degradation Rates of Plastics in the Environment. ACS Sustainable Chemistry and Engineering 8, 3494–3511. doi:10.1021/acssuschemeng.9b06635

Chen, M., Cao, M., Zhang, W., Chen, X., Liu, H., Ning, Z., Peng, L., Fan, C., Wu, D., Zhang, M., Li, Q., 2024. Effect of biodegradable PBAT microplastics on the C and N accumulation of functional organic pools in tropical latosol. Environment International 183, 108393. doi:10.1016/j.envint.2023.108393

Chen, S., Zhou, Y., Chen, Y., Gu, J., 2018. fastp: an ultra-fast all-in-one FASTQ preprocessor. Bioinformatics 34, i884–i890. doi:10.1093/bioinformatics/bty560

Chen, Y., Liu, X., Leng, Y., Wang, J., 2020. Defense responses in earthworms (*Eisenia fetida*) exposed to low-density polyethylene microplastics in soils. Ecotoxicology and Environmental Safety 187, 109788. doi:10.1016/j.ecoenv.2019.109788

Cheng, Y., Song, W., Tian, H., Zhang, K., Li, B., Du, Z., Zhang, W., Wang, Jinhua, Wang, Jun, Zhu, L., 2021. The effects of high-density polyethylene and polypropylene microplastics on the soil and earthworm *Metaphire guillelmi* gut microbiota. Chemosphere 267, 129219. doi:10.1016/j.chemosphere.2020.129219

Corradini, F., Casado, F., Leiva, V., Huerta-Lwanga, E., Geissen, V., 2021. Microplastics occurrence and frequency in soils under different land uses on a regional scale. Science of The Total Environment 752, 141917. doi:10.1016/j.scitotenv.2020.141917

Corradini, F., Meza, P., Eguiluz, R., Casado, F., Huerta-Lwanga, E., Geissen, V., 2019. Evidence of microplastic accumulation in agricultural soils from sewage sludge disposal. Science of the Total Environment 671, 411–420. doi:10.1016/j.scitotenv.2019.03.368

Curry, J.P., Schmidt, O., 2007. The feeding ecology of earthworms – A review. Pedobiologia 50, 463–477. doi:10.1016/j.pedobi.2006.09.001

de Souza Machado, A.A., Lau, C.W., Kloas, W., Bergmann, J., Bachelier, J.B., Faltin, E., Becker, R., Gorlich, A.S., Rillig, M.C., 2019. Microplastics Can Change Soil Properties and Affect Plant Performance. Environmental Science & Technology 53, 6044–6052. doi:10.1021/acs.est.9b01339

de Souza Machado, A.A., Lau, C.W., Till, J., Kloas, W., Lehmann, A., Becker, R., Rillig, M.C., 2018. Impacts of Microplastics on the Soil Biophysical Environment. Environmental Science & Technology 52, 9656–9665. doi:10.1021/acs.est.8b02212

Decaëns, Thibaud., 2000. Degradation dynamics of surface earthworm casts in grasslands of the eastern plains of Colombia. Biology and Fertility of Soils 32, 149–156. doi:10.1007/s003740000229

Ding, W., Li, Z., Qi, R., Jones, D.L., Liu, Qiuyun, Liu, Qin, Yan, C., 2021. Effect thresholds for the earthworm *Eisenia fetida*: Toxicity comparison between conventional and biodegradable microplastics. Science of The Total Environment 781, 146884. doi:10.1016/j.scitotenv.2021.146884

Doube, B.M., Schmidt, O., Killham, K., Correll, R., 1997. Influence of mineral soil on the palatability of organic matter for lumbricid earthworms: A simple food preference study. Soil Biology Biochemistry 29, 569–575.

Drake, H.L., Horn, M.A., 2007. As the worm turns: The earthworm gut as a transient habitat for soil microbial biomes. Annual Review of Microbiology. doi:10.1146/annurev.micro.61.080706.093139

European Bioplastics, 2023a. BIOPLASTICS facts and figures. https://docs.european-bioplastics.org/publications/EUBP_Facts_and_figures.pdf

European Bioplastics, 2023b. Q&A on certified soil-biodegradable mulch films. https://docs.european-

bioplastics.org/publications/EUBP_Q_A_Certified_soil_biodegradable_mulch_films.pdf

European Bioplastics, 2020. Bioplastics Market Development Update 2020.

European Bioplastics, 2019. BIOPLASTICS facts and figures.

Givaudan, N., Wiegand, C., Le Bot, B., Renault, D., Pallois, F., Llopis, S., Binet, F., 2014. Acclimation of earthworms to chemicals in anthropogenic landscapes, physiological mechanisms and soil ecological implications. Soil Biology and Biochemistry 73, 49–58. doi:10.1016/j.soilbio.2014.01.032

Greco, A., Ferrari, F., 2021. Thermal behavior of PLA plasticized by commercial and cardanol-derived plasticizers and the effect on the mechanical properties. Journal of Thermal Analysis and Calorimetry 146, 131–141. doi:10.1007/s10973-020-10403-9

Griffin-LaHue, D., Ghimire, S., Yu, Y., Scheenstra, E.J., Miles, C.A., Flury, M., 2022. In-field degradation of soil-biodegradable plastic mulch films in a Mediterranean climate. Science of The Total Environment 806, 150238. doi:10.1016/j.scitotenv.2021.150238

Guo, J.-J., Huang, X.-P., Xiang, L., Wang, Y.-Z., Li, Y.-W., Li, H., Cai, Q.-Y., Mo, C.-H., Wong, M.-H., 2020. Source, migration and toxicology of microplastics in soil. Environment International 137, 105263. doi:10.1016/j.envint.2019.105263

Guo, Z., Li, P., Yang, X., Wang, Z., Wu, Y., Li, G., Liu, G., Ritsema, C.J., Geissen, V., Xue, S., 2023a. Effects of Microplastics on the Transport of Soil Dissolved Organic Matter in the Loess Plateau of China. Environmental Science & Technology 57, 20138–20147. doi:10.1021/acs.est.3c04023

Hadad, D., Geresh, S., Sivan, A., 2005. Biodegradation of polyethylene by the thermophilic bacterium *Brevibacillus borstelensis*. Journal of Applied Microbiology 98, 1093–1100. doi:10.1111/j.1365-2672.2005.02553.x

Haider, T.P., Völker, C., Kramm, J., Landfester, K., Wurm, F.R., 2019a. Plastics of the Future? The Impact of Biodegradable Polymers on the Environment and on Society. Angewandte Chemie International Edition 58, 50–62. doi:10.1002/anie.201805766

Han, Y., Teng, Y., Wang, X., Wen, D., Gao, P., Yan, D., Yang, N., 2024. Biodegradable PBAT microplastics adversely affect pakchoi (*Brassica chinensis* L.) growth and the rhizosphere ecology: Focusing on rhizosphere microbial community composition, element metabolic potential, and root exudates. Science of The Total Environment 912, 169048. doi:10.1016/j.scitotenv.2023.169048

Han, Y., Teng, Y., Wang, Xia, Ren, W., Wang, Xiaomi, Luo, Y., Zhang, H., Christie, P., 2021. Soil Type Driven Change in Microbial Community Affects Poly(butylene adipate- *co* -terephthalate) Degradation Potential. Environmental Science & Technology 55, 4648–4657. doi:10.1021/acs.est.0c04850

Harkes, P., Suleiman, A.K.A., van den Elsen, S.J.J., de Haan, J.J., Holterman, M., Kuramae, E.E., Helder, J., 2019. Conventional and organic soil management as divergent drivers of resident and active fractions of major soil food web constituents. Scientific

Reports 9, 13521. doi:10.1038/s41598-019-49854-y

Hartmann, N.B., Hüffer, T., Thompson, R.C., Hassellöv, M., Verschoor, A., Daugaard, A.E., Rist, S., Karlsson, T., Brennholt, N., Cole, M., Herrling, M.P., Hess, M.C., Ivleva, N.P., Lusher, A.L., Wagner, M., 2019. Are We Speaking the Same Language? Recommendations for a Definition and Categorization Framework for Plastic Debris. Environmental Science & Technology 53, 1039–1047. doi:10.1021/acs.est.8b05297

Hayes, D.G., Flury, M., 2018. Summary and Assessment of EN 17033:2018, a New Standard for Biodegradable Plastic Mulch Films.

Heinze, W.M., Mitrano, D.M., Lahive, E., Koestel, J., Cornelis, G., 2021. Nanoplastic Transport in Soil via Bioturbation by *Lumbricus terrestris*. Environmental Science & Technology 55, 16423–16433. doi:10.1021/acs.est.1c05614

Hernández-Castellanos, B., Ortíz-Ceballos, A., Martínez-Hernández, S., Noa-Carrazana, J.C., Luna-Guido, M., Dendooven, L., Contreras-Ramos, S.M., 2013. Removal of benzo (a) pyrene from soil using an endogeic earthworm *Pontoscolex corethrurus*. Applied Soil Ecology 70, 62–69. doi:10.1016/j.apsoil.2013.04.009

Hickman, Z.A., Reid, B.J., 2008. Earthworm assisted bioremediation of organic contaminants. Environment International 34, 1072–1081. doi:10.1016/j.envint.2008.02.013

Hink, L., Holzinger, A., Sandfeld, T., Weig, A.R., Schramm, A., Feldhaar, H., Horn, M.A., 2023. Microplastic ingestion affects hydrogen production and microbiomes in the gut of the terrestrial isopod *Porcellio scaber*. Environmental Microbiology. doi:10.1111/1462-2920.16386

Holzinger, A., Hink, L., Sehl, E., Rüppel, N., Lehndorff, E., Weig, A.R., Agarwal, S., Horn, M.A., Feldhaar, H., 2023. Biodegradable polymers boost reproduction in the earthworm *Eisenia fetida*. Science of The Total Environment 892, 164670. doi:10.1016/j.scitotenv.2023.164670

Horn, M.A., Schramm, A., Drake, H.L., 2003. The earthworm gut: An ideal habitat for ingested N_2O-producing microorganisms. Applied and Environmental Microbiology 69, 1662–1669. doi:10.1128/AEM.69.3.1662-1669.2003

Huang, Y., Liu, Q., Jia, W., Yan, C., Wang, J., 2020. Agricultural plastic mulching as a source of microplastics in the terrestrial environment. Environmental Pollution 260, 114096. doi:10.1016/j.envpol.2020.114096

Huerta Lwanga, E., Gertsen, H., Gooren, H., Peters, P., Salánki, T., van der Ploeg, M., Besseling, E., Koelmans, A.A., Geissen, V., 2017a. Incorporation of microplastics from litter into burrows of *Lumbricus terrestris*. Environmental Pollution 220, 523–531. doi:10.1016/j.envpol.2016.09.096

Huerta Lwanga, E., Gertsen, H., Gooren, H., Peters, P., Salánki, T., van der Ploeg, M., Besseling, E., Koelmans, A.A., Geissen, V., 2016. Microplastics in the Terrestrial Ecosystem: Implications for *Lumbricus terrestris* (Oligochaeta, Lumbricidae). Environmental Science & Technology 50, 2685–2691. doi:10.1021/acs.est.5b05478

Huerta Lwanga, E., Mendoza Vega, J., Ku Quej, V., Chi, J. de los A., Sanchez del Cid, L., Chi, C., Escalona Segura, G., Gertsen, H., Salánki, T., van der Ploeg, M., Koelmans, A.A., Geissen, V., 2017b. Field evidence for transfer of plastic debris along a terrestrial food chain. Scientific Reports 7, 14071. doi:10.1038/s41598-017-14588-2

Huerta Lwanga, E., Thapa, B., Yang, X., Gertsen, H., Salanki, T., Geissen, V., Garbeva, P., 2018. Decay of low-density polyethylene by bacteria extracted from earthworm's guts: A potential for soil restoration. Science of the Total Environment 624, 753–757. doi:10.1016/j.scitotenv.2017.12.144

Jiang, X., Chang, Y., Zhang, T., Qiao, Y., Klobucar, G., Li, M., 2020. Toxicological effects of polystyrene microplastics on earthworm (*Eisenia fetida*). Environmental Pollution 259, 113896. doi:10.1016/j.envpol.2019.113896

Jouquet, P., Bottinelli, N., Podwojewski, P., Hallaire, V., Tran Duc, T., 2008. Chemical and physical properties of earthworm casts as compared to bulk soil under a range of different land-use systems in Vietnam. Geoderma 146, 231–238. doi:10.1016/j.geoderma.2008.05.030

Ju, H., Yang, X., Osman, R., Geissen, V., 2023. Effects of microplastics and chlorpyrifos on earthworms (*Lumbricus terrestris*) and their biogenic transport in sandy soil. Environmental Pollution 316, 120483. doi:10.1016/j.envpol.2022.120483

Ju, H., Yang, X., Tang, D., Osman, R., Geissen, V., 2024. Pesticide bioaccumulation in radish produced from soil contaminated with microplastics. Science of The Total Environment 910, 168395. doi:10.1016/j.scitotenv.2023.168395

Ju, H., Zhu, D., Qiao, M., 2019. Effects of polyethylene microplastics on the gut microbial community, reproduction and avoidance behaviors of the soil springtail, *Folsomia candida*. Environmental Pollution 247, 890–897. doi:10.1016/j.envpol.2019.01.097

Kamiya, M., Asakawa, S., Kimura, M., 2007. Molecular analysis of fungal communities of biodegradable plastics in two Japanese soils. Soil Science and Plant Nutrition 53, 568–574. doi:10.1111/j.1747-0765.2007.00169.x

Kim, S.W., Leifheit, E.F., Maaß, S., Rillig, M.C., 2021. Time-Dependent Toxicity of Tire Particles on Soil Nematodes. Frontiers in Environmental Science 9. doi:10.3389/fenvs.2021.744668

Kwak, J. Il, An, Y.-J., 2021. Microplastic digestion generates fragmented nanoplastics in soils and damages earthworm spermatogenesis and coelomocyte viability. Journal of Hazardous Materials 402, 124034. doi:10.1016/j.jhazmat.2020.124034

Lan, T., Dong, X., Liu, S., Zhou, M., Li, Y., Gao, X., 2024. Coexistence of microplastics and Cd alters soil N transformation by affecting enzyme activity and ammonia oxidizer abundance. Environmental Pollution 342, 123073. doi:10.1016/j.envpol.2023.123073

Li, B., Song, W., Cheng, Y., Zhang, K., Tian, H., Du, Z., Wang, Jinhua, Wang, Jun, Zhang, W., Zhu, L., 2021. Ecotoxicological effects of different size ranges of industrial-grade polyethylene and polypropylene microplastics on earthworms *Eisenia fetida*. Science of The Total Environment 783, 147007. doi:10.1016/j.scitotenv.2021.147007

Li, T., Lu, M., Xu, B., Chen, H., Li, J., Zhu, Z., Yu, M., Zheng, J., Peng, P., Wu, S., 2022. Multiple perspectives reveal the gut toxicity of polystyrene microplastics on *Eisenia fetida*: Insights into community signatures of gut bacteria and their translocation. Science of The Total Environment 838, 156352. doi:10.1016/j.scitotenv.2022.156352

Li, W., Wufuer, R., Duo, J., Wang, S., Luo, Y., Zhang, D., Pan, X., 2020. Microplastics in agricultural soils: Extraction and characterization after different periods of polythene film mulching in an arid region. Science of The Total Environment 749, 141420. doi:10.1016/j.scitotenv.2020.141420

Liao, J., Chen, Q., 2021. Biodegradable plastics in the air and soil environment: Low degradation rate and high microplastics formation. Journal of Hazardous Materials 418, 126329. doi:10.1016/j.jhazmat.2021.126329

Liu, C., Cui, Y., Li, X., Yao, M., 2021. *microeco* : an R package for data mining in microbial community ecology. FEMS Microbiology Ecology 97. doi:10.1093/femsec/fiaa255

Liu, E.K., He, W.Q., Yan, C.R., 2014. 'White revolution' to 'white pollution'—agricultural plastic film mulch in China. Environmental Research Letters 9, 091001. doi:10.1088/1748-9326/9/9/091001

Liu, H., Yang, X., Liu, G., Liang, C., Xue, S., Chen, H., Ritsema, C.J., Geissen, V., 2017. Response of soil dissolved organic matter to microplastic addition in Chinese loess soil. Chemosphere 185, 907–917. doi:10.1016/j.chemosphere.2017.07.064

Liu, J., Wang, P., Wang, Y., Zhang, Yujia, Xu, T., Zhang, Yiqiong, Xi, J., Hou, L., Li, L., Zhang, Z., Lin, Y., 2022. Negative effects of poly(butylene adipate-co-terephthalate) microplastics on *Arabidopsis* and its root-associated microbiome. Journal of Hazardous Materials 437, 129294. doi:10.1016/j.jhazmat.2022.129294

Liu, L., Zou, G., Zuo, Q., Li, S., Bao, Z., Jin, T., Liu, D., Du, L., 2022. It is still too early to promote biodegradable mulch film on a large scale: A bibliometric analysis. Environmental Technology & Innovation 27, 102487. doi:10.1016/j.eti.2022.102487

Liu, M., Feng, J., Shen, Y., Zhu, B., 2023. Microplastics effects on soil biota are dependent on their properties: A meta-analysis. Soil Biology and Biochemistry 178, 108940. doi:10.1016/j.soilbio.2023.108940

Louca, S., Parfrey, L.W., Doebeli, M., 2016. Decoupling function and taxonomy in the global ocean microbiome. Science 353, 1272–1277. doi:10.1126/science.aaf4507

Luo, Y., Li, L., Feng, Y., Li, R., Yang, J., Peijnenburg, W.J.G.M., Tu, C., 2022. Quantitative tracing of uptake and transport of submicrometre plastics in crop plants using lanthanide chelates as a dual-functional tracer. Nature Nanotechnology 17, 424–431. doi:10.1038/s41565-021-01063-3

Lwanga, E.H., Beriot, N., Corradini, F., Silva, V., Yang, X., Baartman, J., Rezaei, M., van Schaik, L., Riksen, M., Geissen, V., 2022. Review of microplastic sources, transport pathways and correlations with other soil stressors: a journey from agricultural sites into the environment. Chemical and Biological Technologies in Agriculture 9, 20. doi:10.1186/s40538-021-00278-9

Magoč, T., Salzberg, S.L., 2011. FLASH: fast length adjustment of short reads to improve genome assemblies. Bioinformatics 27, 2957–2963. doi:10.1093/bioinformatics/btr507

Marhan, S., Scheu, S., 2005. Effects of sand and litter availability on organic matter decomposition in soil and in casts of *Lumbricus terrestris* L. Geoderma 128, 155–166. doi:10.1016/j.geoderma.2004.07.001

Mariani, L., Jiménez, J.J., Asakawa, N., Thomas, R.J., Decaëns, T., 2007. What happens to earthworm casts in the soil? A field study of carbon and nitrogen dynamics in Neotropical savannahs. Soil Biology and Biochemistry 39, 757–767. doi:10.1016/j.soilbio.2006.09.023

Martinkosky, L., Barkley, J., Sabadell, G., Gough, H., Davidson, S., 2017. Earthworms (*Eisenia fetida*) demonstrate potential for use in soil bioremediation by increasing the degradation rates of heavy crude oil hydrocarbons. Science of The Total Environment 580, 734–743. doi:10.1016/j.scitotenv.2016.12.020

Meng, F., Fan, T., Yang, X., Riksen, M., Xu, M., Geissen, V., 2020. Effects of plastic mulching on the accumulation and distribution of macro and micro plastics in soils of two farming systems in Northwest China. PeerJ 8, e10375. doi:10.7717/peerj.10375

Meng, F., Harkes, P., van Steenbrugge, J.J.M., Geissen, V., 2023. Effects of microplastics on common bean rhizosphere bacterial communities. Applied Soil Ecology 181. doi:10.1016/j.apsoil.2022.104649

Meng, F., Yang, X., Riksen, M., Xu, M., Geissen, V., 2021. Response of common bean (*Phaseolus vulgaris* L.) growth to soil contaminated with microplastics. Science of The Total Environment 755, 142516. doi:10.1016/j.scitotenv.2020.142516

Meng, K., Lwanga, E.H., van der Zee, M., Munhoz, D.R., Geissen, V., 2023a. Fragmentation and depolymerization of microplastics in the earthworm gut: A potential for microplastic bioremediation? Journal of Hazardous Materials 447. doi:10.1016/j.jhazmat.2023.130765

Meng, K., Ren, W., Teng, Y., Wang, B., Han, Y., Christie, P., Luo, Y., 2019. Application of biodegradable seedling trays in paddy fields: Impacts on the microbial community. Science of The Total Environment 656, 750–759. doi:10.1016/j.scitotenv.2018.11.438

Meng, K., Teng, Y., Ren, W., Wang, B., Geissen, V., 2023b. Degradation of commercial biodegradable plastics and temporal dynamics of associated bacterial communities in soils: A microcosm study. Science of The Total Environment 865, 161207. doi:10.1016/j.scitotenv.2022.161207

Moliner, C., Finocchio, E., Arato, E., Ramis, G., Lagazzo, A., 2020. Influence of the Degradation Medium on Water Uptake, Morphology, and Chemical Structure of Poly(Lactic Acid)-Sisal Bio-Composites. Materials 13, 3974. doi:10.3390/ma13183974

Nechitaylo, T.Y., Timmis, K.N., Golyshin, P.N., 2009. '*Candidatus* Lumbricincola', a novel lineage of uncultured *Mollicutes* from earthworms of family *Lumbricidae*.

Environmental Microbiology 11, 1016–1026. doi:10.1111/j.1462-2920.2008.01837.x

Nelson, T.F., Baumgartner, R., Jaggi, M., Bernasconi, S.M., Battagliarin, G., Sinkel, C., Künkel, A., Kohler, H.-P.E., McNeill, K., Sander, M., 2022. Biodegradation of poly(butylene succinate) in soil laboratory incubations assessed by stable carbon isotope labelling. Nature Communications 13, 5691. doi:10.1038/s41467-022-33064-8

Nelson, T.F., Remke, S.C., Kohler, H.-P.E., McNeill, K., Sander, M., 2020. Quantification of Synthetic Polyesters from Biodegradable Mulch Films in Soils. Environmental Science & Technology 54, 266–275. doi:10.1021/acs.est.9b05863

Ng, E.L., Lin, S.Y., Dungan, A.M., Colwell, J.M., Ede, S., Huerta Lwanga, E., Meng, K., Geissen, V., Blackall, L.L., Chen, D., 2021. Microplastic pollution alters forest soil microbiome. Journal of Hazardous Materials 409, 124606. doi:10.1016/j.jhazmat.2020.124606

Orellana, L.H., Francis, T. Ben, Ferraro, M., Hehemann, J.-H., Fuchs, B.M., Amann, R.I., 2022. Verrucomicrobiota are specialist consumers of sulfated methyl pentoses during diatom blooms. The ISME Journal 16, 630–641. doi:10.1038/s41396-021-01105-7

Otake, Y., Kobayashi, T., Asabe, H., Murakami, N., Ono, K., 1995. Biodegradation of low - density polyethylene, polystyrene, polyvinyl chloride, and urea formaldehyde resin buried under soil for over 32 years. Journal of Applied Polymer Science 56, 1789–1796. doi:10.1002/app.1995.070561309

Palacios-Mateo, C., Meng, K., Legaz-Pol, L., Steen Redeker, E., Huerta-Lwanga, E., Blank, L.M., 2023. Enzymes for microplastic-free agricultural soils. Ecotoxicology and Environmental Safety 258, 114982. doi:10.1016/j.ecoenv.2023.114982

Peng, B.Y., Chen, Z.B., Chen, J.B., Yu, H.R., Zhou, X.F., Criddle, C.S., Wu, W.M., Zhang, Y.L., 2020. Biodegradation of Polyvinyl Chloride (PVC) in *Tenebrio molitor* (Coleoptera: Tenebrionidae) larvae. Environment International 145. doi:ARTN 106106 10.1016/j.envint.2020.106106

Peng, B.Y., Chen, Z.B., Chen, J.B., Zhou, X.F., Wu, W.M., Zhang, Y.L., 2021. Biodegradation of polylactic acid by yellow mealworms (larvae of *Tenebrio molitor*) via resource recovery: A sustainable approach for waste management. Journal of Hazardous Materials 416. doi:ARTN 125803 10.1016/j.jhazmat.2021.125803

Peng, B.Y., Su, Y., Chen, Z., Chen, J., Zhou, X., Benbow, M.E., Criddle, C.S., Wu, W.M., Zhang, Y., 2019. Biodegradation of Polystyrene by Dark (*Tenebrio obscurus*) and Yellow (*Tenebrio molitor*) Mealworms (Coleoptera: Tenebrionidae). Environmental Science & Technology 53, 5256–5265. doi:10.1021/acs.est.8b06963

Peng, B.Y., Sun, Y., Wu, Z.Y., Chen, J.B., Shen, Z., Zhou, X.F., Wu, W.M., Zhang, Y.L., 2022. Biodegradation of polystyrene and low-density polyethylene by *Zophobas atratus* larvae: Fragmentation into microplastics, gut microbiota shift, and microbial functional enzymes. Journal of Cleaner Production 367. doi:ARTN 132987 10.1016/j.jclepro.2022.132987

Phillips, H.R.P., Guerra, C.A., Bartz, M.L.C., Briones, M.J.I., Brown, G., Crowther, T.W., Ferlian, O., Gongalsky, K.B., van den Hoogen, J., Krebs, J., Orgiazzi, A., Routh, D., Schwarz, B., Bach, E.M., Bennett, J.M., Brose, U., Decaëns, T., König-Ries, B., Loreau, M., Mathieu, J., Mulder, C., van der Putten, W.H., Ramirez, K.S., Rillig, M.C., Russell, D., Rutgers, M., Thakur, M.P., de Vries, F.T., Wall, D.H., Wardle, D.A., Arai, M., Ayuke, F.O., Baker, G.H., Beauséjour, R., Bedano, J.C., Birkhofer, K., Blanchart, E., Blossey, B., Bolger, T., Bradley, R.L., Callaham, M.A., Capowiez, Y., Caulfield, M.E., Choi, A., Crotty, F. V., Crumsey, J.M., Dávalos, A., Diaz Cosin, D.J., Dominguez, A., Duhour, A.E., van Eekeren, N., Emmerling, C., Falco, L.B., Fernández, R., Fonte, S.J., Fragoso, C., Franco, A.L.C., Fugère, M., Fusilero, A.T., Gholami, S., Gundale, M.J., López, M.G., Hackenberger, D.K., Hernández, L.M., Hishi, T., Holdsworth, A.R., Holmstrup, M., Hopfensperger, K.N., Lwanga, E.H., Huhta, V., Hurisso, T.T., Iannone, B. V., Iordache, M., Joschko, M., Kaneko, N., Kanianska, R., Keith, A.M., Kelly, C.A., Kernecker, M.L., Klaminder, J., Koné, A.W., Kooch, Y., Kukkonen, S.T., Lalthanzara, H., Lammel, D.R., Lebedev, I.M., Li, Y., Jesus Lidon, J.B., Lincoln, N.K., Loss, S.R., Marichal, R., Matula, R., Moos, J.H., Moreno, G., Morón-Ríos, A., Muys, B., Neirynck, J., Norgrove, L., Novo, M., Nuutinen, V., Nuzzo, V., Pansu, J., Paudel, S., Pérès, G., Pérez-Camacho, L., Piñeiro, R., Ponge, J.-F., Rashid, M.I., Rebollo, S., Rodeiro-Iglesias, J., Rodríguez, M.Á., Roth, A.M., Rousseau, G.X., Rozen, A., Sayad, E., van Schaik, L., Scharenbroch, B.C., Schirrmann, M., Schmidt, O., Schröder, B., Seeber, J., Shashkov, M.P., Singh, J., Smith, S.M., Steinwandter, M., Talavera, J.A., Trigo, D., Tsukamoto, J., de Valença, A.W., Vanek, S.J., Virto, I., Wackett, A.A., Warren, M.W., Wehr, N.H., Whalen, J.K., Wironen, M.B., Wolters, V., Zenkova, I. V., Zhang, W., Cameron, E.K., Eisenhauer, N., 2019. Global distribution of earthworm diversity. Science 366, 480–485. doi:10.1126/science.aax4851

Plastics Europe, 2023. Plastics – the fast Facts 2023. https://plasticseurope.org/knowledge-hub/plastics-the-fast-facts-2023/

Plastics Europe, 2019. Plastics - the Facts 2020. An analysis of European plastics production, demand and waste data. https://plasticseurope.org/knowledge-hub/plastics-the-facts-2020/

Poh, L., Wu, Q., Chen, Y., Narimissa, E., 2022. Characterization of industrial low-density polyethylene: a thermal, dynamic mechanical, and rheological investigation. Rheologica Acta 61, 701–720. doi:10.1007/s00397-022-01360-1

Prendergast-Miller, M.T., Katsiamides, A., Abbass, M., Sturzenbaum, S.R., Thorpe, K.L., Hodson, M.E., 2019. Polyester-derived microfibre impacts on the soil-dwelling earthworm *Lumbricus terrestris*. Environmental Pollution 251, 453–459. doi:10.1016/j.envpol.2019.05.037

Qi, Y., Beriot, N., Gort, G., Huerta Lwanga, E., Gooren, H., Yang, X., Geissen, V., 2020. Impact of plastic mulch film debris on soil physicochemical and hydrological properties. Environmental Pollution 266, 115097. doi:10.1016/j.envpol.2020.115097

Qi, Y., Ossowicki, A., Yang, X., Huerta Lwanga, E., Dini-Andreote, F., Geissen, V., Garbeva, P., 2020c. Effects of plastic mulch film residues on wheat rhizosphere and soil

properties. Journal of Hazardous Materials 387. doi:10.1016/j.jhazmat.2019.121711

Qi, Y., Yang, X., Pelaez, A.M., Huerta Lwanga, E., Beriot, N., Gertsen, H., Garbeva, P., Geissen, V., 2018. Macro- and micro- plastics in soil-plant system: Effects of plastic mulch film residues on wheat (*Triticum aestivum*) growth. Science of The Total Environment 645, 1048–1056. doi:10.1016/j.scitotenv.2018.07.229

Rambacher, J., Pantos, O., Hardwick, S., Cameron, E.Z., Gaw, S., 2023. Transforming Encounters: A review of the drivers and mechanisms of macrofaunal plastic fragmentation in the environment. Cambridge Prisms: Plastics 1–33. doi:10.1017/plc.2023.6

Ren, X., Tang, J., Liu, X., Liu, Q., 2020. Effects of microplastics on greenhouse gas emissions and the microbial community in fertilized soil. Environmental Pollution 256, 113347. doi:10.1016/j.envpol.2019.113347

Rezaei, M., Riksen, M.J.P.M., Sirjani, E., Sameni, A., Geissen, V., 2019. Wind erosion as a driver for transport of light density microplastics. Science of The Total Environment 669, 273–281. doi:10.1016/j.scitotenv.2019.02.382

Rezaei Rashti, M., Hintz, J., Esfandbod, M., Bahadori, M., Lan, Z., Chen, C., 2023. Detecting microplastics in organic-rich materials and their potential risks to earthworms in agroecosystems. Waste Management (New York, N.Y.) 166, 96–103. doi:10.1016/j.wasman.2023.04.047

Rillig, M.C., Kim, S.W., Zhu, Y.G., 2023. The soil plastisphere. Nature Reviews Microbiology. doi:10.1038/s41579-023-00967-2

Rillig, M.C., Ziersch, L., Hempel, S., 2017. Microplastic transport in soil by earthworms. Scientific Reports 7, 1362. doi:10.1038/s41598-017-01594-7

Rodriguez-Seijo, A., Lourenco, J., Rocha-Santos, T.A.P., da Costa, J., Duarte, A.C., Vala, H., Pereira, R., 2017. Histopathological and molecular effects of microplastics in *Eisenia andrei* Bouche. Environmental Pollution 220, 495–503. doi:10.1016/j.envpol.2016.09.092

Sanchez-Hernandez, J.C., Capowiez, Y., Ro, K.S., 2020. Potential Use of Earthworms to Enhance Decaying of Biodegradable Plastics. ACS Sustainable Chemistry & Engineering 8, 4292–4316. doi:10.1021/acssuschemeng.9b05450

Sanchez-Hernandez, J.C., Mazzia, C., Capowiez, Y., Rault, M., 2009. Carboxylesterase activity in earthworm gut contents: Potential (eco) toxicological implications. Comparative Biochemistry and Physiology C-Toxicology & Pharmacology 150, 503–511. doi:10.1016/j.cbpc.2009.07.009

Sander, M., 2019. Biodegradation of Polymeric Mulch Films in Agricultural Soils: Concepts, Knowledge Gaps, and Future Research Directions. Environmental Science & Technology 53, 2304–2315. doi:10.1021/acs.est.8b05208

Sanluis-Verdes, A., Colomer-Vidal, P., Rodriguez-Ventura, F., Bello-Villarino, M., Spinola-Amilibia, M., Ruiz-Lopez, E., Illanes-Vicioso, R., Castroviejo, P., Aiese Cigliano, R., Montoya, M., Falabella, P., Pesquera, C., Gonzalez-Legarreta, L., Arias-Palomo, E.,

Solà, M., Torroba, T., Arias, C.F., Bertocchini, F., 2022. Wax worm saliva and the enzymes therein are the key to polyethylene degradation by *Galleria mellonella*. Nature Communications 13, 5568. doi:10.1038/s41467-022-33127-w

Satti, S.M., Shah, A.A., Marsh, T.L., Auras, R., 2018. Biodegradation of Poly(lactic acid) in Soil Microcosms at Ambient Temperature: Evaluation of Natural Attenuation, Bio-augmentation and Bio-stimulation. Journal of Polymers and the Environment 26, 3848–3857. doi:10.1007/s10924-018-1264-x

Scheurer, M., Bigalke, M., 2018. Microplastics in Swiss Floodplain Soils. Environmental Science & Technology 52, 3591–3598. doi:10.1021/acs.est.7b06003

Schrader, S., Zhang, H., 1997. Earthworm casting: Stabilization or destabilization of soil structure? Soil Biology and Biochemistry 29, 469–475.

Schulmann, O., Tiunov, A., 1999. Leaf litter fragmentation by the earthworm *Lumbricus terrestris* L. Pedobiologia 43, 453–458.

Segata, N., Izard, J., Waldron, L., Gevers, D., Miropolsky, L., Garrett, W.S., Huttenhower, C., 2011. Metagenomic biomarker discovery and explanation. Genome Biology 12. doi:10.1186/gb-2011-12-6-r60

Shipitalo, M.J., Protz, R., 1989. Chemistry and Micromorphology of Aggregation in Earthworm Casts. Geoderma 45, 357–374.

Shogren, R.L., Doane, W.M., Garlotta, D., Lawton, J.W., Willett, J.L., 2003. Biodegradation of starch/polylactic acid/poly(hydroxyester-ether) composite bars in soil. Polymer Degradation and Stability 79, 405–411. doi:Pii S0141-3910(02)00356-7 Doi 10.1016/S0141-3910(02)00356-7

Shumway, D., Koide, R., 1994. Seed preferences of *Lumbricus terrestris* L. Applied Soil Ecology 1.

Sintim, H.Y., Bary, A.I., Hayes, D.G., English, M.E., Schaeffer, S.M., Miles, C.A., Zelenyuk, A., Suski, K., Flury, M., 2019. Release of micro- and nanoparticles from biodegradable plastic during in situ composting. Science of The Total Environment 675, 686–693. doi:10.1016/j.scitotenv.2019.04.179

Sintim, H.Y., Bary, A.I., Hayes, D.G., Wadsworth, L.C., Anunciado, M.B., English, M.E., Bandopadhyay, S., Schaeffer, S.M., DeBruyn, J.M., Miles, C.A., Reganold, J.P., Flury, M., 2020. In situ degradation of biodegradable plastic mulch films in compost and agricultural soils. Science of The Total Environment 727, 138668. doi:10.1016/j.scitotenv.2020.138668

Slezak, R., Krzystek, L., Puchalski, M., Krucińska, I., Sitarski, A., 2023. Degradation of bio-based film plastics in soil under natural conditions. Science of the Total Environment 866. doi:10.1016/j.scitotenv.2023.161401

Song, B., Shang, S., Cai, F.M., Liu, Z., Fang, J., li, N., Adams, J.M., Razavi, B.S., 2023. Microbial resistance in rhizosphere hotspots under biodegradable and conventional microplastic amendment: Community and functional sensitivity. Soil Biology and Biochemistry 180, 108989. doi:10.1016/J.SOILBIO.2023.108989

Song, Y., Qiu, R., Hu, J., Li, X., Zhang, X., Chen, Y., Wu, W.M., He, D., 2020. Biodegradation and disintegration of expanded polystyrene by land snails *Achatina fulica*. Science of the Total Environment 746, 141289. doi:10.1016/j.scitotenv.2020.141289

Sun, Y., Zhao, L., Li, X., Hao, Y., Xu, H., Weng, L., Li, Y., 2019. Stimulation of earthworms (*Eisenia fetida*) on soil microbial communities to promote metolachlor degradation. Environmental Pollution 248, 219–228. doi:10.1016/j.envpol.2019.01.058

Suthar, S., 2008. Metal remediation from partially composted distillery sludge using composting earthworm *Eisenia fetida*. Journal of Environmental Monitoring 10, 1099. doi:10.1039/b807908k

Tang, R., Ying, M., Luo, Y., El-Naggar, A., Palansooriya, K.N., Sun, T., Cao, Y., Diao, Z., Zhang, Y., Lian, Y., Chen, K., Yan, Y., Lu, X., Cai, Y., Chang, S.X., 2023. Microplastic pollution destabilized the osmoregulatory metabolism but did not affect intestinal microbial biodiversity of earthworms in soil. Environmental Pollution 320, 121020. doi:10.1016/j.envpol.2023.121020

Taylor, A.R., Taylor, A.F.S., 2013. Assessing daily egestion rates in earthworms: using fungal spores as a natural soil marker to estimate gut transit time. Biology and Fertility of Soils 50, 179–183. doi:10.1007/s00374-013-0823-5

Thompson, R.C., Olsen, Y., Mitchell, R.P., Davis, A., Rowland, S.J., John, A.W.G., McGonigle, D., Russell, A.E., 2004. Lost at Sea: Where Is All the Plastic? Science 304, 838–838. doi:10.1126/science.1094559

Van Groenigen, J.W., Van Groenigen, K.J., Koopmans, G.F., Stokkermans, L., Vos, H.M.J., Lubbers, I.M., 2019. How fertile are earthworm casts? A meta-analysis. Geoderma 338, 525–535. doi:10.1016/j.geoderma.2018.11.001

Von Burkersroda, F., Schedl, L., Opferich, A.G., 2002. Why degradable polymers undergo surface erosion or bulk erosion. Biomaterials 23, 4221–4231.

Vos, H.M.J., Koopmans, G.F., Beezemer, L., de Goede, R.G.M., Hiemstra, T., van Groenigen, J.W., 2019. Large variations in readily-available phosphorus in casts of eight earthworm species are linked to cast properties. Soil Biology and Biochemistry 138. doi:10.1016/j.soilbio.2019.107583

Wang, C., Zhao, J., Xing, B., 2021. Environmental source, fate, and toxicity of microplastics. Journal of Hazardous Materials 407, 124357. doi:10.1016/J.JHAZMAT.2020.124357

Wang, J., Coffin, S., Sun, C., Schlenk, D., Gan, J., 2019. Negligible effects of microplastics on animal fitness and HOC bioaccumulation in earthworm *Eisenia fetida* in soil. Environmental Pollution 249, 776–784. doi:10.1016/j.envpol.2019.03.102

Wang, L., Peng, Y., Xu, Y., Zhang, J., Liu, C., Tang, X., Lu, Y., Sun, H., 2022. Earthworms' Degradable Bioplastic Diet of Polylactic Acid: Easy to Break Down and Slow to Excrete. Environmental Science & Technology 56, 5020–5028. doi:10.1021/acs.est.1c08066

Ward, C.P., Reddy, C.M., Edwards, B., Perri, S.T., 2024. To curb plastic pollution, industry

and academia must unite. Nature 625, 658–662. doi:10.1038/d41586-024-00155-z

Wei, X.-F., Bohlén, M., Lindblad, C., Hedenqvist, M., Hakonen, A., 2021. Microplastics generated from a biodegradable plastic in freshwater and seawater. Water Research 198, 117123. doi:10.1016/j.watres.2021.117123

Willis, A.D., 2019. Rarefaction, Alpha Diversity, and Statistics. Frontiers in Microbiology 10. doi:10.3389/fmicb.2019.02407

Wohlleben, W., Rückel, M., Meyer, L., Pfohl, P., Battagliarin, G., Hüffer, T., Zumstein, M., Hofmann, T., 2023. Fragmentation and Mineralization of a Compostable Aromatic–Aliphatic Polyester during Industrial Composting. Environmental Science & Technology Letters. doi:10.1021/acs.estlett.3c00394

Wolińska, A., Kuźniar, A., Zielenkiewicz, U., Izak, D., Szafranek-Nakonieczna, A., Banach, A., Błaszczyk, M., 2017. Bacteroidetes as a sensitive biological indicator of agricultural soil usage revealed by a culture-independent approach. Applied Soil Ecology 119, 128–137. doi:10.1016/j.apsoil.2017.06.009

Xu, G., Yu, Y., 2021. Polystyrene microplastics impact the occurrence of antibiotic resistance genes in earthworms by size-dependent toxic effects. Journal of Hazardous Materials 416, 125847. doi:10.1016/j.jhazmat.2021.125847

Yang, J., Schrader, S., Tebbe, C.C., 2024. Legacy effects of earthworms on soil microbial abundance, diversity, and community dynamics. Soil Biology and Biochemistry 190, 109294. doi:10.1016/j.soilbio.2023.109294

Yang, J., Yang, Y., Wu, W.-M., Zhao, J., Jiang, L., 2014. Evidence of Polyethylene Biodegradation by Bacterial Strains from the Guts of Plastic-Eating Waxworms. Environmental Science & Technology 48, 13776–13784. doi:10.1021/es504038a

Yang, L., Gao, J., Liu, Y., Zhuang, G., Peng, X., Wu, W.-M., Zhuang, X., 2021. Biodegradation of expanded polystyrene and low-density polyethylene foams in larvae of *Tenebrio molitor* Linnaeus (Coleoptera: Tenebrionidae): Broad versus limited extent depolymerization and microbe-dependence versus independence. Chemosphere 262, 127818. doi:10.1016/j.chemosphere.2020.127818

Yoshida, S., Hiraga, K., Takehana, T., Taniguchi, I., Yamaji, H., Maeda, Y., Toyohara, K., Miyamoto, K., Kimura, Y., Oda, K., 2016. A bacterium that degrades and assimilates poly(ethylene terephthalate). Science 351, 1196–1199. doi:10.1126/science.aad6359

Yu, H., Shi, L., Fan, P., Xi, B., Tan, W., 2022. Effects of conventional versus biodegradable microplastic exposure on oxidative stress and gut microorganisms in earthworms: A comparison with two different soils. Chemosphere 307, 135940. doi:10.1016/j.chemosphere.2022.135940

Yu, M., van der Ploeg, M., Lwanga, E.H., Yang, X., Zhang, S., Ma, X., Ritsema, C.J., Geissen, V., 2019. Leaching of microplastics by preferential flow in earthworm (*Lumbricus terrestris*) burrows. Environmental Chemistry 16, 31. doi:10.1071/EN18161

Zeb, A., Li, S., Wu, J., Lian, J., Liu, W., Sun, Y., 2020. Insights into the mechanisms underlying the remediation potential of earthworms in contaminated soil: A critical

review of research progress and prospects. Science of The Total Environment 740, 140145. doi:10.1016/j.scitotenv.2020.140145

Zettler, E.R., Mincer, T.J., Amaral-Zettler, L.A., 2013. Life in the "Plastisphere": Microbial Communities on Plastic Marine Debris. Environmental Science & Technology 47, 7137–7146. doi:10.1021/es401288x

Zhang, G.S., Liu, Y.F., 2018. The distribution of microplastics in soil aggregate fractions in southwestern China. Science of the Total Environment 642, 12–20. doi:10.1016/j.scitotenv.2018.06.004

Zhang, H., Schrader, S., 1993. Earthworm effects on selected physical and chemical properties of soil aggregates. Biology and Fertility of Soils 15, 229–234. doi:10.1007/BF00361617

Zhang, J., Gao, D., Li, Q., Zhao, Y., Li, L., Lin, H., Bi, Q., Zhao, Y., 2020. Biodegradation of polyethylene microplastic particles by the fungus *Aspergillus flavus* from the guts of wax moth *Galleria mellonella*. Science of the Total Environment 704, 135931. doi:10.1016/j.scitotenv.2019.135931

Zhang, L., Sintim, H.Y., Bary, A.I., Hayes, D.G., Wadsworth, L.C., Anunciado, M.B., Flury, M., 2018. Interaction of *Lumbricus terrestris* with macroscopic polyethylene and biodegradable plastic mulch. Science of The Total Environment 635, 1600–1608. doi:10.1016/j.scitotenv.2018.04.054

Zhang, X., Yu, K., Zhang, H., Liu, Y., He, J., Liu, X., Jiang, J., 2020. A novel heating-assisted density separation method for extracting microplastics from sediments. Chemosphere 256, 127039. doi:10.1016/j.chemosphere.2020.127039

Zhang, Y., Cai, C., Gu, Y., Shi, Y., Gao, X., 2022. Microplastics in plant-soil ecosystems: A meta-analysis. Environmental Pollution 308, 119718. doi:10.1016/j.envpol.2022.119718

Zhang, Y., Tao, J., Bai, Y., Wang, F., Xie, B., 2023. Incomplete degradation of aromatic–aliphatic copolymer leads to proliferation of microplastics and antibiotic resistance genes. Environment International 181. doi:10.1016/j.envint.2023.108291

Zhao, T., Lozano, Y.M., Rillig, M.C., 2021. Microplastics Increase Soil pH and Decrease Microbial Activities as a Function of Microplastic Shape, Polymer Type, and Exposure Time. Frontiers in Environmental Science 9. doi:10.3389/fenvs.2021.675803

Zhou, G.-W., Yang, X.-R., Sun, A.-Q., Li, H., Lassen, S.B., Zheng, B.-X., Zhu, Y.-G., 2019. Mobile Incubator for Iron(III) Reduction in the Gut of the Soil-Feeding Earthworm *Pheretima guillelmi* and Interaction with Denitrification. Environmental Science & Technology 53, 4215–4223. doi:10.1021/acs.est.8b06187

Zhou, J., Gui, H., Banfield, C.C., Wen, Y., Zang, H., Dippold, M.A., Charlton, A., Jones, D.L., 2021. The microplastisphere: Biodegradable microplastics addition alters soil microbial community structure and function. Soil Biology and Biochemistry 156, 108211. doi:10.1016/j.soilbio.2021.108211

Zhou, Y., Wang, J., Zou, M., Jia, Z., Zhou, S., Li, Y., 2020. Microplastics in soils: A review

of methods, occurrence, fate, transport, ecological and environmental risks. Science of The Total Environment 748, 141368. doi:10.1016/j.scitotenv.2020.141368

Zhu, D., Ma, J., Li, G., Rillig, M.C., Zhu, Y.-G., 2022. Soil plastispheres as hotspots of antibiotic resistance genes and potential pathogens. The ISME Journal 16, 521–532. doi:10.1038/s41396-021-01103-9

Zhu, G., Du, R., Du, D., Qian, J., Ye, M., 2021. Keystone taxa shared between earthworm gut and soil indigenous microbial communities collaboratively resist chlordane stress. Environmental Pollution 283, 117095. doi:10.1016/j.envpol.2021.117095

Zrimec, J., Kokina, M., Jonasson, S., Zorrilla, F., Zelezniak, A., 2021. Plastic-Degrading Potential across the Global Microbiome Correlates with Recent Pollution Trends. MBio 12. doi:10.1128/mBio.02155-21

Zumstein, M.T., Schintlmeister, A., Nelson, T.F., Baumgartner, R., Woebken, D., Wagner, M., Kohler, H.-P.E., McNeill, K., Sander, M., 2018. Biodegradation of synthetic polymers in soils: Tracking carbon into CO_2 and microbial biomass. Science Advances 4. doi:10.1126/sciadv.aas9024

Summary

Since the 1950s, plastics have been widely used for multiple purposes, with a strong increase since the 1990s. In agricultural systems, the extensive use and incomplete recycling of plastics, such as mulch films and irrigation pipes have resulted in the release and accumulation of plastic residues in soils. Plastic debris with a diameter of <5 mm is called microplastic (MP), the presence of which in soils has raised increasing concerns due to its potential risks to the soil ecosystem. Studies have shown that MPs can affect soil physicochemical properties, the growth and production of plants, the composition and function of soil microbial communities and potentially the soil nutrient cycles. In recent years, biodegradable plastics have been promoted to replace non-biodegradable plastics in agricultural production. One of the purposes is to reduce plastic contamination in soils. However, the current standards and labels for certifying/labeling the soil-biodegradable mulch films, such as EN 17033:2018, ISO 23517:2021 and OK biodegradable SOIL, use testing conditions that are not comparable with various natural soils and climates. As a result, the degradation rate of biodegradable plastics in soils can be much slower than expected, leading to the potential accumulation of biodegradable MPs in soils.

Earthworms are important soil engineers that maintain soil fertility, optimize soil structure, stimulate soil microbial activity, and adjust soil nutrient cycles. Previous studies have reported that earthworms play a key role in easing the stress caused by various pollutants in the soil ecosystem. Pioneer studies have also shed light on the interactions between different earthworm species and different types and dosages of MPs in soils. Inspired by existing findings, the current thesis presents one of the first attempts to explore the potential of earthworms to mitigate MPs contamination in soils.

We explored and evaluated earthworms' potential to reduce MPs pollution in the soil by studying the physicochemical changes and contents of MPs during the passage through earthworm gut and during cast aging. To simulate a contamination pattern that can represent the present legacy of plastic use and the future agricultural practices, three polymers that are widely used to produce agricultural mulch films, low-density polyethylene (LDPE) and biodegradable mulch films, i.e. polylactic acid (PLA) and polybutylene adipate terephthalate (PBAT) were tested in the thesis. A widespread anecic earthworm *Lumbricus terrestris* was used as a model species due to its relatively large body size, high stress tolerance and wide range of feeding sources.

Chapter 2 presents an exploration of the physical and chemical changes of MPs during the passage through the earthworm's gut in a Petri Dish system and a mesocosm system. In the Petris Dish experiment, *L. terrestris* was exposed to only moist MPs for 4 days at 16 °C. In the mesocosm experiment, *L. terrestris* was incubated in 1.5 kg MP-free soil and MPs-spiked soils (1%, w/w) for 35 days at 16 °C. The average sizes of MPs were 362 ± 119 µm (LDPE), 300 ± 167 µm (PLA), and 234 ± 139 µm (PBAT). The results show that the ingestion of MPs by *L. terrestris* was not particle size dependent. Earthworms survived in the MPs-spiked soil (0% mortality in 35 days) but barely when exposed solely to microplastics (30-80% mortality in 4 days). We found significantly more small-sized MPs

in the earthworm gut compared to the pre-ingestion soil or pure MPs, indicating that the tested MPs could be physically fragmented in the earthworm's gut. In addition, by checking chemical properties of the two polyester MPs (PLA and PBAT), we found that PLA underwent substantial depolymerization (weight-average molar mass reduced by 17.7% with clear shift in molecular weight distribution). Suspected depolymerization of PBAT was observed in the worm gut, but further evidence is needed. By contrast, no change in the molar weight distribution was observed for PLA and PBAT MPs in the bulk soil. Chapter 2 shows that the earthworm's gut could function as a microenvironment where ingested MPs are subjected to a certain level of physical and chemical deterioration.

The findings in chapter 2 naturally led to the question of what happens to MPs during the cast aging process once they are excreted back to the environment. The answer to this question provided key understanding not only for assessing the potential risks of MPs, but also for evaluating the feasibility of bioremediation of MPs with earthworms.

Therefore, **chapter 3** presents a comprehensive picture about the fate of MPs during the earthworm's cast aging process. The experiment was carried out using a microcosm system that mimics the aging of earthworm casts deposited on the soil surface for up to 180 days (0, 15, 60 and 180 days). Earthworms were fed with MPs-spiked soils (1%, w/w) to generate casts. The average sizes of prepared pristine MPs were 419 ± 160 μm (LDPE), 465 ± 107 μm (PLA), and 338 ± 215 μm (PBAT). To study MP concentrations in the soil and cast during experiment, we applied two extraction–quantification approaches based on different principles for PLA MPs and PBAT MPs: (1) density separation followed by gravimetric quantification (for all MPs). (2) Soxhlet extraction followed by proton nuclear magnetic resonance quantification (Sox-NMR) (for residual PLA and PBAT polymers). The physicochemical properties of MPs were characterized by multiple techniques (ATR-FTIR, DSC, ^{1}H–NMR). The results show that PLA MPs and PBAT MPs could be fragmented in the gut within a very short time span (<1 d). The fate of MPs during the cast aging process is polymer type dependent. LDPE MPs stayed unaffected. Two phenomena were observed for biodegradable MPs: one is faster degradation than in the bulk soil (for PLA MPs only); The other is immobilization of MPs in aged casts (for both PLA and PBAT), which led to declined recovery performance by the density separation method. It is speculated that the degradation mechanism of PLA MPs during cast aging is surface erosion and fragmentation of PLA MPs occurred during the degradation process.

Another import aspect from which we can evaluate the strategy—bioremediating MPs contaminated soils with earthworms—is to study the microbial responses to MPs. The changes in the microbial community composition and function could help explain the mechanisms of the potential MPs degradation in the gut and cast, and help assessing the potential influence of MPs on the soil microbiome.

Chapter 4 presents the influence of MPs on the physicochemical properties of earthworm's cast and bacterial communities in different niches during the soil–gut–cast journey based on the experiment performed in Chapter 3. The bacterial communities were profiled by 16S rRNA sequencing (DNA) and 16S cDNA sequencing (RNA) so that we could get information on the total bacterial community and the active community. Different niches, e.g., pre-ingestion soil (Soil), gut content (Gut) and casts aged for 0–180 days (C0–

C18O) were studied. The results show that the tested MPs (LDPE, PLA and PBAT) enlarged the gut passage-derived difference between pre-ingestion soil and the fresh cast in terms of pH, ammonium contents, nitrate/nitrite contents, and dissolved organic carbon contents. However, such effects gradually disappeared during cast aging. The composition and, alpha and beta diversity of both total (DNA) and active (RNA) bacterial communities were shaped by its niche, rather than by the presence/absence or the types of MPs. Nevertheless, a few biomarkers indicative of PBAT were identified, and the functional prediction (by FAPROTAX) for the active community showed that PBAT was associated with higher potential for aliphatic and aromatic hydrocarbon degradation. We also identified a soil-related core community and a gut-related core community, which might have neutralized MPs' effects and maintained the main structure and function of bacterial communities during the Soil–Gut–Cast journey. The findings of chapter 4 indicate that the tested MPs exerted minor influence on the bacterial communities during the cast aging process, MPs in aged casts might not add additional influence on the soil microbial community when they are finally incorporated into the soil. Future studies testing different soil types, polymer types, earthworm species, and field conditions are recommended to help enhance current knowledge on the influence of MPs on earthworms' cast microbiome.

Altogether, our findings suggest that earthworms are resistant to moderate (1%, w/w) MPs contamination in soils. The gut process of earthworms can cause physical fragmentation of MPs in the ingested soil, and such phenomenon is more pronounced for biodegradable plastics. Among the tested polymers, only PLA can be deteriorated by the earthworm's gut process and degraded to some extent during cast aging process. Earthworm's cast could function as either a microenvironment with high microbial activity and suitable physicochemical conditions that favor the degradation of certain polymers (e.g., PLA) or as a sink (before cast disintegration) and potentially as a source (after cast disintegration) of earthworm induced secondary MPs in the soil ecosystem.

Based on these results, we propose that earthworms possess the potential to help solve MPs contamination of certain polymer types under certain conditions. A good option could be the vermicomposting of biodegradable MPs. In this scenario, earthworms are exposed to MPs in a relatively closed bioactive environment, where MPs in the matrix could be repeatedly treated with the earthworm's gut process, the reduction of MPs sizes could in return accelerate the degradation of biodegradable polymers. Another good option could be using earthworms to mitigate the accumulation of biodegradable MPs in soils. The degradation of biodegradable polymers can happen faster in the cast than in the soil. By introducing earthworms into fields where biodegradable mulch films or other biodegradable plastic products are being used, the fragments derived from biodegradable plastics can be processed by earthworms' gut and immobilized in the cast and further exposed to faster biodegradation. However, for fields contaminated mainly with inert plastics (e.g. LDPE), the introduction of earthworms may not be an appropriate solution.

Acknowledgements

My stay at the Soil Physics and Land Management (SLM) group was like a 4.5- year sweet dream. The Netherlands is a unique and beautiful country, and Wageningen is a peaceful small city where people have the leisure to think and study. I really enjoyed my PhD life here.

First, I would like to express my gratitude to Violette and Esperanza, for making a great supervision team with me. When I arrived in October 2019, I was given a lot of time and freedom to think about which topic to select for my PhD project. After many rounds of intensive but insightful discussions with both of you we finalized the PhD proposal, and it was directly approved by the peer review committee without the suggestion to revise (it was a big surprise!). During implementing the PhD project, we kept good communications with each other, and everything went smoothly. Besides research-related activities, we also shared many good memories. On Thursdays (sometimes also on Fridays), Violette, I and other PhDs often went to play basketball together. During games, we could always hear you shouting, “You are not alone!”, which means you want to get the ball! The potluck events at your house were also unforgettable experiences, where I enjoyed nice food from SLM people from all around the world! I still remember that Esperanza showed me how to collect and distinguish worms from the field and how to dissect earthworms in an effective way. In addition, you were like a mentor to me whenever I felt confused and stressed. Thank you both for your company and support, which backed me throughout my PhD journey!

I would also like to sincerely thank the people who worked with me during my PhD for their help and efforts. Thank you, Davi, for being my all-time comrade on science! My research life has become more colorful with you involved! We have been closely working on many interesting things together since 2021. We went to sample plastic debris in south NL, we conceived the idea of “earthworm engineers equipped with AI-backpacks”, we explored instruments for measuring carbon dioxide during plastic degradation, we organized WSC 2023 Masterclass, we carried out Alice’s research practice together… these are just a few cases among all our collaborations. It has been a great pleasure to work with you! Thank you, Maarten, for sharing your professional knowledge and critical input with me throughout my PhD! I really learnt a lot from you on polymer science and I sincerely felt that your contributions have made our research more rigorous! Thank you, Paula, for guiding me through the molecular biology experiments and bioinformatics analysis! It was also great fun to work with you in the lab! I also want to extend my thanks to Xiaomei, who helped and guided me like an elder sister. I really appreciate that you can always help me see more clearly from a Chinese perspective. Finally, I would also like to thank Harm, Piet, Hennie, and Rima from SLM group, Fritz and Annie from Aquatic Ecology and Water Quality Management group, Yanzhang from Magnefy, and Wouter, Evelien and Herman from Wageningen Food & Biobased Research for your valuable help that supported my PhD research.

Of course, one’s PhD life can never be perfect without friends. It was a great pleasure and

honor to share the same office with you, Nikola Rakonjac, during the past years. You are my BFF with whom I talk about everything. I hope you, Ljubica and Olga have a happy and healthy life in the future! Please come to China, I will be your personal guide to travel around! I also want to thank Hui, my good buddy with whom we travelled together, carried out experiments together during COVID. And more importantly you also acted as my personal hairdresser ^ ^. Thank you, Darrel, for always sharing your imaginative ideas with me. I could still remember our trip to Germany and Cyprus, and the nice summer BBQs at the front yard of your old studio. I was also very happy to be one of the paranymphs for your promotion! Thank you, Dennis, for being an always progressing ping pong player and an unstable (when you wear glasses) but competitive pool player. It was great fun to play sports, vent out, and chill together with you. Thank you, Valdrich, for being the geek in our office, we exchanged exciting things about coding, and we tried our first cigars together, it was an interesting experience. I would like to thank all my friends at SLM for your support and company during my PhD life!

Finally, I would like to thank my family, my father, my mother, and my girlfriend Lixue Xie for always supporting me no matter what happens. I feel so lucky to have such a warm and loving family. Your unconditional love and support encouraged me to go through all my adventures.

About the author

Ke Meng (left) and Nikola Rakonjac (right)

Ke Meng was born on the 22nd of January 1994 in Zhenjiang, a beautiful and peaceful city in eastern China. Since his childhood he has shown an enthusiasm in keeping the order and cleanness of the environment of his neighborhood, which also contributed partially to his future decision of doing environment-related research. After 3 years of happy study life in Jiangsu Provincial Zhenjiang No.1 High School, he was admitted to China University of Geosciences (CUG) in 2012.

Ke Meng majored in geochemistry during his bachelor's study, which provided him opportunities to visit different labs and reserve basic knowledge on instrumental chemistry. Besides his study in CUG, he also did research practices in Guangzhou Institute of Geochemistry, Chinese Academy of Sciences (Jan–Feb 2015) and Nanjing University (July 2015), where he developed great interests in environmental research. After 4 years, he was admitted (exam-free) to University of Chinese Academy of Sciences (UCAS) and Institute of Soil Science, Chinese Academy of Sciences (ISSCAS) to pursue a master's degree.

Under the supervision of Prof. Dr Ying Teng and the help of Assoc. Prof. Dr Wenjie Ren, Ke Meng devoted himself to studying the degradation and ecological effects of biodegradable plastic products in paddy soils. Besides experimental work in the lab, in 2018 he also went to fields where biodegradable plastic products were used. Such experience increased his concerns over the potential risks caused by the use of biodegradable plastics, that's why he decided to continue relevant study for his PhD project.

In 2019, Ke Meng got in contact with Prof. Violette Geissen and was successfully granted with the financial support by the China Scholarship Council (CSC). From Oct 7, 2019, he joined Soil Physics and Land Management (SLM) Group, Wageningen University & Research (WUR), under the supervision of Dr Violette Geissen and Dr Esperanza Huerta Lwanga. During his PhD, he and his supervision team explored whether earthworm gut related activities can help reduce microplastic pollution in soils. Besides his main topic, he also participated in the supervision of a master's thesis and a master's research practice.

His permanent contact email address is: jasonmengke@126.com

Scientific publications

Meng, K., Van der Zee, M., Munhoz, D.R., Lwanga, E.H. & Geissen, V. Fate of microplastics during the aging of earthworm casts: immobilization and degradation. (To be submitted)

Meng, K., Harkes, P., Lwanga, E.H. & Geissen, V. Microplastics exert minor influence on bacterial community succession during the aging of earthworm (*Lumbricus terrestris*) casts. (submitted to ***Soil Biology and Biochemistry***, in revision)

Munhoz, D.R., **Meng, K.**, Wang L., Lwanga, E.H., Geissen, V., & Harkes, P. (2024). Exploring the potential of earthworm gut bacteria for plastic degradation. ***Science of The Total Environment***, 927, 172175. https://doi.org/10.1016/j.scitotenv.2024.172175

Meng, K., Lwanga, E.H., Van der zee, M., Munhoz, D.R., & Geissen, V. (2023). Fragmentation and depolymerization of microplastics in the earthworm gut: A potential for microplastic bioremediation? ***Journal of Hazardous Materials***, 447, Article 130765. https://doi.org/10.1016/j.jhazmat.2023.130765

Meng, K., Teng, Y., Ren, W., Wang, B., & Geissen, V. (2023). Degradation of commercial biodegradable plastics and temporal dynamics of associated bacterial communities in soils: A microcosm study. ***Science of The Total Environment***, 865, 161207. http://doi.org/10.1016/j.scitotenv.2022.161207

Palacios-Mateo, C., **Meng, K.**, Legaz-Pol, L., Steen Redeker, E., Huerta-Lwanga, E., & Blank, L.M. (2023). Enzymes for microplastic-free agricultural soils. ***Ecotoxicology and Environmental Safety***, 258, 114982. https://doi.org/10.1016/j.ecoenv.2023.114982

Wang, B., Teng, Y., Li, R., **Meng, K.**, Xu, Y., Liu, S., & Luo, Y. (2023). Exploring the PAHs dissipation and indigenous bacteria response in soil amended with two different microbial inoculants. ***Science of The Total Environment***, 859, 160186. https://doi.org/10.1016/j.scitotenv.2022.160186.

Lwanga, E.H., Van Roshum, I., Munhoz, D.R., **Meng, K.**, Rezaei, M., Goossens, D., Bijsterbosch, J., Alexandre, N., Oosterwijk, J., Krol, M., Peters, P., Geissen, V., & Ritsema, C. (2023). Microplastic appraisal of soil, water, ditch sediment and airborne dust: The case of agricultural systems. ***Environmental Pollution***, 316, 120513. https://doi.org/10.1016/j.envpol.2022.120513

Cohen, Q.M., Glaese, M., **Meng, K.**, Geissen, V., & Huerta-Lwanga, E. (2022). Parks and Recreational Areas as Sinks of Plastic Debris in Urban Sites: The Case of Light-Density Microplastics in the City of Amsterdam, The Netherlands. ***Environment***s, 9, 5. https://doi.org/10.3390/environments9010005

Ng, E.L., Lin, S.Y., Dungan, A.M., Colwell, J.M., Ede, S., Huerta Lwanga, E., **Meng, K.**, Geissen, V., Blackall, L.L., & Chen, D. (2021). Microplastic pollution alters forest soil microbiome. ***Journal of Hazardous Materials***, 409, 124606. https://doi.org/10.1016/j.jhazmat.2020.124606

Meng, K., Ren, W., Teng, Y., Wang, B., Han, Y., Christie, P., & Luo, Y. (2019). Application of biodegradable seedling trays in paddy fields: Impacts on the microbial community.

Science of The Total Environment, 656, 750–759. https://doi.org/10.1016/j.scitotenv.2018.11.438

Xu, Y., Dai, S., **Meng, K.**, Wang, Y., Ren, W., Zhao, L., Christie, P., & Teng, Y. (2018). Occurrence and risk assessment of potentially toxic elements and typical organic pollutants in contaminated rural soils. ***Science of The Total Environment***, 630, 618-629. https://doi.org/10.1016/j.scitotenv.2018.02.212

Co-author affiliations

Violette Geissen

Soil Physics and Land Management Group, Wageningen University & Research, Wageningen, the Netherlands

Esperanza Huerta Lwanga

Soil Physics and Land Management Group, Wageningen University & Research, Wageningen, the Netherlands

Agroecología, El Colegio de la Frontera Sur, Unidad Campeche, Campeche, Mexico

Maarten van der Zee

Wageningen Food & Biobased Research, Wageningen University & Research, Wageningen, The Netherlands

Davi Renato Munhoz

Soil Physics and Land Management Group, Wageningen University & Research, Wageningen, the Netherlands

Paula Harkes

Soil Physics and Land Management Group, Wageningen University & Research, Wageningen, the Netherlands

Netherlands Research School for the
Socio-Economic and Natural Sciences of the Environment

D I P L O M A

for specialised PhD training

The Netherlands research school for the
Socio-Economic and Natural Sciences of the Environment
(SENSE) declares that

Ke Meng

born on 22nd of January 1994 in Zhenjiang, China

has successfully fulfilled all requirements of the
educational PhD programme of SENSE.

Wageningen, 10th of June 2024

SENSE coordinator PhD education

Dr Ir Peter Vermeulen

The SENSE Director

Dr Jampel Dell'Angelo

The SENSE Research School declares that **Ke Meng** has successfully fulfilled all requirements of the educational PhD programme of SENSE with a work load of 31.9 EC, including the following activities:

SENSE PhD Courses

- Environmental research in context (2019)
- Research in context activity: 'WSC 2023 Masterclass: assessing the fate of microplastics in soils' (2023)

Other PhD and Advanced MSc Courses

- Microbial Ecology, Wageningen University (2022)
- Bioinformatics with Linux and Python, WIMEK and VLAG (2023)
- R and Big data, PE&RC (2023)
- Big data exploration and object-oriented programming with Python, WIMEK (2023)
- Big Data in the Life Sciences, VLAG (2023)
- Intensive Writing Week, Wageningen University (2024)

Management and Didactic Skills Training

- Supervising a MSc student with thesis titled "Degradation of microplastics in soil by enzymes" (2022)
- Supervising a MSc student during their internship (2023)

Oral and Poster Presentations

- *Exploring the potential use of earthworms to mitigate microplastic pollution in the soil.* 12th International Symposium on Earthworm Ecology, 10-15 July 2022, Rennes, France
- *The fate of egested conventional and bio/biodegradable microplastics during the earthworm's cast ageing process*. 18th International Conference On Chemistry And The Environment, 11-15 June 2023, Venice, Italy

Colophon

The research described in this thesis was conducted at Soil Physics and Land Management Group, Wageningen University. This research described in this thesis was financially supported by the EU Horizon 2020 project MIcro- and NAno-Plastics in AGRIcultural Soils (MINAGRIS) and the China Scholarship Council (CSC: 201904910443)

Layout by: Ke Meng

Cover designed by: Ke Meng and Fenna Schaap (Proefschriftmaken)

Printed by: Proefschriftmaken || www.proefschriftmaken.nl